

# Efficient and minimal length parametric conformal prediction regions

Daniel J. Eck<sup>1</sup> and Forrest W. Crawford<sup>2,3,4,5</sup>

1. Department of Statistics, University of Illinois Urbana-Champaign
2. Department of Biostatistics, Yale School of Public Health
3. Department of Statistics & Data Science, Yale University
4. Department of Ecology & Evolutionary Biology, Yale University
5. Yale School of Management

October 29, 2019

## Abstract

Conformal prediction methods construct prediction regions for iid data that are valid in finite samples. We provide two parametric conformal prediction regions that are applicable for a wide class of continuous statistical models. This class of statistical models includes generalized linear models (GLMs) with continuous outcomes. Our parametric conformal prediction regions possess finite sample validity, even when the model is misspecified, and are asymptotically of minimal length when the model is correctly specified. The first parametric conformal prediction region is constructed through binning of the predictor space, guarantees finite-sample local validity and is asymptotically minimal at the  $\sqrt{\log(n)/n}$  rate when the dimension  $d$  of the predictor space is one or two, and converges at the  $O\{(\log(n)/n)^{1/d}\}$  rate when  $d > 2$ . The second parametric conformal prediction region is constructed by transforming the outcome variable to a common distribution via the probability integral transform, guarantees finite-sample marginal validity, and is asymptotically minimal at the  $\sqrt{\log(n)/n}$  rate. We develop a novel concentration inequality for maximum likelihood estimation that induces these convergence rates. We analyze prediction region coverage properties, large-sample efficiency, and robustness properties of four methods for constructing conformal prediction intervals for GLMs: fully nonparametric kernel-based conformal, residual based conformal, normalized residual based conformal, and parametric conformal which uses the assumed GLM density as a conformity measure. Extensive simulations compare these approaches to standard asymptotic prediction regions. The utility of the parametric conformal prediction region is demonstrated in an application to interval prediction of glycosylated hemoglobin levels, a blood measurement used to diagnose diabetes.

**Keywords:** conformity measure, maximum likelihood estimation, regression, generalized linear models, exponential families, finite sample validity, concentration inequalities

## 1 Introduction

Vovk et al. [2005] introduced conformal prediction to construct finite sample valid prediction regions for predictions from nearest-neighbor methods, support-vector machines, and sequential classification and both

linear and ridge regression problems. The goal in conformal prediction is to construct a prediction region  $C_n$  from an iid random sample  $Y_1, \dots, Y_n$ , such that the probability of a future observation  $Y_{n+1}$  belonging to the region  $C_n$  exceeds a desired coverage level [Shafer and Vovk, 2008]. That is, given  $Y_1, \dots, Y_n$ , we seek a set  $C_n = C_n(Y_1, \dots, Y_n)$  such that for  $0 < \alpha < 1$ ,

$$\mathbb{P}(Y_{n+1} \in C_n) \geq 1 - \alpha. \quad (1)$$

Lei et al. [2013] extended the framework of Shafer and Vovk [2008] to provide a framework for which the prediction region  $C_n$  is also asymptotically of minimal length. These prediction regions make use of a conformity measure  $\sigma$  which measures the agreement of a point  $y$  with a probability measure  $P$ . For example, when  $y \in \mathbb{R}$ , the probability density function  $p$  corresponding to  $P$  is a conformity measure  $\sigma$ . Lei et al. [2013] proposed nonparametric kernel density estimation of  $p$  to construct conformal prediction regions that are asymptotically minimal under smoothness conditions on  $p$ . Beyond real-valued outcomes, conformal methods have been proposed for functional data [Lei et al., 2015], nonparametric regression [Lei and Wasserman, 2014], time series data [Chernozhukov et al., 2018b], high-dimensional regression problems [Lei et al., 2018], random effects [Dunn and Wasserman, 2018], causal inference [Chernozhukov et al., 2018a], machine learning [Vovk et al., 2005, Gammernan and Vovk, 2007, Papadopoulos et al., 2011, Vovk, 2012, Burnaev and Vovk, 2014, Balasubramanian et al., 2014, Johansson et al., 2018, Wang et al., 2018], and quantile regression [Romano et al., 2019a,b, Sesia and Candés, 2019]. The finite sample validity property of conformal prediction regions has broad appeal in many scientific domains, including astrophysics [Ciollaro et al., 2018], medical applications [Lambrou et al., 2009, Devetyarov et al., 2012, Eklund et al., 2015, Bosc et al., 2019], genetics [Norinder et al., 2018b,a], and chemistry [Cortés-Ciriano and Bender, 2018, Ji et al., 2018, Svensson et al., 2018a,b, Toccaceli et al., 2017].

However, usefulness of the finite sample validity property of conformal prediction regions in regression may be offset by the size of the prediction region. Recently, Cortés-Ciriano and Bender [2019] stated that “a major issue in conformal prediction applied to regression is the low efficiency of most conformal prediction models. . . Such large intervals are not informative and thus hamper the practical usefulness of conformal prediction”, calling for the development of non-conformity functions to reduce the size of the predicted confidence regions [Cortés-Ciriano and Bender, 2019]. The parametric conformal prediction regions that we develop in this paper answer the call made by Cortés-Ciriano and Bender [2019] in the context of regression. We show that when one uses the parametric density with maximum likelihood estimators (MLEs) of model parameters plugged in for modeling parameters as the conformity measure, then one can construct conformal predictions that are asymptotically minimal length and our sharp under our proof technique. Our parametric conformal prediction regions possess the same finite-sample validity guarantees as existing conformal prediction procedures, even under model misspecification.

In a recent paper, Chernozhukov et al. [2019] proposed parametric conformal prediction regions based on regression models for conditional distributions, establishing the conditional validity of the resulting prediction intervals under consistent estimation of the conditional distributions. Their proposed prediction method is based on modeling the entire conditional distribution (rather than the conditional mean) and thereby generates conditionally valid prediction sets that fully utilize the information in the covariates [Chernozhukov et al., 2019]. In another recent paper, Izbicki et al. [2019] proposed parametric conformal prediction regions that are asymptotically minimal length, without providing explicit convergence rates.

We build upon the frameworks outlined by Chernozhukov et al. [2019] and Izbicki et al. [2019] by providing two methods for constructing parametric conformal prediction regions which are asymptotically of minimal length with desirable rates of convergence. Both methods are constructed by using the maximum likelihood estimator as a plugin estimate of unknown modeling parameters in the underlying density and distribution

functions. The first of these is conditionally valid in local regions of the predictor space [Lei and Wasserman, 2014, pg. 72], and is asymptotically conditionally valid for point predictions. The rate of convergence for this parametric conformal prediction region is  $O\{\sqrt{\log(n)/n}\}$  when the dimension of predictor space is  $d \leq 2$  and is  $O\{(\log(n)/n)^{1/d}\}$  when  $d > 2$  where the predictor region of interest shrinks at a suitable rate. The construction of this conformal prediction region follows the binning technique in Lei and Wasserman [2014]. The  $O\{(\log(n)/n)^{1/d}\}$  rate is a consequence of how quickly the predictor region of interest shrinks. The second parametric conformal prediction region is obtained by first transforming the outcome variable to a “common” distribution via the probability integral transform, and conducting conformal prediction with respect to this common distributions to obtain a finite sample marginally valid prediction region, and then backtransforming this region to the scale of the original outcome variables. We leverage the estimated density to obtain estimates of the quantiles corresponding to the minimal length  $(1 - \alpha) \times 100\%$  prediction region before we backtransform to the scale of the response. We show that this parametric conformal prediction region is asymptotically minimal at rate  $O\{\sqrt{\log(n)/n}\}$ . The convergence rates for both parametric conformal regions are appreciably faster than that presented by Lei and Wasserman [2014] which gave rates of  $\{\log(n)/n\}^{1/(d+3)}$  for nonparametric conformal prediction regions in the same regression context.

Chernozhukov et al. [2019] developed a similar transformation conformal prediction region that is motivated by the probability integral transform. Their conformal prediction technique is based on the  $\alpha/2$  and  $1 - \alpha/2$  quantiles of the underlying data generating model. This technique will return asymptotically minimal length prediction regions when the data generating model is symmetric. However, this asymptotic property will not hold for non-symmetric distributions. Moreover, Chernozhukov et al. [2019] did not provide convergence rates for their transformation based conformal prediction region. Izbicki et al. [2019] developed a similar binned and transformation parametric conformal prediction regions which are asymptotically minimal length. However, Izbicki et al. [2019] did not provide convergence rates for either conformal prediction region. Furthermore, their transformation conformal prediction region may obtain larger regions than necessary when the underlying distribution is neither symmetric nor unimodal [Izbicki et al., 2019, Section 2]. We show that maximum likelihood estimation within a class of models that possess subexponential tail behavior and additional mild regularity conditions is necessary for our convergence rates to hold. Furthermore, the asymptotic properties for both of our conformal prediction regions hold for nonsymmetric and multimodal distributions.

We motivate our parametric conformal prediction techniques through the application of GLMs with continuous outcomes. GLMs are widely used regression models for outcomes that follow an exponential family distribution [McCullagh and Nelder, 1989]. GLMs are popular in empirical research in the biomedical and social sciences; procedures for fitting GLMs is incorporated into every major statistical software package. Often predictive inference from a fitted GLM serves the primary scientific goals of the analysis. Point predictions from these models are usually combined with variance estimates from the bootstrap or delta method to construct prediction intervals. For example, interval predictions on the outcome scale may be constructed using the `predict.glm` function in R [R Core Team, 2019] to construct Wald type intervals for either the mean response or its distribution. We show that our parametric conformal regions provide a useful alternative to such approaches.

In an extensive simulation study, we analyze marginal, local, and conditional prediction interval coverage, and large-sample efficiency of four methods for constructing conformal prediction intervals from fitted GLMs: fully nonparametric kernel-based prediction [Lei and Wasserman, 2014], prediction for residuals and locally weighted residuals [Lei et al., 2018], and prediction using the parametric density as conformity measure. We find that when sample sizes are moderate – large enough to estimate regression coefficients reasonably precisely, but before asymptotic arguments guarantee good conditional coverage – conformal

prediction methods outperform traditional methods in terms of finite sample marginal, local, and conditional coverage. Importantly, we find that parametric conformal prediction regions perform extremely well under mild model misspecification, they are calibrated to give valid finite sample coverage and they are not too large for meaningful inference in this setting. We demonstrate the utility of conformal prediction methods for GLMs in an application to diabetes diagnosis via interval prediction of glycosylated hemoglobin levels of subjects participating in a community-based study [Willems et al., 1997].

## 2 Background

### 2.1 Conformal prediction for continuous outcomes

The basic intuition underlying the conformal prediction method is that, given an independent sample  $Y_1, \dots, Y_n$  from distribution  $P$  defined on  $\mathbb{R}^r$ , the iid hypothesis that  $(Y_1, \dots, Y_n, Y_{n+1}) \sim P$  using observation  $(Y_1, \dots, Y_n, y)$  is tested for each  $y \in \mathbb{R}^r$ , and a prediction region  $\widehat{C}^{(\alpha)}$  is created by inverting this test [Lei et al., 2013, Vovk et al., 2005, Shafer and Vovk, 2008]. More formally, suppose that  $(Y_1, \dots, Y_n, Y_{n+1}) \sim P$ . Let  $\widehat{P}_{n+1}$  be the corresponding empirical distribution and note that  $\widehat{P}_{n+1}$  is symmetric in its  $n + 1$  arguments. The conformity rank is  $\pi_{n+1,i} = (n + 1)^{-1} \sum_{j=1}^{n+1} \mathbb{1} \left\{ \sigma(\widehat{P}_{n+1}, Y_j) \leq \sigma(\widehat{P}_{n+1}, Y_i) \right\}$  where  $\sigma(\cdot, \cdot)$  is a conformity measure which measures the ‘‘agreement’’ of a point  $y$  with respect to a distribution  $P$  [Lei et al., 2013]. Informally, a conformity measure should be large when there is agreement between  $y$  and  $P$ . One important example of a conformity measure is the density function  $p$  of  $P$  (when it exists); this idea is used in Section 3. Exchangeability of  $(\pi_{n+1,i} : 1 \leq i \leq n + 1)$  follows from exchangeability of the random variables  $\{\sigma(\widehat{P}_{n+1}, Y_i) : 1 \leq i \leq n + 1\}$ . Define  $\pi(y) = \pi_{n+1,n+1} |_{Y_{n+1}=y}$  as the random variable  $\pi_{n+1,n+1}$  evaluated at  $Y_{n+1} = y$ . The conformal prediction region for  $Y_{n+1}$  is  $\widehat{C}^{(\alpha)}(Y_1, \dots, Y_n) = \{y : \pi(y) \geq \tilde{\alpha}\}$ , where  $\tilde{\alpha} = \lfloor (n + 1)\alpha \rfloor / (n + 1)$ . Then by construction,  $\mathbb{P}(\pi(Y_{n+1}) \geq \tilde{\alpha}) \geq 1 - \alpha$ , which implies that  $\mathbb{P} \left\{ Y_{n+1} \in \widehat{C}^{(\alpha)}(Y_1, \dots, Y_n) \right\} \geq 1 - \alpha$ . Any conformity measure  $\sigma$  can be used to construct prediction regions with finite sample validity.

**Lemma 1.** [Lei et al., 2013]. *Suppose  $Y_1, \dots, Y_n, Y_{n+1}$  is an independent random sample from  $P$ . Then  $\mathbb{P} \left\{ Y_{n+1} \in \widehat{C}^{(\alpha)} \right\} \geq 1 - \alpha$ , for all probability measures  $P$ , and hence  $\widehat{C}^{(\alpha)}$  is valid.*

Figure 1 shows schematically how this conformal prediction region is constructed.

### 2.2 Notions of finite sample validity in regression

Several notions of finite sample validity exist in the context of regression. Suppose that we have an iid sample  $(X_i, Y_i)$ ,  $i = 1, \dots, n$  where the predictor is  $X \in \mathbb{R}^m$  and  $Y \in \mathbb{R}$  is the outcome. We will suppose that  $d$  of the  $X$ ’s are main effects, where  $d \leq m$ , and the other  $m - d$  terms in  $X$  are functions of the  $d$  main effects. We will suppose that  $X$  has support  $\mathcal{X} = [0, 1]^d$ .

**Definition 1** (marginal validity). *Let  $0 < \alpha < 1$  be a desired error tolerance. Let  $(X_i, Y_i)$ ,  $i = 1, \dots, n$  be an iid sample from a continuous distribution  $P$ . The prediction region  $\widehat{C}^{(\alpha)}$  has finite sample marginal validity if  $\mathbb{P} \left\{ Y_{n+1} \in \widehat{C}^{(\alpha)}(X_{n+1}) \right\} \geq 1 - \alpha$ , where  $(X_{n+1}, Y_{n+1}) \sim P$ .*

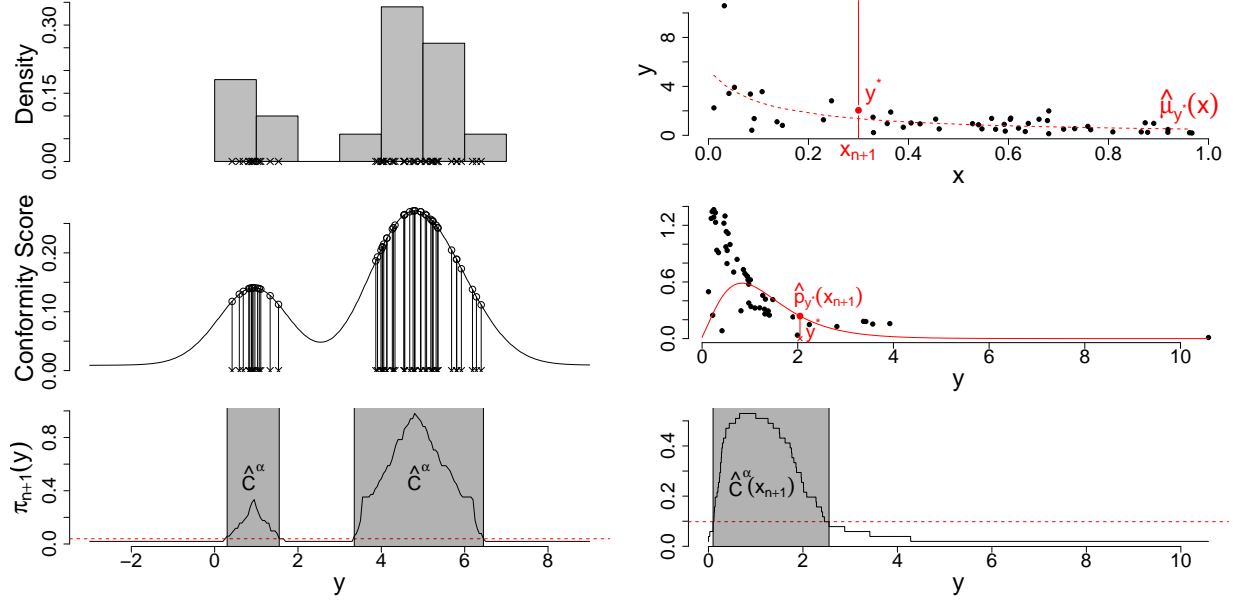


Figure 1: How conformal prediction regions are constructed. The left panel shows conformal prediction for a univariate outcome  $y$ : the top row shows the data points and corresponding histogram; middle row shows conformity scores for a nonparametric kernel smoother; bottom panel shows  $\pi_{n+1,i}$  for each  $i$ , and the conformal prediction set  $\widehat{C}^{(\alpha)}$ . The right panel show conformal prediction for a univariate regression with predictor  $x$  and outcome  $y$ : the top row shows the  $(x_i, y_i)$  pairs, and a regression estimate  $\hat{\mu}_y(x)$  computed using the additional point  $(x_{n+1}, y^*)$ ; middle panel shows the conformity scores obtained by using the estimated density as the conformity measure; bottom panel shows  $\pi(y)$  at  $x_{n+1}$ , the proportion of density scores lower than the density score at candidate  $y$ , and the conformal prediction set  $\widehat{C}^{(\alpha)}(x_{n+1})$ .

Finite sample marginal validity is guaranteed for conformal prediction methods by construction. Finite sample marginal validity alone may not be desirable when variability of the outcome is not constant across the support of the predictor. A second notion of finite sample validity arises by considering coverage of the prediction region conditional on a particular value of the predictor.

**Definition 2** (conditional validity). *Let  $0 < \alpha < 1$  be a desired error tolerance. Let  $(X_i, Y_i)$ ,  $i = 1, \dots, n$  be an iid sample from a continuous distribution  $P$ . The prediction region  $\widehat{C}^{(\alpha)}$  has finite sample conditional validity at  $x$  when  $\mathbb{P}\{Y_{n+1} \in \widehat{C}^{(\alpha)}(x) | X_{n+1} = x\} \geq 1 - \alpha$ , where  $(X_{n+1}, Y_{n+1}) \sim P$ .*

However, conditional validity at every  $x$  is unattainable if we insist that  $\widehat{C}^{(\alpha)}$  is asymptotically of minimal length. Let  $p(y|x)$  be the conditional density corresponding to regression of  $y$  on  $x$ . Define  $s_x^{(\alpha)}$  to be the value such that  $P(Y_{n+1} \in \{y : p(y|x) \geq s_x^{(\alpha)}\} | X = x) = 1 - \alpha$  and define  $C(x) = \{y : p(y|x) \geq s_x^{(\alpha)}\}$  to be the optimal conditional prediction region (i.e., the minimal length prediction region). Let  $\nu$  be Lebesgue measure and let  $\Delta$  denote the symmetric set difference operator. Then there does not exist a finite sample conditional valid prediction region  $\widehat{C}^{(\alpha)}(x)$  such that  $\sup_{x \in \mathcal{X}} \nu\{\widehat{C}^{(\alpha)}(x) \Delta C(x)\} \xrightarrow{P} 0$  holds, a result due to Lemma 1 of Lei and Wasserman [2014]. A third notion of finite sample validity relaxes the stringent requirement of conditional validity at every possible  $x$ .

**Definition 3** (local validity). *Let  $0 < \alpha < 1$  be a desired error tolerance. Let  $(X_i, Y_i)$ ,  $i = 1, \dots, n$  be an*

iid sample from a continuous distribution  $P$ . Let  $\mathcal{A} = \{A_k : k \geq 1\}$  be a partition of  $\mathcal{X}$ . We say that the prediction region  $\widehat{C}^{(\alpha)}$  has finite sample local validity when  $\mathbb{P} \left\{ Y_{n+1} \in \widehat{C}^{(\alpha)}(X_{n+1}) | X_{n+1} \in A_k \right\} \geq 1 - \alpha$ , for all  $A_k \in \mathcal{A}$  where  $(X_{n+1}, Y_{n+1}) \sim P$ .

Local validity offers a bridge between marginal validity – which is inappropriate in the presence of heterogeneity – and conditional validity – which is unattainable when we require that the prediction interval is asymptotically minimal [Lei and Wasserman, 2014]. The nonparametric conformal prediction region in Section 4.1 satisfies finite sample local validity and is asymptotically conditional valid [Lei and Wasserman, 2014]. In Section 3 we show that the parametric conformal prediction region also satisfies finite sample local validity and is asymptotically conditional valid at rate faster than its nonparametric counterpart.

### 3 Conformal prediction for parametric models

We now introduce parametric conformal prediction regions for a wide class of parametric families with continuous outcomes. We show that this class of parametric families includes continuous regular full exponential families, and hence GLMs by extension. Two parametric conformal prediction regions are provided. The first of these guarantees finite-sample local validity using a similar binning technique as Lei and Wasserman [2014]. The second guarantees finite-sample marginal validity via transformation to a “common” distribution.

Suppose, for simplicity, that the support of the predictors is  $\mathcal{X} = [0, 1]^d$ . Let  $(X, Y) \sim P$  and let  $(X_i, Y_i) \sim P$ ,  $i = 1, \dots, n$  be an iid sample where  $P$  is a continuous distribution,  $Y \in \mathbb{R}$ ,  $X \in \mathbb{R}^m$  with  $d \leq m$  main effects. We will denote the true conditional density of the regression model as  $p_\psi(\cdot|x)$  and define  $\psi \in \mathbb{R}^r$ . For each  $x$ , we define  $t_x^{(\alpha)}$  to be the point such that  $\mathbb{P} \left( \{y : p_\psi(y|x) \geq t_x^{(\alpha)}\} | X = x \right) = 1 - \alpha$  for  $0 < \alpha < 1$ . The optimal or minimal length prediction region at  $x$  is  $C_P^{(\alpha)}(x) = \{y : p_\psi(y|x) \geq t_x^{(\alpha)}\}$ . Define the moment generating function (MGF)  $M_{Y,x,\psi}(t)$  corresponding to the conditional density  $p_\psi(\cdot|x)$ . The parameter space for this parametric family is

$$\mathfrak{N}_{\mathcal{X}} = \{ \psi : \nabla_\psi \log p_\psi(y|x) = O(y), M_{Y,x,\psi}(t) \text{ exists for all } t \text{ in a neighborhood of } 0, \text{ all } x \in \mathcal{X} \}.$$

#### 3.1 Local validity via binning

Let  $\mathcal{A} = \{A_k : k \geq 1\}$  be a partition  $\mathcal{X}$  and define the rates  $r_n = O(\sqrt{\log(n)/n})$  and  $z_n = O\{(\log(n)/n)^{1/d}\}$ . The number of elements in the partition  $\mathcal{A}$  increases at rate  $1/r_n$  when  $d \leq 2$  and  $1/z_n$  when  $d > 2$ . When we restrict the partition to be formed of equilateral cubes, we let the widths of these cubes decrease at rate  $r_n$  or  $z_n$ . Let  $p_\psi(y|x)$  be the true conditional density function and let  $\hat{p}_\psi(\cdot|\cdot)$  be the estimated density fit using the original data and define  $\hat{p}_\psi^{(x,y)}(\cdot|\cdot)$  as the estimated density fit to the augmented data  $\{(X_1, Y_1), \dots, (X_n, Y_n), (x, y)\}$ . We will use this estimated density as our conformity measure. The local conformal prediction region is then

$$\widehat{C}_{n,k}^{(\alpha)}(x) = \left\{ y : \frac{1}{n_k + 1} \sum_{i=1}^{n+1} \mathbb{1} \{X_i \in A_k\} \mathbb{1} \left\{ \hat{p}_\psi^{(x,y)}(Y_i | X_i) \leq \hat{p}_\psi^{(x,y)}(y|x) \right\} \geq \tilde{\alpha}_k \right\}, \quad (2)$$

where  $\tilde{\alpha}_k = \lfloor (n_k + 1)\alpha \rfloor / (n_k + 1)$  for  $0 < \alpha < 1$ .

A schematic of how this conformal prediction region is constructed is displayed in the right-hand side of Figure 1. We now establish local validity for  $\widehat{C}_{n,k}^{(\alpha)}$ .

**Lemma 2.** *Let  $\mathcal{A}$  be a partition of  $\mathcal{X}$  and let  $\widehat{C}_{n,k}^{(\alpha)}(x)$  be as defined in (2). Then  $\widehat{C}_{n,k}^{(\alpha)}(x)$  is finite sample locally valid for  $x \in A_k \in \mathcal{A}$ .*

*Proof.* The proof follows from the proof of [Lei and Wasserman, 2014, Proposition 2]. Fix  $k$  and let  $\{i_1, \dots, i_{n_k}\} = \{i : 1 \leq i \leq n, X_i \in A_k\}$ . Let  $(X_{n+1}, Y_{n+1}) \sim P$  be another independent sample. Let  $i_{n_k+1} = n+1$  and  $\sigma_{i_j} = \hat{p}_{\psi}^{(x,y)}(Y_{i_j} | X_{i_j})$  for all  $1 \leq j \leq n_k+1$ . Then conditioning on  $X_{n+1} \in A_k$  and  $(i_1, \dots, i_{n_k})$ , the sequence  $(\sigma_{i_1}, \dots, \sigma_{i_{n_k}}, \sigma_{i_{n_k+1}})$  is exchangeable.  $\square$

We now establish that the parametric conformal prediction region  $\widehat{C}_{n,k}^{(\alpha)}$  is asymptotically of minimum length over  $\mathcal{X}$ .

**Assumption 1** (Assumption 1 (a) of Lei and Wasserman [2014]). Let  $\mathcal{X}$  be the support of  $X$  and assume that  $\mathcal{X} = [0, 1]^d$ . The marginal density of  $X$  satisfies  $0 < b_1 \leq p_X(x) \leq b_2 < \infty$  for all  $x \in \mathcal{X}$ .

**Assumption 2.** The conditional density  $p_{\psi}(\cdot|x)$  is Lipschitz in both  $x$  and  $\psi$ , there exists some  $L_1, L_2 \in \mathbb{R}$  such that,  $\|p_{\psi}(\cdot|x_1) - p_{\psi}(\cdot|x_2)\|_{\infty} \leq L_1 \|x_1 - x_2\|$ , and  $\|p_{\psi_1}(\cdot|x) - p_{\psi_2}(\cdot|x)\|_{\infty} \leq L_2 \|\psi_1 - \psi_2\|$ .

**Assumption 3** (smoothness condition of Lei and Wasserman [2014]). There exists positive constants  $\varepsilon, \gamma, c_1$ , and  $c_2$  such that, for all  $x \in \mathcal{X}$ , and all  $\psi \in \mathfrak{N}_{\mathcal{X}}$ ,

$$c_1 \varepsilon^{\gamma} \leq \mathbb{P}[\{y : |p_{\psi}(y|x) - t_x^{(\alpha)}|X = x\}] \leq c_2 \varepsilon^{\gamma},$$

for all  $\varepsilon \leq \varepsilon_0$ . Moreover,  $\inf_x t_x^{(\alpha)} \geq t_0 > 0$ .

**Theorem 1.** *Let  $Y|X = x$  be a random variable with conditional density  $p_{\psi}(\cdot|x)$  and parameter space  $\mathfrak{N}_{\mathcal{X}}$ . Assume that  $p_{\psi}(\cdot|x)$  is twice differentiable in  $\psi$  and satisfies Assumptions 2 and 3. Let  $(X_1, Y_1), \dots, (X_n, Y_n)$  be independent and identically distributed copies of  $(X, Y)$ . Let  $\psi \in \mathbb{R}^r$ . Let  $\hat{\psi}$  be the MLE of  $\psi$ . Augment the sample data with a new point  $(x, y)$ , and let  $\hat{\psi}^{(x,y)}$  be the MLE of  $\psi$  with respect to the augmented data. Let  $\hat{p}_{\psi}^{(x,y)}(\cdot|x)$  be the conditional density with  $\hat{\psi}^{(x,y)}$  plugged in for  $\psi$ . Suppose that Assumption 1 holds. Let  $0 < \alpha < 1$  and  $\widehat{C}_{n,k}^{(\alpha)}$  be the prediction band given by (2). Then, for a given  $\lambda > 0$ , there exists a numerical constant  $\zeta_{\lambda}$  such that*

$$\mathbb{P} \left[ \sup_{x \in \mathcal{X}} \nu \left\{ \widehat{C}_{n,k}^{(\alpha)}(x) \triangle C_P^{(\alpha)}(x) \right\} \geq \zeta_{\lambda} (z_n \vee r_n) \right] = O \left( n^{-\lambda} \right), \quad (3)$$

where  $r_n = O(\sqrt{\log(n)/n})$ .

### Remarks:

1. The proof of Theorem 1 is given in the Appendix. The rates  $r_n$  and  $z_n$  are appreciably faster than that of the nonparametric conformal prediction band which has a convergence rate of  $w_n = O\{\log(n)/n\}^{1/(d+3)}$  when the underlying  $p_{\psi}(y|x)$  has parameter space  $\mathfrak{N}_{\mathcal{X}}$ . The difference between the convergence speed of the parametric and nonparametric conformal prediction regions originates from the differences in the rates of MLEs and nonparametric techniques and the speed at which the bin widths shrink.

2. The following Lemma governs how fast the bins can shrink while still maintaining that  $n_k \rightarrow \infty$ .

**Lemma 3** (Lemma 9 in Lei and Wasserman [2014]). *Under Assumption 1, there exists constants  $C_1$  and  $C_2$  such that*

$$\mathbb{P}\left(\forall k : b_1 n w_n^d / 2 \leq n_k \leq 3b_2 n w_n^d / 2\right) \geq 1 - C_1 w_n^{-d} \exp(-C_2 n w_n^d),$$

with  $b_1$  and  $b_2$  defined in Assumption 1.

3. The key term in Lemma 3 is the  $n w_n^d$  term appearing in the exponent. The proof of Theorem 1 reveals that the rate of convergence of the parametric conformal prediction region is limited by Lemma 3. This is not the case for the nonparametric conformal prediction region where the limiting factor is the rate of convergence of the kernel density estimator.
4. The proof of Theorem 1 requires a new concentration inequality for MLEs which is stated below as Theorem 2. The proof technique that we employ for Theorem 1 involves sandwiching  $\widehat{C}_{n,k}^{(\alpha)}(x)$  by two estimated level sets, formalized as Lemma 10 in the Appendix. The convergence rate of these sandwiching level sets depends on  $r_n$ ,  $z_n$ , and the convergence rate of  $\sup_{x \in \mathcal{X}} \|\widehat{p}_\psi^{(x,y)}(\cdot|x) - p_\psi(\cdot|x)\|_\infty$ , see Lemma 9 in the Appendix. We verify that

$$\sup_{x \in \mathcal{X}} \|\widehat{p}_\psi^{(x,y)}(\cdot|x) - p_\psi(\cdot|x)\|_\infty = O\left(|\widehat{\psi} - \psi|\right),$$

where  $\psi \in \mathbb{R}^r$  are the parameters in density  $p_\psi(\cdot|x)$  and  $\widehat{\psi}$  be the MLE of  $\psi$ , hence the need for Theorem 2.

Let  $|\cdot|$  denote the  $L^1$  norm of a vector or the absolute value of a scalar.

**Theorem 2.** *Let  $Y|X = x$  be a random variable with conditional density  $p_\psi(\cdot|x)$  and parameter space  $\aleph_{\mathcal{X}}$ . Assume that  $p_\psi(\cdot|x)$  is twice differentiable in  $\psi$  and satisfies Assumption 2. Let  $(X_1, Y_1), \dots, (X_n, Y_n)$  be independent and identically distributed copies of  $(X, Y)$ . Let  $\psi \in \mathbb{R}^r$ . Let  $\widehat{\psi}$  be the MLE of  $\psi$ . Then for any  $\lambda > 0$ , there exists a numerical constant  $A_\lambda$ , such that*

$$\mathbb{P}\left\{\sqrt{n}|\widehat{\psi} - \psi| \geq A_\lambda \sqrt{\log(n)}\right\} = O\left(n^{-\lambda}\right). \quad (4)$$

The concentration inequality given in Theorem 2 is a generalization of Theorem 3.3 in Miao [2010] to subexponential random variables with powers of  $\log(n)/n$  replacing  $r$ , provided that the underlying density is parameterized with  $\aleph_{\mathcal{X}}$ . Theorem 3.3 in Miao [2010] only holds for subgaussian random variables. Our extension is possible because of subexponential concentration theory and the score function is of the same order as the outcome variable. These results circumvent the necessity for the use of optimal transport theory [Bobkov and Götze, 1999, Ledoux, 1999, 2001, Djellout et al., 2004, Villani, 2008] to prove Theorem 3.3 in Miao [2010].

## 3.2 Transformation conformal

Transformation parametric conformal prediction was proposed by Chernozhukov et al. [2019] to construct a  $(1 - \alpha) \times 100\%$  prediction region using the lower and upper  $\alpha/2$  quantiles of the assumed parametric



distribution. We build on this framework to propose transformation based parametric conformal prediction regions that are asymptotically minimal length at rate  $r_n$ . Let  $m(x, \psi)$  be the number of modes of  $p_\psi(\cdot|x)$  and suppose that  $\sup_{x \in \mathcal{X}, \psi \in \mathbb{N}_X} m(x, \psi) = m < \infty$ . With this specification we can construct  $C_P(x)$  as a finite union of intervals. Let  $F(\cdot|x)$  be the conditional distribution function with density  $p_\psi(\cdot|x)$  and let  $\hat{F}(\cdot|x)$  be the estimate of  $F(\cdot|x)$  with the MLE  $\hat{\psi}$  plugged in. Let  $\hat{F}^{(x,y)}(\cdot|\cdot)$  be the estimate of  $F(\cdot|\cdot)$  with the MLE corresponding to the augmented data  $\hat{\psi}^{(x,y)}$  plugged in. Let  $(X_{n+1}, Y_{n+1}) = (x, y)$  be a candidate data point.

The logic of transformation conformal prediction is as follows. We first augment the original data by adding the point  $(x, y)$ . We then estimate model parameters via maximum likelihood estimation with respect to this augmented dataset, and denote this estimator as  $\hat{\psi}^{(x,y)}$ . The estimator  $\hat{\psi}^{(x,y)}$  is then used to estimate the distribution function  $F(\cdot|\cdot)$  by  $\hat{F}^{(x,y)}(\cdot|\cdot)$  via plugin. We then transform outcomes by computing  $\hat{U}_i^{(x,y)} = \hat{F}^{(x,y)}(Y_i|X_i)$  for  $i = 1, \dots, n+1$ . Define  $\tilde{\pi}(y) = (n+1)^{-1} \sum_{i=1}^{n+1} \mathbb{1} \left\{ \sigma \left( \hat{U}_i^{(x,y)} \right) \leq \sigma \left( \hat{U}_{n+1}^{(x,y)} \right) \right\}$ , and the conformal prediction region

$$\tilde{C}^{(\alpha)}(x) = \{y : \tilde{\pi}(y) \geq \alpha'\}, \quad (5)$$

where  $0 < \alpha' \leq \alpha < 1$ .

**Lemma 4.** *Let  $\tilde{C}^{(\alpha)}(x)$  be as defined in (5). Then  $\tilde{C}^{(\alpha)}(x)$  is finite sample marginally valid.*

*Proof.* The proof follows from the proof of Lemma 2. Let  $(X_{n+1}, Y_{n+1}) \sim P$  be another independent sample. The random variables  $\hat{U}_i^{(x,y)}$ ,  $1 \leq i \leq n+1$ , are exchangeable. Then, conditioning on  $X_{n+1} = x$ , the sequence  $(\sigma(\hat{U}_1^{(x,y)}), \dots, \sigma(\hat{U}_{n+1}^{(x,y)}))$  is exchangeable. Marginal validity follows by construction.  $\square$

A particular choice of the conformity measure  $\sigma(\cdot)$  and  $\alpha'$  yields an asymptotically minimal length conformal prediction region at rate  $r_n$ . First, let  $\hat{U}_{n+1}^{(x,y)} = \hat{F}^{(x,y)}(y|x)$  be the transformed augmented outcome. We can find a minimal length  $1 - \alpha$  high density region based on the estimated density  $\hat{p}_\psi^{(x,y)}(\cdot|x)$  through solution of the optimization problem

$$\hat{A}(x) = \operatorname{argmin}_{A(x)} \nu(A(x)), \quad \text{subject to} \quad \int_{A(x)} \hat{p}_\psi^{(x,y)}(y'|x) dy' = 1 - \alpha, \quad (6)$$

where the solution  $\hat{A}(x) = \cup_{k=1}^{m'(x)} (\hat{a}_k(x), \hat{b}_k(x))$  is a union of  $m'(x)$  disjoint intervals. Because  $p_\psi(\cdot|x)$  has  $m < \infty$  modes for every  $x \in \mathcal{X}$ , the number of intervals in the union is  $m'(x) \leq m$ . Let

$$\hat{U}_{\text{lwr},k}^{(x,y)} = \hat{F}^{(x,y)}(\hat{a}_k(x)|x) \quad \text{and} \quad \hat{U}_{\text{upr},k}^{(x,y)} = \hat{F}^{(x,y)}(\hat{b}_k(x)|x)$$

be the transformed values corresponding to the lower and upper limits of the prediction set for each  $x \in \mathcal{X}$ .

Then, for each  $k$ , find intervals in the transformed observed values that contain  $(\hat{a}_k(x), \hat{b}_k(x))$ ,

$$\tilde{U}_{\text{lwr},k}^{(x,y)} = \begin{cases} \hat{U}_{\lfloor (n+1)\hat{U}_{\text{lwr},k}^{(x,y)} \rfloor}^{(x,y)} & \text{if } \lfloor (n+1)\hat{U}_{\text{lwr},k}^{(x,y)} \rfloor \geq 1 \\ 0 & \text{otherwise} \end{cases}$$

and  $\tilde{U}_{\text{upr},k}^{(x,y)} = \hat{U}_{\lceil (n+1)\hat{U}_{\text{upr},k}^{(x,y)} \rceil}^{(x,y)}$  where  $\hat{U}_{[j]}^{(x,y)}$  is the  $j$ th order statistic of the transformed values. Define the set consisting of the union of these intervals

$$\hat{B}^{(x,y)} = \cup_{k=1}^{m'(x)} (\tilde{U}_{\text{lwr},k}^{(x,y)}, \tilde{U}_{\text{upr},k}^{(x,y)}),$$

and define the conformity measure as the indicator that the value  $u$  is in the estimated high density region,  $\sigma(u) = \mathbb{1}\{u \in \widehat{B}^{(x,y)}\}$ . Let the threshold be

$$\alpha' = 1 - \sum_{k=1}^{m'(x)} \left( \frac{\lceil (n+1)\widetilde{U}_{\text{upr},k}^{(x,y)} \rceil}{n+1} - \frac{\lfloor (n+1)\widetilde{U}_{\text{lwr},k}^{(x,y)} \rfloor}{n+1} \right) \leq \alpha.$$

With these specifications, the conformal prediction region (5) becomes

$$\widehat{C}_{\text{trans}}^{(\alpha)}(x) = \left\{ y : \widehat{U}_{n+1}^{(x,y)} \in \cup_{k=1}^{m'(x)} \left( \widetilde{U}_{\text{lwr},k}^{(x,y)}, \widetilde{U}_{\text{upr},k}^{(x,y)} \right) \right\}, \quad (7)$$

where  $y \in \widehat{C}_{\text{trans}}^{(\alpha)}(x)$  implies that  $\sigma(\widehat{U}_{n+1}^{(x,y)}) = 1$ .

While this procedure may appear complicated, it is motivated by a simple observation. When the parametric model is correctly specified, the  $\widehat{U}_i^{(x,y)}$  random variables have an approximate Uniform[0, 1] distribution in finite samples and are asymptotically Uniform[0, 1]. By conducting the conformal prediction procedure in the transformed space, we can leverage distributional information from the estimated density  $\hat{p}_{\psi}^{(x,y)}(\cdot|x)$  to mimic a highest density region while ensuring nominal marginal coverage. Even when the model is misspecified, this procedure is designed to guarantee nominal marginal coverage.

We now establish that the transformation parametric conformal prediction region  $\widehat{C}_{\text{trans}}^{(\alpha)}$  is asymptotically of minimum length over  $\mathcal{X}$  at rate  $r_n$ .

**Assumption 4.** Let  $Y|X = x$  be a random variable with conditional density  $p_{\psi}(\cdot|x)$  and parameter space  $\aleph_{\mathcal{X}}$ . Let  $F(y|x)$  be the conditional distribution function corresponding to  $p_{\psi}(\cdot|x)$ . Further assume that  $|\nabla_{\psi} F(v|x)|$  is bounded for all  $v$  and all  $\psi \in \aleph_{\mathcal{X}}$ .

**Theorem 3.** Let  $Y|X = x$  be a random variable with conditional density  $p_{\psi}(\cdot|x)$  and parameter space  $\aleph_{\mathcal{X}}$ . Assume that  $p_{\psi}(\cdot|x)$  has  $m$  modes, is twice differentiable in  $\psi$ , and satisfies Assumption 2. Assume that the corresponding distribution function satisfies Assumption 4. Let  $(X_1, Y_1), \dots, (X_n, Y_n)$  be independent and identically distributed copies of  $(X, Y)$ . Let  $\psi \in \mathbb{R}^r$  and let  $\hat{\psi}$  be the MLE of  $\psi$ . Augment the sample data with a new point  $(x, y)$ , and let  $\hat{\psi}^{(x,y)}$  be the MLE of  $\psi$  with respect to the augmented data. Let  $\hat{p}_{\psi}^{(x,y)}(\cdot|x)$  be the conditional density with  $\hat{\psi}^{(x,y)}$  plugged in for  $\psi$ . Suppose that Assumption 1 holds. Let  $0 < \alpha < 1$  and  $\widehat{C}_{\text{trans}}^{(\alpha)}$  be the prediction band given by (7). Then, for a given  $\lambda > 0$ , there exists a numerical constant  $\chi_{\lambda}$  such that

$$\mathbb{P} \left[ \sup_{x \in \mathcal{X}} \nu \left\{ \widehat{C}_{\text{trans}}^{(\alpha)}(x) \Delta C_P^{(\alpha)}(x) \right\} \geq \chi_{\lambda} r_n \right] = O \left( n^{-\lambda} \right). \quad (8)$$

#### Remarks:

1. In the simple case when  $p_{\psi}(y|x)$  is unimodal, the optimization problem (6) is replaced with,

$$(\hat{a}(x), \hat{b}(x)) = \underset{(a,b)}{\operatorname{argmin}} (b - a), \quad \text{subject to} \quad \int_a^b \hat{p}_{\psi}^{(x,y)}(u|x) du = 1 - \alpha, \text{ and } b - a > 0. \quad (9)$$

In this case, we then construct  $\widehat{U}_{\text{lwr}}^{(x,y)} = \widehat{F}^{(x,y)}(\hat{a}(x)|x)$  and  $\widehat{U}_{\text{upr}}^{(x,y)} = \widehat{F}^{(x,y)}(\hat{b}(x)|x)$ , and set  $\widetilde{B}^{(x,y)} = (\widehat{U}_{\text{lwr}}^{(x,y)}, \widehat{U}_{\text{upr}}^{(x,y)})$ . From these quantities, we construct the conformity measure  $\sigma(u) = \mathbb{1}_{(\widetilde{B}^{(x,y)})}(u)$ , specify that

$$\alpha' = 1 - \left( \frac{\lceil (n+1)\widehat{U}_{\text{upr}}^{(x,y)} \rceil}{n+1} - \frac{\lfloor (n+1)\widehat{U}_{\text{lwr}}^{(x,y)} \rfloor}{n+1} \right) \leq \alpha,$$

and build  $\widetilde{C}^{(\alpha)}(x)$  with respect to these specifications as

$$\widetilde{C}^{(\alpha)}(x) = \left\{ y : \widehat{U}_{\lfloor (n+1)\widehat{U}_{\text{lwr}}^{(x,y)} \rfloor}^{(x,y)} \leq \widehat{U}_{n+1}^{(x,y)} \leq \widehat{U}_{\lceil (n+1)\widehat{U}_{\text{upr}}^{(x,y)} \rceil}^{(x,y)} \right\}, \quad (10)$$

where  $y \in \widetilde{C}^{(\alpha)}(x)$  implies that  $\sigma(\widehat{U}_{n+1}^{(x,y)}) = 1$ .

2. The proof of Theorem 3 is given in the Appendix. Our proof technique is for the  $m = 1$  case. The proof of Theorem 3 requires the concentration inequality for MLEs stated in Theorem 2. Under our proof technique the convergence rate  $r_n = \sqrt{\log(n)/n}$  of  $\widehat{C}_{\text{trans}}^{(\alpha)}$  is sharp.
3. The rates  $r_n$  is appreciably faster than that of the nonparametric conformal prediction band and the binned parametric conformal prediction region  $\widehat{C}_{n,k}^{(\alpha)}$  in (2) when the underlying density  $p_\psi(y|x)$  has parameter space  $\aleph_{\mathcal{X}}$ . The region  $\widehat{C}_{n,k}^{(\alpha)}$  converges more slowly slower than  $\widehat{C}_{\text{trans}}^{(\alpha)}$  because the former prediction region is hampered by  $n_k$ , the number of observations per bin, as the bin widths shrink at rate  $w_n$ . However, our simulation studies show that  $\widehat{C}_{n,k}^{(\alpha)}$  performs better than  $\widehat{C}_{\text{trans}}^{(\alpha)}$  when modest departures from the assumed model are present, due to its finite sample local validity guarantees.
4. The transformation parametric conformal prediction region in Chernozhukov et al. [2019] has generality beyond the context of the maximum likelihood estimation based methodology that we propose. However, explicit convergence rates for their conformal prediction rates are not given and we speculate that they would be slower for the entire class of models for which their methodology is appropriate. In addition, our methodology leverages the underlying true distribution to construct the minimal length  $(1 - \alpha) \times 100\%$  prediction region under the assumed model when on the scale of the approximately uniform random variables. This is instead of choosing the end points corresponding to the lower and upper  $\alpha/2$  quantiles of the transformed approximate uniform variables. Our focus on minimal length prediction regions and relatively fast convergence rates addresses the efficiency and utility concerns of conformal prediction in the context of regression which were raised in Cortés-Ciriano and Bender [2019].

### 3.3 Example: exponential family distributions and generalized linear models

In this Section we show that a broad class of continuous GLMs can be parameterized by  $\aleph_{\mathcal{X}}$  so that the conformal prediction methodology is applicable. The exponential families that we consider have densities  $p_\theta : \mathbb{R}^p \rightarrow \mathbb{R}$  defined by

$$p_\theta(y) = e^{\langle y, \theta \rangle - c(\theta)}. \quad (11)$$

We refer to  $y$  and  $\theta$  as the canonical statistic and canonical parameter respectively. Densities of the form  $p_\theta$  are integrated with respect to a *generating measure*  $\mu$ , where  $c(\theta)$  is the cumulant function defined as  $c(\theta) = \log \int \exp(\langle y, \theta \rangle) \mu(dy)$ . The *effective domain* of  $c$  is  $\text{dom } c = \{\theta \in \mathbb{R} : c(\theta) < +\infty\}$ . The exponential family is *full* if  $\Theta = \text{dom } c$  and is *regular* if  $\Theta$  is an open set.

We will only consider scalar outcome variables. However, we can extend our setup to multidimensional canonical statistics, the normal distribution being an example with canonical statistic  $z \mapsto (z, z^2)'$ . Thus we will assume that the canonical statistic vector lies on a one-dimensional manifold in the event that the canonical statistic is multidimensional.

When the density (11) corresponds to a generalized linear regression model we will re-parameterize  $\theta = f(x'\beta, \phi)$ , where  $f : \mathbb{R}^p \rightarrow \mathbb{R}^p$  is continuous in both arguments, the vectors  $x \in \mathbb{R}^m$  and  $\beta \in \mathbb{R}^m$  are a predictors and regression coefficients respectively, and  $\phi \in \mathbb{R}^{p-1}$  is a vector of nuisance parameters. Let  $\psi = (\beta, \phi)$  and set  $r = m + p - 1$ . We specify that the base set (main effects) of predictors have support  $\mathcal{X} \in \mathbb{R}^d$ ,  $d \leq m$ . Here we assume, without loss of generality, that  $\mathbb{E}(Y_1|x) = g^{-1}(x'\beta)$  where  $g : \mathbb{R} \rightarrow \mathbb{R}$  is a link function and  $Y_1$  is the first component of the canonical statistic vector. As an example of this reparameterization, consider the simple linear regression model with homoskedastic normal errors with variance given by  $\sigma^2$ . In this example  $d = m = 1$ ,  $r = 2$ , and  $\phi = \sigma^2$ . The link function  $g$  is taken to be the identity function and  $\mu_x = \mathbb{E}(Y|x) = x'\beta$ .

The reparameterized density corresponding to the generalized linear regression model is then

$$p_\psi(y|x) = \exp [\langle y, f(x'\beta, \phi) \rangle - c \{f(x'\beta, \phi)\}] \quad (12)$$

with respect to generating measure  $\mu$ . We will further assume that  $\mathcal{X}$  is bounded and that the exponential family is full with parameter space given by  $\Theta_{\mathcal{X}} = \{\beta \in \mathbb{R}^m, \phi \in \mathbb{R}^{p-1} : c \{f(x'\beta, \phi)\} < \infty, \text{ for all } x \in \mathcal{X}\}$ . Consider the multiple linear regression model with homoskedastic normal errors with variance given by  $\sigma^2$ . Here we have  $f(x'\beta, \phi) = (x'\beta, \sigma^2)'$  and  $\Theta_{\mathcal{X}} = \{(\beta', \sigma^2)' : \beta \in \mathbb{R}^m, \sigma > 0, x \in \mathcal{X}\}$ . We will assume that the link function of the generalized linear regression model is known, the model is correctly specified, and that  $\hat{\beta}$  is a  $\sqrt{n}$ -consistent estimator of the regression coefficients  $\beta$ . All of the continuous exponential families implemented in the `glm` function in R have densities that can be parameterized as (12). Moreover, we have that  $\Theta_{\mathcal{X}} \subseteq \mathfrak{N}_{\mathcal{X}}$  since,

$$\begin{aligned} \frac{\partial}{\partial \psi} \log p_\psi(y|x) &= \frac{\partial}{\partial \psi} (\langle y, f(x'\beta, \phi) \rangle - c \{f(x'\beta, \phi)\}) \\ &= \left( \frac{\partial f(x'\beta, \phi)}{\partial \psi} \right) \left( y - \frac{\partial}{\partial f(x'\beta, \phi)} c \{f(x'\beta, \phi)\} \right) = O(y), \end{aligned}$$

and  $M_{Y,x,\psi}(t)$  exists for all  $t$  in a neighborhood of 0, for all  $x \in \mathcal{X}$ , and  $\psi \in \Theta_{\mathcal{X}}$ . Therefore our conformal prediction regions are appropriate for the GLMs parameterized in this Section. We show that our GLM parameterization satisfies Assumptions 2 and 3 in the Supplementary Materials.

We describe some related work on conformal prediction techniques for regression settings in the next sections. Finite-sample performance of our parametric conformal prediction region and these related methods is assessed in Section 5.

## 4 Existing conformal prediction techniques in regression

### 4.1 The nonparametric kernel estimator

Lei and Wasserman [2014] proposed a nonparametric conformal prediction region for continuous outcomes that satisfies finite sample local validity. Partitioning of the predictor space is performed so that the nonparametric conformal prediction region within each partition achieves finite sample marginal validity. When we

restrict the partition to be formed of equilateral cubes, we let the widths of these cubes decrease at rate  $w_n$ . Let  $n_k = \sum_{i=1}^n \mathbb{1}(X_i \in A_k)$ . Let  $K(\cdot)$  be a non-negative kernel function. The estimated local marginal density of  $Y$  is  $\tilde{p}(v|A_k) = (n_k h_n)^{-1} \sum_{i=1}^n \mathbb{1}\{X_i \in A_k\} K((Y_i - v)/h_n)$  where  $h_n$  is the bandwidth. The density estimate given a new pair  $(x, y) \in A_k \times \mathbb{R}$  is

$$\tilde{p}^{(x,y)}(v|A_k) = \frac{n_k}{n_k + 1} \tilde{p}(v|A_k) + \frac{1}{(n_k + 1)h_n} K\left(\frac{v - y}{h_n}\right).$$

The local conformity rank is then

$$\tilde{\pi}_{n,k}(x, y) = \frac{1}{n_k + 1} \sum_{i=1}^{n+1} \mathbb{1}(X_i \in A_k) \mathbb{1}\left\{\tilde{p}^{(x,y)}(Y_i|A_k) \leq \tilde{p}^{(x,y)}(Y_{n+1}|A_k)\right\},$$

and the conformal prediction band is  $\widehat{C}_{\text{loc}}^{(\alpha)}(x) = \{y : \tilde{\pi}_{n,k}(x, y) \geq \alpha\}$ , for all  $x \in A_k$ . The intuition for constructing the conformal prediction region in this manner is that, asymptotically, the width  $w_n$  shrinks so that the conditional distributions  $Y|X = x$  for all  $x \in A_k$  become very similar to that of  $Y|X = x$  for any particular  $x \in A_k$ . Lei and Wasserman [2014] provided that rate of convergence for which  $\widehat{C}_{\text{loc}}^{(\alpha)}(x)$  is asymptotically of minimal length. In the Supplementary Materials we show that when the underlying model is a GLM,  $\widehat{C}_{\text{loc}}^{(\alpha)}(x)$  is asymptotically of minimal length at rate  $w_n$ .

The nonparametric conformal prediction region is desirable when the underlying distribution is unknown or analytically intractable. However, its convergence is slow when compared with its parametric counterpart. Our analytical results and simulation studies show that the parametric conformal prediction region is preferable to the nonparametric conformal prediction region when the GLM is reasonably close to correctly specified. In the Supplementary Materials, we verify that the nonparametric conformal region of Lei and Wasserman [2014] is appropriate for the class of GLMs that we consider.

## 4.2 Normalized residuals

Lei et al. [2018] proposed a prediction region obtained from conformal prediction for residuals, which is appropriate when errors are symmetric about the mean function  $\mu(x)$ . Lei et al. [2018, Section 5.2] also proposed an extension of their conformal prediction procedure that is appropriate when the errors about  $\mu(x)$  exhibit heterogeneity but remain symmetric. This extension involves a dispersion function  $\rho(x)$  that captures the changing variability across  $x$  and is used to weight the residuals so that these weighted residuals have the same magnitude, on average, across  $x$ . The conformal procedure of Lei et al. [2018, Section 5.2], denoted in this paper as the least squares locally weighted (LSLW) prediction region, proceeds as follows. When the mean regression estimator  $\hat{\mu}(x)$  of  $\mu(x)$  is a symmetric function of the data points, augment the original data with a new point  $(x, y)$ , and estimate the mean function  $\hat{\mu}_y$  and the dispersion function  $\hat{\rho}_y$  with respect to the augmented data.

Define the normalized absolute residuals as  $R_{y,i} = |Y_i - \hat{\mu}_y(X_i)|/\hat{\rho}_y(X_i)$ , for  $i = 1, \dots, n+1$ . The normalized absolute residual  $R_{y,n+1}$  is an example of an anti-conformity measure, in which a low value of  $R_{y,n+1}$  indicates agreement between  $y$  and the estimated regression function. As in Lei et al. [2018], we specify the dispersion function as the conditional mean absolute deviation of  $(Y - \mu(X))|X = x$  as a function of  $x$ . Let  $\pi_{\text{LSLW}}(y) = (n+1)^{-1} \sum_{i=1}^{n+1} \mathbb{1}\{R_{y,i} \leq R_{y,n+1}\}$  be the proportion of points with normalized residuals smaller than the proposed normalized residual  $R_{y,n+1}$ . Define the LSLW conformal prediction regions as  $C_{\text{LSLW}}^{(\alpha)}(x) = \{y \in \mathbb{R} : (n+1)\pi_{\text{LSLW}}(y) \leq \lceil(1-\alpha)(n+1)\rceil\}$ . The least squares (LS) conformal

prediction region is constructed as in  $C_{\text{LSLW}}^{(\alpha)}(x)$  with no weighting with respect to residuals,  $\hat{\rho}_y = 1$ . These conformal prediction regions achieve finite sample marginal validity as a consequence of exchangeability of the data and symmetry of  $\hat{\mu}_y$  in its arguments [Lei et al., 2018].

In our simulation studies we find that this approach to conformal prediction performs well when there are slight deviations from the symmetric error assumption. However, in such settings these conformal prediction regions can be larger than desired, give larger than desired coverage, or give larger prediction errors than other conformal prediction regions. Large departures from the symmetric errors assumption prove problematic for the LSLW conformal prediction region.

## 5 Simulation study

We consider three simulation settings to evaluate the performance of conformal prediction regions under correct model specification and model misspecification. These simulation settings are:

- A) Gamma regression with  $\beta = [1.25, -1]'$  and  $n = 150$ . Data are generated from a Gamma regression model, and the parametric conformal and highest density prediction regions are correctly specified. A cubic regression model is assumed for the LS and LSLW conformal prediction regions.
- B) Gamma regression with  $\beta = [0.5, 1]'$  and  $n = 150$ . Data are generated from a Gamma regression model, and a cubic regression model with homoskedastic normal errors is assumed for the highest density prediction region and the misspecified parametric, LS, and LSLW conformal prediction regions.
- C) Simple linear regression with  $\beta = [2, 5]'$ , and normal errors with constant variance  $\sigma^2 = 1$ . Results are considered for sample sizes  $n \in \{150, 250, 500\}$ . In this setting the regression model is correctly specified for the highest density prediction region and the parametric, LS, and LSLW conformal prediction regions.

The prediction regions under consideration are the transformation based parametric, binned parametric, binned nonparametric, LSLW, and LS conformal prediction regions and the highest density (HD) prediction region under an assumed model. The transformation based parametric, binned parametric, and binned nonparametric are fit using the `conformal.glm` R package [Eck, 2018] with default settings employed which specifies line search precision at 0.005. The LSLW and LS are fit using the `conformalInference` R package [Tibshirani, 2016] with the default settings employed which specifies that the number of grid points is 100. The HD prediction region is fit using using the `HDInterval` R package [Meredith and Kruschke, 2018]. Following the bin width asymptotics of Lei and Wasserman [2014], the number of bins used to form the binned parametric and nonparametric conformal prediction regions is 2 when  $n = 150$  and 3 when  $n = 250, 500$ . All simulations correspond to univariate regressions and the predictor variables were generated as  $X \sim U(0, 1)$ . Figure 2 shows four example conformal regions for simulation setting A, B, and C with  $n = 150$ .

Several diagnostic measures are used to compare conformal prediction regions. These diagnostic measures compare prediction regions by their prediction error, volume, and coverage properties. Our prediction error diagnostic metric will be an average of the squared distances of observations outside of the prediction region

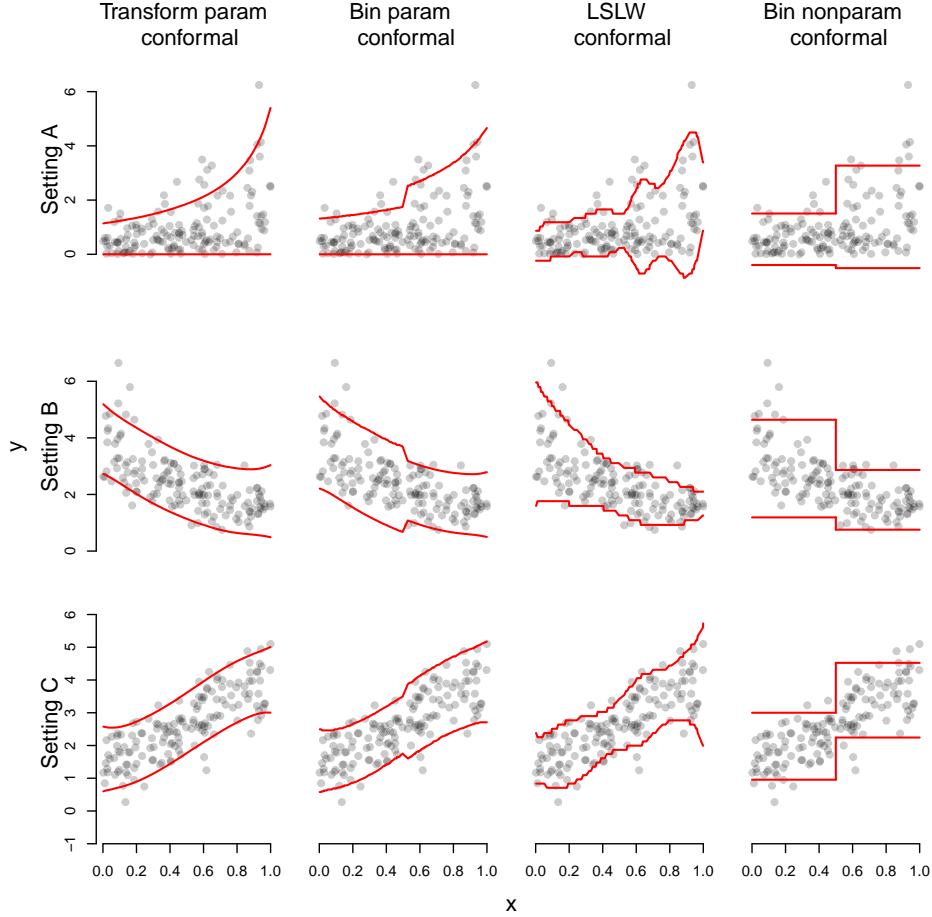


Figure 2: Illustration of conformal prediction regions. The top, middle, and bottom rows correspond to simulation setting A with shape parameter equal to 1, simulation setting B with shape parameter equal to 10, and simulation setting C respectively. The first column depicts the transformation based parametric conformal prediction region which is misspecified in row 2. The second column depicts the binned parametric conformal prediction region which is misspecified in row 2. The third column depicts the locally weighted conformal prediction region. The fourth column depicts the nonparametric conformal prediction region.

to the closest boundary of the prediction region, averaged over all observations. An observation that falls within the prediction region has an error of 0. More formally this prediction error metric is

$$\text{prediction error} = n^{-1} \sum_{i=1}^n \mathbb{1} \left\{ Y_i \notin C^{(\alpha)}(X_i) \right\} \left( \min_{j=1, \dots, m_i} \{ \min\{|Y_i - a_{i,j}|, |Y_i - b_{i,j}|\} \} \right)^2,$$

where  $a_{i,j}$  and  $b_{i,j}$  are, respectively, the lower and upper boundaries of possible  $j = 1, \dots, m_i$  disjoint intervals forming the prediction region.

The volume of each prediction region will be estimated by the average of the upper boundary minus the lower boundary across observed  $\mathcal{X}$ , written as

$$\text{area} = n^{-1} \sum_{i=1}^n \sum_{j=1}^{m_i} (b_{i,j} - a_{i,j}).$$

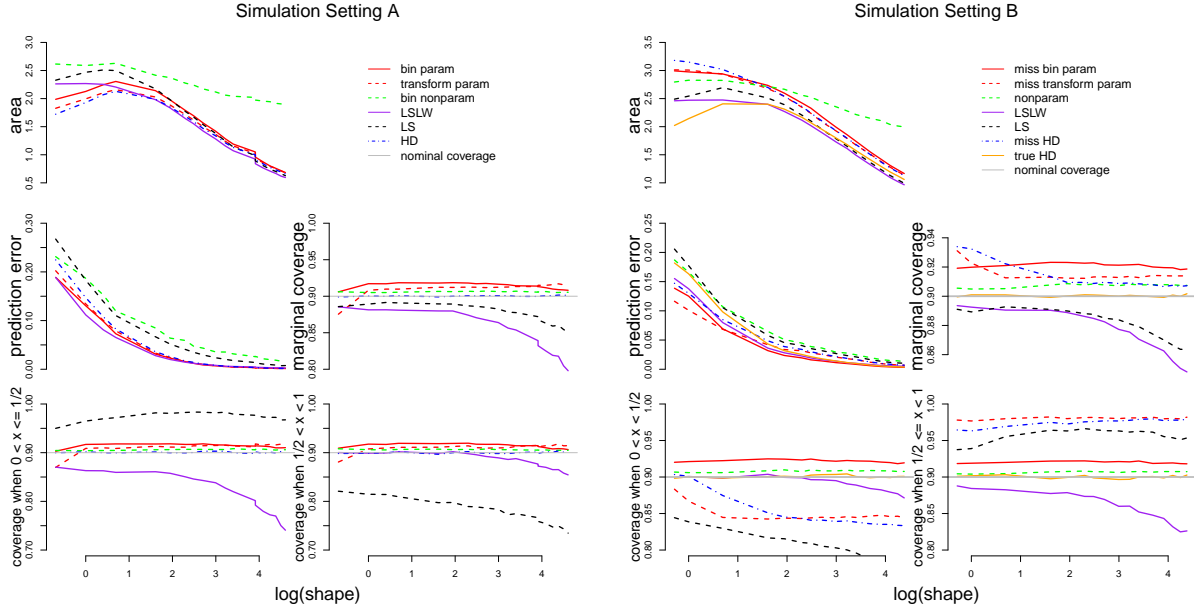


Figure 3: Area, prediction error, and bin-wise coverage for parametric, nonparametric, LS, LSLW conformal prediction region, and the highest density prediction region for Gamma GLM regression with  $n = 150$  and  $\alpha = 0.1$ . Simulation setting A is shown at left, and setting B at right. The average of 250 samples at each shape parameter value in these simulation settings form the lines that are depicted in both plots of this figure.

To assess finite sample marginal validity we calculate the proportion of responses that fall within the prediction region. To assess finite sample local validity with respect to binning we first bin the predictor data and then, for each bin, we calculate the proportion of responses that fall within the prediction region. The same procedure is used to assess finite sample conditional validity, but we use a much finer binning regime than what was used to assess finite sample local validity.

In our simulations, we find that the parametric conformal prediction regions perform well even when the model is moderately misspecified. By construction, the binned parametric conformal prediction region, along with the binned nonparametric conformal prediction region, maintains finite sample local validity with respect to binning as seen in the bottom row of both plots in Figure 3 and Table 1. However, these prediction regions have different shapes conditional on  $x$ , as seen in Figure 2, and give different prediction errors as seen in the top row of both plots in Figure 3 and Table 1. Both parametric conformal prediction regions adapt naturally to the data when the model is correctly specified or when modest deviations from the specified model are present. However, large deviations from model misspecification are not handled well as seen in the top row of the right hand side of Figure 3, although the transformation and binned parametric conformal prediction region give nominal marginal and local coverage respectively as seen in the middle row in the right hand side of Figure 3. Note that the default precision allowed the transformation based parametric conformal prediction region to exhibit undercoverage for small values of  $x$ , and note overcoverage for large values of  $x$  in the bottom row of the right hand side of Figure 3. On the other hand, the nonparametric conformal prediction region does not adapt well to data obtained from a Gamma regression model, and the former is not data adaptive in our linear regression setting.

The LS conformal prediction region obtains marginal validity [Lei et al., 2018] but performs poorly when



		OLS trans conformal	OLS bin conformal	bin nonparametric conformal	LS conformal	LSLW conformal	HD region
$n = 150$	marginal coverage	0.911	0.919	0.911	0.878	0.883	0.904
	local coverage when $0 < x < 1/2$	0.912	0.918	0.911	0.878	0.886	0.903
	local coverage when $1/2 \leq x < 1$	0.909	0.92	0.911	0.878	0.881	0.904
	area	1.88	1.994	2.408	1.775	1.782	1.872
	prediction error	0.01	0.007	0.011	0.012	0.011	0.01
$n = 250$	marginal coverage	0.908	0.916	0.909	0.875	0.878	0.902
	local coverage when $0 < x < 1/3$	0.9	0.916	0.909	0.87	0.882	0.896
	local coverage when $1/3 \leq x < 2/3$	0.914	0.913	0.909	0.879	0.876	0.907
	local coverage when $2/3 \leq x < 1$	0.909	0.92	0.909	0.877	0.876	0.904
	area	1.877	1.974	2.139	1.751	1.754	1.864
prediction error	0.009	0.007	0.01	0.013	0.012	0.01	
$n = 500$	marginal coverage	0.908	0.907	0.904	0.875	0.873	0.902
	local coverage when $0 < x < 1/3$	0.911	0.908	0.906	0.878	0.875	0.905
	local coverage when $1/3 \leq x < 2/3$	0.907	0.907	0.904	0.874	0.871	0.902
	local coverage when $2/3 \leq x < 1$	0.905	0.907	0.904	0.874	0.875	0.899
	area	1.886	1.904	2.098	1.735	1.731	1.86
prediction error	0.009	0.009	0.011	0.013	0.013	0.01	

Table 1: Diagnostics for conformal prediction regions for linear regression models with normal errors and constant variance. Local and marginal coverage properties, areas, and prediction errors are presented for the transformation based and binned parametric conformal prediction regions, binned nonparametric conformal prediction region, LS conformal prediction region, LSLW conformal prediction region, and HD prediction region.

deviations about the estimated mean function are either not symmetric, not constant, or both. When heterogeneity is present, the LS conformal prediction region exhibits undercoverage in regions where variability about the mean function is large and over-coverage in regions where variability about the mean function is small. Clear evidence of these features are seen in Figure 3 and 2. This conformal prediction region is very sensitive to model misspecification. The LSLW conformal prediction region also guarantees marginal validity [Lei et al., 2018, Section 5.2], although our simulations reveal that the default software implementation struggles to guarantee this in practice. That being said, the LSLW region appears to exhibit flexibility under mild model misspecification as evidenced in the second row of Figure 2 and our Supplementary Materials. This region is far less sensitive to model misspecification than the LS conformal prediction region, and it performs well under modest model misspecification. However, the LSLW conformal prediction region is not appropriate when deviations about an estimated mean function are obviously not symmetric, as evidenced in the top row of Figure 2. Results from additional simulations corresponding to settings A and B are provided in the Supplementary Materials. The findings from these additional simulations are consistent with the conclusions of the simulations presented in this Section.

## 6 Predicting the risk of diabetes

Diabetes is a group of metabolic diseases associated with long-term damage, dysfunction, and failure of different organs, especially the eyes, kidneys, nerves, heart, and blood vessels [American Diabetes Association, 2010]. In 2017 approximately 5 million adult deaths worldwide were attributable to diabetes; global healthcare expenditures on people with diabetes are estimated USD 850 billion [Cho et al., 2018]. Diabetes remains undiagnosed for an estimated 30% of the people who have the disease [Heikes et al., 2008]. One way to address the problem of undiagnosed diabetes is to develop simple, inexpensive diagnostic tools that can identify people who are at high risk of pre-diabetes or diabetes using only readily-available clinical or

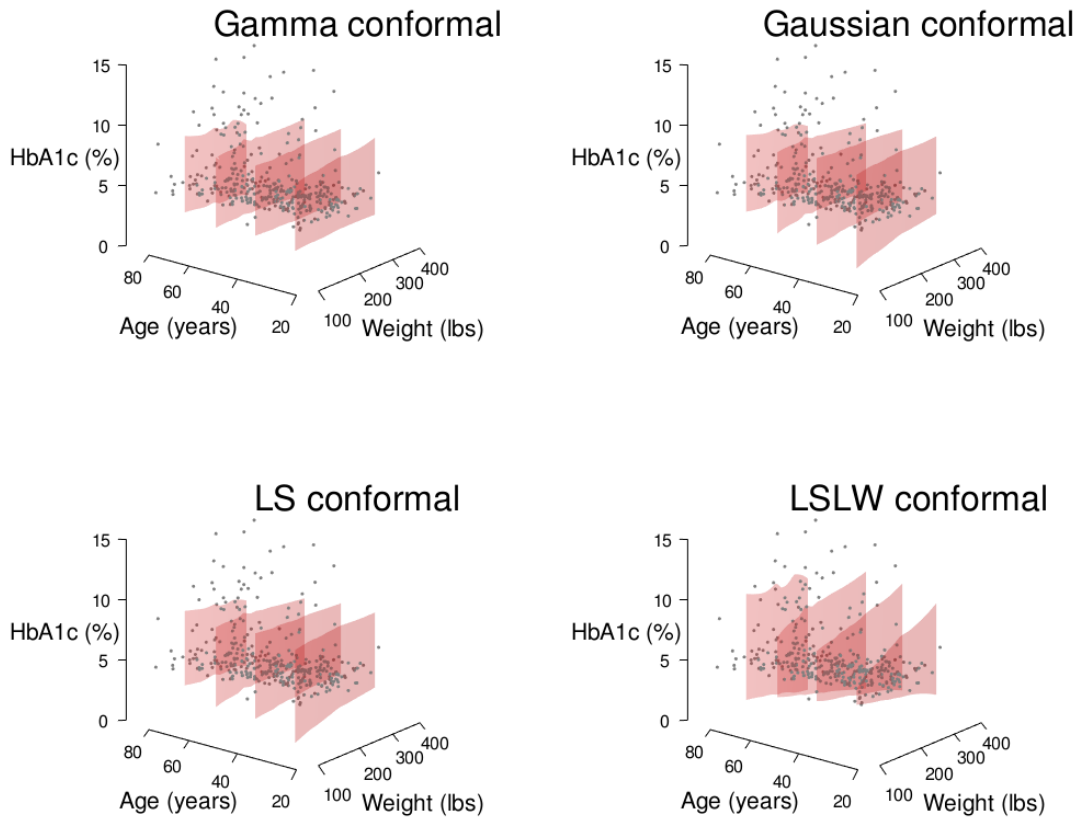


Figure 4: Conformal prediction regions for glycosylated hemoglobin projected onto the age and weight predictor axes. Upper and lower bounds of the conformal prediction region are loess smoothed for visual appearance.

demographic information [Heikes et al., 2008].

We examine the influence of several variables on blood sugar, or glycosylated hemoglobin percentage (also known as HbA1c), an important risk factor for diabetes. A glycosylated hemoglobin value of 6.5% can be used as a cutoff for positive diagnosis of diabetes [World Health Organization, 2011]. We predict an individual’s glycosylated hemoglobin from their height, weight, age, and gender, all of which are easy to measure, inexpensive, and do not require any laboratory testing. The data in this analysis come from a population-based sample of 403 rural African-Americans in Virginia [Willems et al., 1997], taken from the `faraway` R package [Faraway, 2016]. We considered a gamma regression model that only includes linear terms for each covariate, a linear regression model with homoskedastic normal errors and the same linear terms for each covariate, and a linear regression model with homoskedastic normal errors that also included quadratic terms for each covariate. Of these considered models, the gamma regression model fit the data best: it had the lowest AIC value and gives the best predictive performance as measured by the sum of squares prediction error.

Based on these covariates, conformal prediction regions provide finite sample valid prediction regions for glycosylated hemoglobin that may be useful for diagnosing diabetes in this study population. Six conformal prediction regions are considered for predicting glycosylated hemoglobin percentage. These conformal prediction regions are the binned and transformation parametric conformal prediction region with a Gamma model fit, the binned and transformation parametric conformal prediction region with a Gaussian model fit, the LS conformal prediction region, and the LSLW conformal prediction region. All conformal prediction regions correspond to models that only include linear terms for each of the covariates. The binned Gamma and Gaussian parametric conformal prediction regions were computed with binning across the binary gender factor variable, the predictor space is partitioned across genders. However, no additional binning structure within the levels of gender was employed.

	Gamma trans conformal	Gaussian trans conformal	Gamma bin conformal	Gaussian bin conformal	LSLW conformal	LS conformal
marginal coverage	0.901	0.924	0.909	0.906	0.880	0.888
volume	7.656	8.560	7.349	7.730	8.574	7.103
pred error	0.653	0.425	0.931	0.849	0.803	1.012
avg.cond.coverage	0.856	0.888	0.874	0.849	0.863	0.827

Table 2: Diagnostics for prediction regions. Marginal coverage ( $\alpha = 0.10$ ), prediction region volume, prediction error, and average conditional coverage make up the first four rows.

Diagnostics from the six conformal prediction regions are depicted in Table 6. The error tolerance for all prediction regions was set at  $\alpha = 0.10$ . We see that parametric conformal prediction regions maintain their advertised finite sample marginal validity for the predictions of glycosylated hemoglobin. These prediction regions provide a balance between marginal coverage, size, prediction error, and average conditional coverage (the average of the coverage probabilities taken over small subregions of the predictor space). The transformation Gamma conformal prediction region balances these criteria particularly nicely. This prediction region is relatively small, has relatively small prediction error, and it gives near nominal desired coverage. This finding is expected when the underlying estimated density used as the parametric conformity measure is a good approximation of the data generating model.

Plots of three dimensional conformal prediction region are displayed in Figure 4. These plots are projections of each conformal prediction regions to the age (in years), weight (in pounds), and glycosylated hemoglobin percentage three dimensional space.

## 7 Discussion

The finite sample validity properties of conformal prediction regions have been verified in broader methodological contexts, including support vector machines, ridge regression, nearest neighbor regression, neural networks, and decision decision trees [Vovk et al., 2005, Gammerman and Vovk, 2007, Papadopoulos et al., 2011, Vovk, 2012]. While any conformity measure function will achieve finite sample validity, a careful choice may make the returned conformal prediction regions more useful in applications [Papadopoulos et al., 2011]. The developments of conformal prediction in the machine learning literature show how empirically successful prediction methods in machine learning can be hedged to give valid predictions in finite samples [Gammerman and Vovk, 2007]. The developments of conformal prediction in the statistics literature show that specification of the conformity measure to incorporate knowledge about the data generating

process can lead to conformal prediction regions which are also asymptotically of minimal length [Lei and Wasserman, 2014, Dunn and Wasserman, 2018]. Our parametric conformal prediction regions for parametric regression models falls within this line of research, which addresses efficiency concerns of conformal prediction methodology raised by Cortés-Ciriano and Bender [2019]. This line of research shows that when uncertainty about point predictions is considered, regression modeling provides smaller prediction regions when we require regions to guarantee valid finite sample coverage.

Because GLMs are widely used by empiricists conducting regression analyses, parametric conformal prediction for GLM regression therefore may offer an appealing compromise for the applied researcher: when the GLM is correctly specified, conformal prediction regions are asymptotically minimal, finite sample local and marginal validity holds, and the rate of convergence is fast; when the GLM is incorrectly specified, asymptotic minimality is not guaranteed, but local finite sample validity still holds by construction. Researchers who currently use GLMs to compute prediction intervals for the mean regression function may be able to easily integrate conformal prediction into their data analysis workflow, since specification and fitting of the GLM is unchanged. A software package that accompanies this paper implements the parametric and nonparametric conformal prediction regions [Eck, 2018].

The robustness properties of conformal prediction come at a substantial computational cost [Vovk, 2012]. In our software implementation of the conformal methodology, two line searches are performed to determine the boundaries of the possibly disjoint conformal prediction region at every point at which a prediction region is desired. The conformity scores must be recomputed with respect to augmented data at every iteration of these line searches. This involves refitting the parametric model to augmented data at every iteration of the line search to construct the parametric conformal prediction region. Furthermore, when sample sizes are very large, conformal prediction may not offer much additional benefit beyond the parametric conditional prediction regions available in popular software packages for regression. However, when sample sizes are moderate, conformal prediction may substantially outperform traditional methods in terms of finite sample marginal, local, and conditional coverage.

The asymptotic optimality properties of parametric conformal prediction regions follow from our concentration inequality for maximum likelihood estimation stated in Theorem 2. We conjecture that a similar concentration inequality may hold for random variables whose score functions do not have functional subexponential behavior (see Appendix), and/or a non-existent MGF. This concentration inequality will likely induce convergence rates that are slower than  $\sqrt{\log(n)/n}$ . Dunn and Wasserman [2018] showed that finite sample validity holds in the presence of random effects. We expect that asymptotic optimality properties for parametric conformal prediction regions can be extended to their settings and to the class of generalized linear mixed models.

**Supplementary Materials:** Additional simulation results are available in the accompanying Supplementary Materials document (appended at the end of the main text). An accompanying R package is available at <https://github.com/DEck13/conformal.glm> [Eck, 2018]. A technical report that includes the data and all of the code necessary to reproduce the findings, tables, and figures in this manuscript is available at <https://github.com/DEck13/conformal.glm/tree/master/techreport>.

**Acknowledgments:** We are grateful to Peter M. Aronow, Karl Oskar Ekvall, Jing Lei, Aaron J. Molstad, Molly Offer-Westort, Cyrus Samii, Fredrik Sävje, and Larry Wasserman for helpful comments. This work was supported by NIH grant NICHD 1DP2HD091799-01.

## Appendix: Mathematical details

### Subexponential random variables

The following definition and two lemmas are taken from Wainwright [2019, Chapter 2].

**Definition 4.** A mean zero random variable  $Y$  is said to be subexponential with parameters  $(\tau^2, b)$  if  $\mathbb{E}\{\exp(tY)\} \leq \exp(t^2\tau^2/2)$  for all  $|t| \leq 1/b$ .

**Lemma 5.** For a mean zero random variable  $Y$ , the following are equivalent: (a)  $Y$  is subexponential with parameters  $(\tau^2, b)$ ; (b) There is a positive number  $c_0 > 0$  such that  $\mathbb{E}(e^{tY}) < \infty$  for all  $|t| < c_0$ ; (c)  $\mathbb{P}\{Y \geq \mathbb{E}(Y) + t\} \leq \max\left(e^{-\frac{t^2}{2\tau^2}}, e^{-\frac{t}{2b}}\right)$ .

**Lemma 6.** Let  $Y_i$  be independent mean zero subexponential random variables with parameters  $(\tau_i^2, b_i)$ . Then  $\sum_{i=1}^n Y_i$  is subexponential with parameters  $(\sum_{i=1}^n \tau_i^2, b_\star)$  where  $b_\star = \max_i(b_i)$  and

$$\mathbb{P}\left\{\left|\frac{1}{n}\sum_{i=1}^n Y_i\right| \geq t\right\} \leq 2 \exp\left\{-\min\left(\frac{nt^2}{2n^{-1}\sum_{i=1}^n \tau_i^2}, \frac{nt}{2b_\star}\right)\right\}. \quad (13)$$

Let  $l_\psi(Y|x) = \log p_\psi(Y|x)$  be the log likelihood for the random variable  $Y|X = x$  and let  $\nabla_\psi l_\psi(Y|x)$  be the corresponding score function. We will now motivate the construction of the parameter space  $\mathfrak{N}_\mathcal{X}$ . This parameter space requires a notion of functional subexponential that we will now define and examine.

**Definition 5** (functional subexponential). Let  $Y$  be a random variable and suppose that  $f : \mathbb{R} \rightarrow \mathbb{R}$  is a function such that  $E\{f(Y)\} = 0$ . We say that  $f$  is functional subexponential with respect to  $Y$  with parameters  $(\tau^2, b)$  if  $\mathbb{E}\{\exp(tf(Y))\} \leq \exp(t^2\tau^2/2)$  for all  $|t| \leq 1/b$ .

**Definition 6** (multivariate functional subexponential). Let  $Y$  be a random variable and suppose that  $f : \mathbb{R} \rightarrow \mathbb{R}^r$  is a function such that  $E\{f(Y)\} = 0$ . We say that  $f$  is multivariate functional subexponential with respect to  $Y$  with parameters  $(\tau^2, b)$  if  $\mathbb{E}\{\exp(t'f(Y))\} \leq \exp(|t|^2\tau^2/2)$  for all  $|t| \leq 1/b$ .

**Lemma 7.** Let  $Y$  be a random variable and suppose that  $f : \mathbb{R} \rightarrow \mathbb{R}^r$  is a function such that  $E\{f(Y)\} = 0$ . Then  $f(Y)$  is multivariate functional subexponential with respect to  $Y$  if and only if the components of  $f(Y)$  are functional subexponential with respect to  $Y$ .

*Proof.* First suppose that  $f(Y)$  is multivariate functional subexponential with respect to  $Y$ . Let  $s_j$  be the  $r$  dimensional zeros vector with an  $s$  in the  $j$ th component. Then  $\mathbb{E}\{\exp(sf_j(Y))\} \leq \exp(s^2\tau^2/2)$  for all  $|s| \leq 1/b$  where  $f_j(Y)$  is the  $j$ th component of  $f(Y)$ . It follows that the components of  $f(Y)$  are functional subexponential with respect to  $Y$ .

Now suppose that the components of  $f(Y)$  are functional subexponential with respect to  $Y$  with parameters  $(\tau_j^2, b_j)$ ,  $j = 1, \dots, r$ . Let  $b = \max(b_j)$  and  $\tau = \max(\tau_j)$ . Then  $\mathbb{E}\{\exp(sf_j(Y))\} \leq \exp(s^2\tau^2/2)$  holds for all  $|s| \leq 1/b$ . Now pick a vector  $t \in \mathbb{R}^r$  such that  $|t| < 1/b$ . Then by multiple applications of Cauchy

Scharwz and the supposition that the components of  $f(Y)$  are functional subexponential we have that

$$\begin{aligned}\mathbb{E} \left\{ \exp(t' f(Y)) \right\} &= \mathbb{E} \left\{ \prod_{j=1}^r \exp(t_j f_j(Y)) \right\} \leq \prod_{j=1}^r \mathbb{E} \left\{ \exp(2^j t_j f_j(Y)) \right\}^{1/2^j} \\ &\leq \prod_{j=1}^r \mathbb{E} \left\{ \exp(2^{2j-1} t_j^2 \tau^2) \right\}^{1/2^j} \leq \prod_{j=1}^r \mathbb{E} \left\{ \exp(2^j t_j^2 \tau^2 / 2) \right\} \leq \exp \left( \frac{|t|^2 2^r \tau^2}{2} \right),\end{aligned}$$

for all  $|t| < 1/b$ . Set  $\tau' = \tau 2^{r/2}$ , then  $f(Y)$  is multivariate subexponential with respect to  $Y$  with parameters  $(\tau', b)$ . The conclusion follows.  $\square$

The following Lemma is the key piece that ties  $\aleph_{\mathcal{X}}$  together with the concentration inequality given in Theorem 2.

**Lemma 8.** *Let  $Y|X = x$  be a random variable and suppose that the moment generating function  $M_{Y,x,\psi}(t)$  exists for all  $t$  in a neighborhood of 0. Let  $p_\psi(y|x)$  be the corresponding probability density function with parameter vector  $\psi \in \mathbb{R}^r$ . Assume that  $p_\psi(y|x)$  is differentiable in both  $y$  and  $\psi$ . Then the score function  $\nabla_\psi \log p_\psi(Y|x)$  is functional subexponential with respect to  $Y|X = x$  provided that  $\nabla_\psi \log p_\psi(y|x) = O(y)$ .*

*Proof.* Let  $\nabla_{\psi_j} \log p_\psi(y|x)$  be the  $j$ th component of  $\nabla_\psi \log p_\psi(y|x)$ . Then,

$$\begin{aligned}\mathbb{E} \left\{ \exp(t_j \nabla_{\psi_j} \log p_\psi(Y|x)) \right\} &= \int \exp(t_j \nabla_{\psi_j} \log p_\psi(y)) p_\psi(y|x) dy \\ &= \int \exp \left\{ t_j y \left( \frac{\nabla_{\psi_j} \log p_\psi(y|x)}{y} \right) \right\} p_\psi(y|x) dy < \infty,\end{aligned}$$

for all  $t_j$  in a neighborhood about 0, and all  $j = 1, \dots, r$ . The same argument as that in Appendix B of Wainwright [2019] implies that the score function  $\nabla_{\psi_j} \log p_\psi(Y)$  is functional subexponential with respect to  $Y|X = x$ . Our conclusion follows from Lemma 7.  $\square$

## Concentration results

We can now prove Theorem 2 from Lemma 8 and our developed notion of functional subexponential random variables.

*Proof of Theorem 2.* From the mean-value theorem, there exists some  $\hat{\psi}_1$  such that  $\hat{\psi}_{1,j} \in (\psi_j \wedge \hat{\psi}_j, \psi_j \vee \hat{\psi}_j)$ ,  $j = 1, \dots, r$ , which satisfies

$$-\nabla_\psi l_n(\psi) = \nabla_{\hat{\psi}_1}^2 l_n(\hat{\psi}_1)(\hat{\psi} - \psi).$$

Rearranging the above yields

$$\sqrt{n}(\hat{\psi} - \psi) = -\sqrt{n} \left\{ \nabla_{\hat{\psi}_1}^2 l_n(\hat{\psi}_1) \right\}^{-1} \nabla_\psi l_n(\psi)$$

where the inverse exists almost surely when  $n > r$ . We see that

$$\begin{aligned} \left| \sqrt{n}(\hat{\psi} - \psi) \right| &= \left| \sqrt{n} \left\{ \nabla_{\psi}^2 l_n(\hat{\psi}_1) \right\}^{-1} \nabla_{\psi} l_n(\psi) \right| \\ &\leq \left| \sqrt{n} \left\{ \nabla_{\psi}^2 l_n(\psi) \right\}^{-1} \nabla_{\psi} l_n(\psi) \right| + |a_n| \\ &\leq \sqrt{n} \left\| \left\{ \nabla_{\psi}^2 l_n(\psi) \right\}^{-1} \right\|_1 |\nabla_{\psi} l_n(\psi)| + |a_n|, \end{aligned}$$

where  $\|\cdot\|_1$  is the induced  $k$ -norm for a matrix with  $k = 1$  and

$$|a_n| = \left| \sqrt{n} \left[ \left\{ \nabla_{\psi}^2 l_n(\hat{\psi}_1) \right\}^{-1} - \left\{ \nabla_{\psi}^2 l_n(\psi) \right\}^{-1} \right] \nabla_{\psi} l_n(\psi) \right|.$$

Choose some  $0 < a_\lambda < A_\lambda$  and let  $B_\lambda = A_\lambda - a_\lambda$ . Then for  $n$  sufficiently large,

$$\begin{aligned} \mathbb{P} \left\{ \sqrt{n} |\hat{\psi} - \psi| \geq A_\lambda \sqrt{\log(n)} \right\} &\leq \mathbb{P} \left\{ \sqrt{n} \left\| \left\{ \nabla_{\psi}^2 l_n(\psi) \right\}^{-1} \right\|_1 |\nabla_{\psi} l_n(\psi)| + |a_n| \geq A_\lambda \sqrt{\log(n)} \right\} \\ &\leq \mathbb{P} \left( \left| \nabla_{\psi} l_n(\psi) \right| \geq \sqrt{\frac{\log(n)}{n}} \frac{B_\lambda}{\left\| \left\{ \nabla_{\psi}^2 l_n(\psi) \right\}^{-1} \right\|_1} \right) \\ &= \mathbb{P} \left( \left| n^{-1} \sum_{i=1}^n \nabla_{\psi} l_i(\psi) \right| \geq \sqrt{\frac{\log(n)}{n}} \frac{B_\lambda}{\left\| n^{-1} \left\{ \nabla_{\psi}^2 l_n(\psi) \right\}^{-1} \right\|_1} \right), \end{aligned}$$

where the second inequality follows from the strong law of large numbers with respect to  $a_n$  and  $l_i(\psi)$  is the log likelihood for each observation. We can now choose some  $D > \left\| \mathbb{E} \left[ \left\{ \nabla_{\psi}^2 l_{n=1}(\psi) \right\}^{-1} \right] \right\|_1$  such that, for  $n$  sufficiently large, we have

$$\begin{aligned} &\mathbb{P} \left( \left| n^{-1} \sum_{i=1}^n \nabla_{\psi} l_i(\psi) \right| \geq \sqrt{\frac{\log(n)}{n}} \frac{B_\lambda}{\left\| n^{-1} \left\{ \nabla_{\psi}^2 l_n(\psi) \right\}^{-1} \right\|_1} \right) \\ &\leq \mathbb{P} \left( \left| n^{-1} \sum_{i=1}^n \nabla_{\psi} l_i(\psi) \right| \geq \sqrt{\frac{\log(n)}{n}} \frac{B_\lambda}{D} \right) \\ &= \mathbb{P} \left( \sum_{j=1}^r \left| n^{-1} \sum_{i=1}^n [\nabla_{\psi} l_i(\psi)]_j \right| \geq \sqrt{\frac{\log(n)}{n}} \frac{B_\lambda}{D} \right) \\ &\leq \sum_{j=1}^r \mathbb{P} \left( \left| n^{-1} \sum_{i=1}^n [\nabla_{\psi} l_i(\psi)]_j \right| \geq \sqrt{\frac{\log(n)}{n}} \frac{B_\lambda}{Dr} \right), \end{aligned}$$

where the first inequality follows from the strong law of large numbers with respect to  $\left\| \mathbb{E} \left[ \left\{ \nabla_{\psi}^2 l_{n=1}(\psi) \right\}^{-1} \right] \right\|_1$ ,

the term  $|n^{-1} \sum_{i=1}^n [\nabla_{\psi} l_i(\psi)]_j|$  is the  $j$ th component of  $\nabla_{\psi} l_i(\psi)$ , and the second inequality follows from sub additivity of probability and the fact that a sum of elements is greater than or equal to a number if at

least one term in the sum is greater than or equal to that number divided by the number of elements in the sum. Then Lemmas 6, 7, and 8 give

$$\sum_{j=1}^r \mathbb{P} \left( \left| n^{-1} \sum_{i=1}^n [\nabla_{\psi} l_i(\psi)]_j \right| \geq \sqrt{\frac{\log(n)}{n}} \frac{B_{\lambda}}{Dr} \right) \leq 2 \sum_{j=1}^r n^{-\frac{B_{\lambda}}{2D\tau_j^2 r}}.$$

We can pick  $A_{\lambda}$  such that  $B_{\lambda}$  can be chosen to satisfy

$$2 \sum_{j=1}^r n^{-\frac{B_{\lambda}}{2D\tau_j^2 r}} = O(n^{-\lambda}).$$

Our conclusion follows. □

The following Corollary extends the concentration inequality for MLEs corresponding to conditional densities  $p_{\psi}(\cdot|x)$  with parameter space  $\mathfrak{N}_{\mathcal{X}}$  in Theorem 2 to the conformal prediction framework.

**Corollary 1.** *Let  $Y|X = x$  be a random variable with conditional density  $p_{\psi}(\cdot|x)$  and parameter space  $\mathfrak{N}_{\mathcal{X}}$ . Assume that  $p_{\psi}(\cdot|x)$  is twice differentiable in  $\psi$ . Let  $(X_1, Y_1), \dots, (X_n, Y_n)$  be independent and identically distributed copies of  $(X, Y)$ . Let  $\psi \in \mathbb{R}^r$ . Let  $\hat{\psi}$  be the MLE of  $\psi$ . Augment the sample data with a new point  $(x, y)$ , and let  $\hat{\psi}^{(x,y)}$  be the MLE of  $\psi$  with respect to the augmented data. Then for any  $\lambda > 0$ , there exists a numerical constant  $A'_{\lambda}$ , such that*

$$\mathbb{P} \left\{ \sqrt{n} \left| \hat{\psi}^{(x,y)} - \psi \right| \geq A'_{\lambda} \sqrt{\log(n)} \right\} = O(n^{-\lambda}). \quad (14)$$

*Proof.* Let  $\hat{\psi}$  be the maximum likelihood estimator of  $\psi$  under the original data. First note that

$$\begin{aligned} \mathbb{P} \left\{ \sqrt{n} \left| \hat{\psi}^{(x,y)} - \psi \right| \geq A'_{\lambda} \sqrt{\log(n)} \right\} &\leq \mathbb{P} \left\{ \sqrt{n} \left| \hat{\psi}^{(x,y)} - \hat{\psi} \right| + \sqrt{n} \left| \hat{\psi} - \psi \right| \geq A'_{\lambda} \sqrt{\log(n)} \right\} \\ &= \mathbb{P} \left\{ \sqrt{n} \left| \hat{\psi} - \psi \right| \geq A'_{\lambda} \sqrt{\log(n)} - \sqrt{n} \left| \hat{\psi}^{(x,y)} - \hat{\psi} \right| \right\}. \end{aligned} \quad (15)$$

We will show that the  $\sqrt{n} \left| \hat{\psi}^{(x,y)} - \hat{\psi} \right|$  term in (15) vanishes quickly enough to yield (14). From the proof Theorem 2 we have that

$$\sqrt{n}(\hat{\psi} - \psi) = -\sqrt{n} \left\{ \nabla_{\psi}^2 l_n(\hat{\psi}_1) \right\}^{-1} \nabla_{\psi} l_n(\psi).$$

where  $l_n(\cdot)$  is the log likelihood of the original data and  $\hat{\psi}_1$  is such that  $\hat{\psi}_{1,j} \in (\psi_j \wedge \hat{\psi}_j, \psi_j \vee \hat{\psi}_j)$ ,  $j = 1, \dots, r$ . Let  $l_n^{(x,y)}(\psi)$  be the likelihood of the augmented data. A similar calculation to that in the proof Theorem 2 yields

$$\sqrt{n}(\hat{\psi}^{(x,y)} - \psi) = -\sqrt{n} \left\{ \nabla_{\psi}^2 l_n^{(x,y)}(\hat{\psi}_1^{(x,y)}) \right\}^{-1} \nabla_{\psi} l_n^{(x,y)}(\psi)$$

with  $\hat{\psi}_1^{(x,y)}$  defined similarly to  $\hat{\psi}_1$ . We have that

$$\nabla_{\psi} l_n^{(x,y)}(\psi) = \nabla_{\psi} l_n(\psi) + \nabla_{\psi} \log p_{\psi}(y|x).$$



These derivations yield

$$\begin{aligned}
\sqrt{n} \left| \hat{\psi}^{(x,y)} - \hat{\psi} \right| &= \left| (\hat{\psi}^{(x,y)} - \psi) - (\hat{\psi} - \psi) \right| \\
&= \left| \sqrt{n} \left\{ \nabla_{\psi}^2 l_n^{(x,y)}(\hat{\psi}_1^{(x,y)}) \right\}^{-1} \nabla_{\psi} l_n^{(x,y)}(\psi) - \sqrt{n} \left\{ \nabla_{\psi}^2 l_n(\hat{\psi}_1) \right\}^{-1} \nabla_{\psi} l_n(\psi) \right| \\
&= \left| \sqrt{n} \left\{ \nabla_{\psi}^2 l_n^{(x,y)}(\hat{\psi}_1^{(x,y)}) \right\}^{-1} [\nabla_{\psi} l_n(\psi) + \nabla_{\psi} \log p_{\psi}(y|x)] \right. \\
&\quad \left. - \sqrt{n} \left\{ \nabla_{\psi}^2 l_n(\hat{\psi}_1) \right\}^{-1} \nabla_{\psi} l_n(\psi) \right| \\
&= \left| \left[ \left\{ \nabla_{\psi}^2 l_n^{(x,y)}(\hat{\psi}_1^{(x,y)}) \right\}^{-1} - \left\{ \nabla_{\psi}^2 l_n(\hat{\psi}_1) \right\}^{-1} \right] \sqrt{n} \nabla_{\psi} l_n(\psi) \right. \\
&\quad \left. + \sqrt{n} \left\{ \nabla_{\psi}^2 l_n^{(x,y)}(\hat{\psi}_1^{(x,y)}) \right\}^{-1} \nabla_{\psi} \log p_{\psi}(y|x) \right| \\
&= \left| \left[ \left\{ \frac{1}{n} \nabla_{\psi}^2 l_n^{(x,y)}(\hat{\psi}_1^{(x,y)}) \right\}^{-1} - \left\{ \frac{1}{n} \nabla_{\psi}^2 l_n(\hat{\psi}_1) \right\}^{-1} \right] \frac{1}{\sqrt{n}} \nabla_{\psi} l_n(\psi) \right. \\
&\quad \left. + \frac{1}{\sqrt{n}} \left\{ \frac{1}{n} \nabla_{\psi}^2 l_n^{(x,y)}(\hat{\psi}_1^{(x,y)}) \right\}^{-1} \nabla_{\psi} \log p_{\psi}(y|x) \right|.
\end{aligned}$$

By the strong law of large numbers and a similar argument to the proof of Theorem 2, we can pick  $A'_\lambda$  such that, for  $n$  sufficiently large, we have that

$$\mathbb{P} \left\{ \sqrt{n} \left| \hat{\psi} - \psi \right| \geq A'_\lambda \sqrt{\log(n)} - \sqrt{n} \left| \hat{\psi}^{(x,y)} - \hat{\psi} \right| \right\} \leq \mathbb{P} \left\{ \sqrt{n} \left| \hat{\psi} - \psi \right| \geq A_\lambda \sqrt{\log(n)} \right\},$$

where  $A_\lambda$  is defined in Theorem 2. Our conclusion follows from Theorem 2.  $\square$

## Proof of Theorem 1

The concentration inequalities in Theorem 2 and Corollary 1 allow us to prove Theorem 1.

**Lemma 9.** *Let  $Y|X = x$  be a random variable with conditional density  $p_{\psi}(\cdot|x)$  and parameter space  $\mathfrak{N}_{\mathcal{X}}$ . Assume that  $p_{\psi}(\cdot|x)$  is twice differentiable in  $\psi$  and satisfies Assumption 2. Let  $(X_1, Y_1), \dots, (X_n, Y_n)$  be independent and identically distributed copies of  $(X, Y)$ . Let  $\psi \in \mathbb{R}^r$ . Let  $\hat{\psi}$  be the MLE of  $\psi$ . Augment the sample data with a new point  $(x, y)$ , and let  $\hat{\psi}^{(x,y)}$  be the MLE of  $\psi$  with respect to the augmented data. Let  $\hat{p}_{\psi}^{(x,y)}(\cdot|x)$  be the conditional density with  $\hat{\psi}^{(x,y)}$  plugged in for  $\psi$ . Given  $\lambda > 0$ , there is a numerical constant  $\xi_\lambda$  such that*

$$\mathbb{P} \left\{ \sup_{x \in \mathcal{X}} \|\hat{p}_{\psi}^{(x,y)}(\cdot|x) - p_{\psi}(\cdot|x)\|_{\infty} \geq \xi_\lambda r_n \right\} = O(n^{-\lambda}).$$

*Proof.* From the Lipschitz property of Assumption 2 and the boundedness of  $\mathcal{X}$ , we can pick an  $M > 0$  such that

$$\sup_{x \in \mathcal{X}} \|\hat{p}_{\psi}^{(x,y)}(\cdot|x) - p_{\psi}(\cdot|x)\|_{\infty} \leq M \|\hat{\psi}^{(x,y)} - \psi\|.$$

Therefore,

$$\mathbb{P} \left\{ \sup_{x \in \mathcal{X}} \|\hat{p}_{\psi}^{(x,y)}(\cdot|x) - p_{\psi}(\cdot|x)\|_{\infty} \geq \xi_\lambda r_n \right\} \leq \mathbb{P} \left\{ M \|\hat{\psi}^{(x,y)} - \psi\| \geq \xi_\lambda r_n \right\}.$$

Choose  $\xi_\lambda$  so that  $A'_\lambda = \xi_\lambda/M$  satisfies the rate of (14) in Corollary 1. Our conclusion then follows from Corollary 1.  $\square$

From the Lipschitz property in Assumption 2, we can pick  $M' > 0$  such that

$$\sup_{x \in A_k} \|\hat{p}_\psi^{(x,y)}(\cdot|x) - p_\psi(\cdot|x)\|_\infty \leq M' \left( \|\hat{\psi}^{(x,y)} - \psi\| + \|\hat{\psi} - \psi\| \right).$$

Let  $a_k$  be the center point of the cube  $A_k$ . Again, from the Lipschitz property in Assumption 2, we can pick  $M'' > 0$  such that

$$\sup_{x \in A_k} \|\hat{p}_\psi(\cdot|x) - \hat{p}_\psi(\cdot|a_k)\|_\infty \leq z_n M'' \|\hat{\psi}\|_\infty.$$

Set  $\lambda > 0$  and pick  $A_\lambda$  as in Theorem 2 and  $A'_\lambda$  as in Corollary 1 and let

$$E_1 = \{ \|\hat{\psi} - \psi\| \leq r_n M' A_\lambda, \|\hat{\psi}^{(x,y)} - \psi\| \leq r_n M' A'_\lambda \},$$

where  $\mathbb{P}(E_1^c) = O(n^{-\lambda})$  by Theorem 2 and Corollary 1. On  $E_1$  we have that

$$\sup_{x \in A_k} \|\hat{p}_\psi^{(x,y)}(\cdot|x) - \hat{p}_\psi(\cdot|x)\|_\infty \leq r_n M' (A_\lambda + A'_\lambda),$$

and

$$\sup_{x \in A_k} \|\hat{p}_\psi(\cdot|x) - \hat{p}_\psi(\cdot|a_k)\|_\infty \leq z_n M'' (\|\psi\| + r_n M' A_\lambda).$$

For  $n$  sufficiently large we can pick  $M''' > 0$  such that

$$z_n M'' (\|\psi\| + r_n M' A_\lambda) \leq z_n M'''$$

and this implies that

$$\sup_{x \in A_k} \|\hat{p}_\psi(\cdot|x) - \hat{p}_\psi(\cdot|a_k)\|_\infty \leq z_n M'''$$

Now let  $\{(X_{i_1}, Y_{i_1}), \dots, (X_{i_{n_k}}, Y_{i_{n_k}})\}$  be the data points that belong to  $A_k$  where the indices  $(i_1, \dots, i_{n_k})$  are conditioned on. Let the data point  $(Y_{(k,\alpha)}, X_{(k,\alpha)})$  be such that  $\hat{p}_\psi(Y_{(k,\alpha)}|a_k)$  is the  $\lfloor n_k \alpha \rfloor$  largest value among all  $\hat{p}_\psi(Y_{i_j}|a_k)$ ,  $1 \leq j \leq n_k$  and define the sandwiching sets,

$$\begin{aligned} \widehat{L}_k^- &= \widehat{L}_k \left( \hat{p}_\psi(Y_{(k,\alpha)}|a_k) + 2r_n M' A'_\lambda + 2z_n M''' \right), \\ \widehat{L}_k^+ &= \widehat{L}_k \left( \hat{p}_\psi(Y_{(k,\alpha)}|a_k) - 2r_n M' A'_\lambda - 2z_n M''' \right), \end{aligned} \tag{16}$$

where the level set  $\widehat{L}_k(t) = \{y : \hat{p}_\psi(y|a_k) \geq t\}$  and  $A''_\lambda = A_\lambda + A'_\lambda$ . The bin sample size has to satisfy  $n_k \rightarrow \infty$  for the sandwiching sets to be of use, this occurs when  $z_n$  is as specified. With this construction, we have

$$\begin{aligned} \widehat{L}_k^- &\subseteq \left\{ y : \frac{1}{n_k + 1} \sum_{i=1}^{n+1} \mathbb{1}\{X_i \in A_k\} \mathbb{1}\{\hat{p}_\psi(Y_i|a_k) + 2r_n M A''_\lambda + 2z_n M''' \leq \hat{p}_\psi(y|a_k)\} \geq \tilde{\alpha}_k \right\} \\ &\subseteq \widehat{C}_{n,k}^{(\alpha)}(x) \\ &\subseteq \left\{ y : \frac{1}{n_k + 1} \sum_{i=1}^{n+1} \mathbb{1}\{X_i \in A_k\} \mathbb{1}\{\hat{p}_\psi(Y_i|a_k) - 2r_n M A''_\lambda - 2z_n M''' \leq \hat{p}_\psi(y|a_k)\} \geq \tilde{\alpha}_k \right\} \\ &\subseteq \widehat{L}_k^+. \end{aligned}$$

Therefore

$$\mathbb{P} \left\{ \widehat{L}_k^- \subseteq \widehat{C}_{n,k}^{(\alpha)}(x) \subseteq \widehat{L}_k^+ \right\} = 1 - O(n^{-\lambda}).$$

We summarize this result in the following Lemma.

**Lemma 10.** *Let  $Y|X = x$  be a random variable with conditional density  $p_\psi(\cdot|x)$  and parameter space  $\mathfrak{N}_\mathcal{X}$ . Assume that  $p_\psi(\cdot|x)$  is twice differentiable in  $\psi$  and satisfies Assumption 2. Let  $(X_1, Y_1), \dots, (X_n, Y_n)$  be independent and identically distributed copies of  $(X, Y)$ . Let  $\psi \in \mathbb{R}^r$ . Let  $\widehat{\psi}$  be the MLE of  $\psi$ . Augment the sample data with a new point  $(x, y)$ , and let  $\widehat{\psi}^{(x,y)}$  be the MLE of  $\psi$  with respect to the augmented data. Suppose that Assumption 1 holds. Let  $0 < \alpha < 1$ . Let the sets  $\widehat{L}_k^-$  and  $\widehat{L}_k^+$  be defined as in (16). Then,*

$$\mathbb{P} \left\{ \widehat{L}_k^- \subseteq \widehat{C}_{n,k}^{(\alpha)}(x) \subseteq \widehat{L}_k^+ \right\} = 1 - O(n^{-\lambda}).$$

*Proof.* The details of this proof are given in the above paragraph. □

We now have enough technical tools to finish the proof of Theorem 1.

*Proof of Theorem 1.* Define  $L_k^l(t) = \{y : \widehat{p}_\psi(y|a_k) \leq t\}$  and  $\widehat{t}_k^{(\alpha)} = \widehat{p}_\psi(Y_{(k,\alpha)}|a_k)$  and  $\alpha_k = \lfloor \alpha n_k \rfloor / n_k$ . We have that

$$\begin{aligned} \widehat{P} \left\{ \widehat{L}_k^l(\widehat{t}_k^{(\alpha)}) | A_k \right\} &= \frac{1}{n_k} \sum_{i=1}^n \mathbb{1} \{X_i \in A_k\} \mathbb{1} \left\{ Y_i \in \widehat{L}_k^l(\widehat{t}_k^{(\alpha)}) \right\} \\ &= \frac{1}{n_k} \sum_{i=1}^n \mathbb{1} \{X_i \in A_k\} \mathbb{1} \left\{ \widehat{p}_\psi(Y_i|a_k) \leq \widehat{p}_\psi(Y_{(k,\alpha)}|a_k) \right\}, \end{aligned}$$

and this implies that  $\widehat{t}_k^{(\alpha)} = \inf \{t \geq 0 : \widehat{P} \left\{ \widehat{L}_k^l(t) | A_k \right\} \geq \alpha_k\}$ . Let

$$R_{n,k} = \sup_{x \in A_k} \|\widehat{p}_\psi(\cdot|x) - \widehat{p}_\psi(\cdot|a_k)\|_\infty,$$

and let  $V_n(x)$  be as in Lei and Wasserman [2014, Lemma 6] with  $z_n$  in place of  $w_n$  and  $p_\psi(\cdot|a_k)$  replacing their  $p(\cdot|A_k)$  in the setup and proof of Lei and Wasserman [2014, Lemma 6]. Define the event

$$E_2 = \left\{ \|\widehat{\psi} - \psi\| \leq r_n M' A_\lambda, \|\widehat{\psi}^{(x,y)} - \psi\| \leq r_n M' A'_\lambda, R_{n,k} \leq z_n M''', V_n(x) \leq z_n \xi_\lambda \right\},$$

where  $z_n$  and  $\xi_\lambda$  are respectively  $r_n$  and  $\xi_{2,\lambda}$  in Lei and Wasserman [2014, Lemma 6]. Note that  $\mathbb{P}(E_2^c) = O(n^{-\lambda})$ . Let  $v_1 = z_n M''' + r_n M'(A_\lambda + A'_\lambda)$  and  $v_2 = z_n \xi_\lambda$  and note that, for sufficiently large  $n$ , these choices satisfy Lei and Wasserman [2014, Lemma 8] which then gives

$$|\widehat{t}_k^{(\alpha)} - t^{(\alpha)}| \leq v_1 + c_1^{-1} v_2,$$

and

$$\mathbb{P} \left[ \sup_x \nu \left\{ \widehat{L}_k^l(\widehat{t}_k^{(\alpha)}) \Delta C_P^{(\alpha)}(x) \right\} \geq \xi_1 v_1 + \xi_2 v_2 \right] = O(n^{-\lambda}),$$

where  $c_1, \xi_1$ , and  $\xi_2$  are all constants that are independent of  $n$ .

Let  $\hat{t}_k^{(\alpha)} = \hat{t}_k^{(\alpha)} + 2r_n M' A_\lambda'' + 2z_n M'''$ . Then, for  $v_3 = 2r_n M' A_\lambda'' + 2z_n M'''$  and constants  $\xi'_j, j = 1, 2, 3$ , Lei and Wasserman [2014, Lemma 8] gives us

$$\mathbb{P} \left[ \sup_x \nu \left\{ \hat{L}_k^- \Delta C_P^{(\alpha)}(x) \right\} \geq \xi'_1 v_1 + \xi'_2 v'_2 + \xi'_3 v_3 \right] = O(n^{-\lambda}).$$

Similarly, for  $v'_3 = -2r_n M' A_\lambda'' - 2z_n M'''$  and constants  $\xi''_j, j = 1, 2, 3$ , Lei and Wasserman [2014, Lemma 8] gives us

$$\mathbb{P} \left[ \sup_x \nu \left\{ \hat{L}_k^+ \Delta C_P^{(\alpha)}(x) \right\} \geq \xi''_1 v_1 + \xi''_2 v''_2 + \xi''_3 v_3 \right] = O(n^{-\lambda}).$$

Then, conditional on  $E_2$ , we have that  $\left\{ \hat{L}_k^- \subseteq \hat{C}_{n,k}^{(\alpha)}(x) \subseteq \hat{L}_k^+ \right\}$ , and this implies that

$$\nu \left\{ \hat{C}_{n,k}^{(\alpha)}(x) \Delta C_P^{(\alpha)}(x) \right\} \leq \nu \left\{ \hat{L}_k^- \Delta C_P^{(\alpha)}(x) \right\} + \nu \left\{ \hat{L}_k^+ \Delta C_P^{(\alpha)}(x) \right\}.$$

Therefore our conclusion holds for some  $\zeta'_\lambda$  at rate  $r_n \vee z_n$ .  $\square$

### Preliminaries for the proof of Theorem 3

We will prove Theorem 3 under the specification that the number of modes of  $p_\psi(\cdot|x)$  is equal to 1 for all  $x \in \mathcal{X}$ , so that (7) and (10) are equivalent. The general case follows a similar argument. With an abuse of notation, let  $(a(x), b(x))$  be the solution to

$$\operatorname{argmin}_{(a(x), b(x))} (b(x) - a(x)), \text{ subject to } \int_{a(x)}^{b(x)} p_\psi(u|x) du = 1 - \alpha, \text{ and } b(x) - a(x) > 0. \quad (17)$$

We now provide a probability bound on the distance between the solutions to (9) and (17). This bound is of fundamental importance for proving Theorem 3.

**Lemma 11.** *Let  $Y|X = x$  be a random variable with conditional density  $p_\psi(\cdot|x)$  and parameter space  $\aleph_{\mathcal{X}}$ . Assume that  $p_\psi(\cdot|x)$  is twice differentiable in  $\psi$  and satisfies Assumption 2. Let  $(X_1, Y_1), \dots, (X_n, Y_n)$  be independent and identically distributed copies of  $(X, Y)$ . Let  $\psi \in \mathbb{R}^r$ . Let  $\hat{\psi}$  be the MLE of  $\psi$ . Augment the sample data with a new point  $(x, y)$ , and let  $\hat{\psi}^{(x,y)}$  be the MLE of  $\psi$  with respect to the augmented data. Suppose that Assumption 1 holds. Let  $0 < \alpha < 1$ . Let  $(\hat{a}(x), \hat{b}(x))$  be the solution to the optimization problem (9) and let  $(a(x), b(x))$  be the solution to the optimization problem (17). Let  $\lambda > 0$  be as is defined in Lemma 9. Then we can pick a number  $\xi'_\lambda$  such that*

$$\mathbb{P} \left( \sup_{x \in \mathcal{X}} |(\hat{a}(x), \hat{b}(x)) - (a(x), b(x))| \geq \xi'_\lambda r_n \right) = O(n^{-\lambda}).$$

*Proof.* Let  $E$  be the event that  $\|\hat{p}_{\hat{\psi}^{(x,y)}}(\cdot|x) - p_\psi(\cdot|x)\|_\infty \leq \xi_\lambda r_n$  with  $\xi_\lambda$  defined in Lemma 9. Note that  $\mathbb{P}(E^c) = O(n^{-\lambda})$ . As a reminder, WLOG we are assuming that the class of densities  $p_\psi$  are unimodal over the parameter space  $\aleph_{\mathcal{X}}$ . In what follows, we will assume that  $a(x) < b(x)$  is an optimization constraint.

On  $E$  we have that,

$$\begin{aligned}
& \sup_{x \in \mathcal{X}} \left\{ \left[ \operatorname{argmin}_{(a(x), b(x))} (b(x) - a(x)), \text{ subject to } \int_{a(x)}^{b(x)} \hat{p}_\psi^{(x,y)}(u|x) du = 1 - \alpha \right] \right. \\
& \quad \left. - \left[ \operatorname{argmin}_{(a(x), b(x))} (b(x) - a(x)), \text{ subject to } \int_{a(x)}^{b(x)} p_\psi(u|x) du = 1 - \alpha \right] \right\} \\
& \leq \sup_{x \in \mathcal{X}} \left\{ \left[ \operatorname{argmin}_{(a(x), b(x))} (b(x) - a(x)), \text{ subject to } \int_{a(x)}^{b(x)} \{p_\psi(u|x) - \xi_\lambda r_n\} du = 1 - \alpha \right] \right. \\
& \quad \left. - \left[ \operatorname{argmin}_{(a(x), b(x))} (b(x) - a(x)), \text{ subject to } \int_{a(x)}^{b(x)} \{p_\psi(u|x) + \xi_\lambda r_n\} du = 1 - \alpha \right] \right\} \\
& = \sup_{x \in \mathcal{X}} \left\{ \left[ \operatorname{argmin}_{(a(x), b(x))} (b(x) - a(x)), \text{ subject to } \int_{a(x)}^{b(x)} p_\psi(u|x) du - (b(x) - a(x))\xi_\lambda r_n = 1 - \alpha \right] \right. \\
& \quad \left. - \left[ \operatorname{argmin}_{(a(x), b(x))} (b(x) - a(x)), \text{ subject to } \int_{a(x)}^{b(x)} p_\psi(u|x) du + (b(x) - a(x))\xi_\lambda r_n = 1 - \alpha \right] \right\}.
\end{aligned}$$

Since the optimization problems above correspond to highest density regions for a uniformly bounded class of densities, it must be the case that  $\inf_{x \in \mathcal{X}} a(x) > -\infty$ ,  $\sup_{x \in \mathcal{X}} b(x) < \infty$ . For all  $\alpha > 0$  in the optimization problems above, there exists an  $N$  and  $M$  such that

$$\int_{a(x)}^{b(x)} p_\psi(u|x) du + (b(x) - a(x))\xi_\lambda r_n \leq \int_{a(x)}^{b(x)} p_\psi(u|x) du + M\xi_\lambda r_n$$

and

$$\int_{a(x)}^{b(x)} p_\psi(u|x) du - (b(x) - a(x))\xi_\lambda r_n \geq \int_{a(x)}^{b(x)} p_\psi(u|x) du - M\xi_\lambda r_n$$

for all  $n > N$ . This yields that

$$\begin{aligned}
& \sup_{x \in \mathcal{X}} \left\{ \left[ \operatorname{argmin}_{(a(x), b(x))} (b(x) - a(x)), \text{ subject to } \int_{a(x)}^{b(x)} p_\psi(u|x) du - (b(x) - a(x))\xi_\lambda r_n = 1 - \alpha \right] \right. \\
& \quad \left. - \left[ \operatorname{argmin}_{(a(x), b(x))} (b(x) - a(x)), \text{ subject to } \int_{a(x)}^{b(x)} p_\psi(u|x) du + (b(x) - a(x))\xi_\lambda r_n = 1 - \alpha \right] \right\} \\
& \leq \sup_{x \in \mathcal{X}} \left\{ \left[ \operatorname{argmin}_{(a(x), b(x))} (b(x) - a(x)), \text{ subject to } \int_{a(x)}^{b(x)} p_\psi(u|x) du - M\xi_\lambda r_n = 1 - \alpha \right] \right. \\
& \quad \left. - \left[ \operatorname{argmin}_{(a(x), b(x))} (b(x) - a(x)), \text{ subject to } \int_{a(x)}^{b(x)} p_\psi(u|x) du + M\xi_\lambda r_n = 1 - \alpha \right] \right\} \\
& = \sup_{x \in \mathcal{X}} \left\{ \left[ \operatorname{argmin}_{(a(x), b(x))} (b(x) - a(x)), \text{ subject to } \int_{a(x)}^{b(x)} p_\psi(u|x) du = 1 - \alpha + M\xi_\lambda r_n \right] \right. \\
& \quad \left. - \left[ \operatorname{argmin}_{(a(x), b(x))} (b(x) - a(x)), \text{ subject to } \int_{a(x)}^{b(x)} p_\psi(u|x) du = 1 - \alpha - M\xi_\lambda r_n \right] \right\}.
\end{aligned}$$

Let  $a_{n,1}(x)$  and  $b_{n,1}(x)$  be the solution to

$$\operatorname{argmin}_{(a(x), b(x))} (b(x) - a(x)), \text{ subject to } \int_{a(x)}^{b(x)} p_\psi(u|x) du = 1 - \alpha + M\xi_\lambda r_n,$$

and let  $a_{n,2}(x)$  and  $b_{n,2}(x)$  be the solution to

$$\operatorname{argmin}_{(a(x), b(x))} (b(x) - a(x)), \text{ subject to } \int_{a(x)}^{b(x)} p_\psi(u|x) du = 1 - \alpha - M\xi_\lambda r_n.$$

Since  $p_\psi$  is unimodal, we have that  $a_{n,1}(x) < a_{n,2}(x)$  and  $b_{n,2}(x) < b_{n,1}(x)$ . The combination of this and the setup of the optimization problems implies that

$$\begin{aligned} & \sup_{x \in \mathcal{X}} \{(a_{n,2}(x) - a_{n,1}(x))p_\psi(a_{n,1}(x)|x) + (b_{n,1}(x) - b_{n,2}(x))p_\psi(b_{n,1}(x)|x)\} \\ &= \sup_{x \in \mathcal{X}} \{(a_{n,2}(x) - a_{n,1}(x)) + (b_{n,1}(x) - b_{n,2}(x))\} p_\psi(a_{n,1}(x)|x) \\ &\leq 2M\xi_\lambda r_n. \end{aligned}$$

The number  $p_\psi(a_{n,1}(x)|x)$  is increasing in  $n$  for all  $x \in \mathcal{X}$  since  $1 - \alpha + M\xi_\lambda r_n$  is decreasing in  $n$ . We can pick a number  $m$  such that  $\inf_{x \in \mathcal{X}} p_\psi(a_{n,1}(x)|x) > m$ . Thus,

$$\sup_{x \in \mathcal{X}} \{(a_{n,2}(x) - a_{n,1}(x)) + (b_{n,1}(x) - b_{n,2}(x))\} \leq \frac{2M\xi_\lambda r_n}{m}.$$

Let  $\xi'_\lambda = 2M\xi_\lambda/m$ . This implies that

$$\sup_{x \in \mathcal{X}} (a_{n,2}(x) - a_{n,1}(x)) \leq \xi'_\lambda r_n \quad \text{and} \quad \sup_{x \in \mathcal{X}} (b_{n,1}(x) - a_{n,2}(x)) \leq \xi'_\lambda r_n.$$

Therefore we have that  $|(\hat{a}(x), \hat{b}(x)) - (a(x), b(x))| \leq \xi'_\lambda r_n$ . Our conclusion follows.  $\square$

**Lemma 12.** *Let  $Y|X = x$  be a random variable with conditional density  $p_\psi(\cdot|x)$  and parameter space  $\mathfrak{N}_\mathcal{X}$ . Assume that  $p_\psi(\cdot|x)$  is twice differentiable in  $\psi$  and satisfies Assumption 2. Let  $F(y|x)$  be the conditional distribution function corresponding to  $p_\psi(\cdot|x)$  and assume that  $F(y|x)$  satisfies Assumption 4. Let  $(X_1, Y_1), \dots, (X_n, Y_n)$  be independent and identically distributed copies of  $(X, Y)$ . Let  $\psi \in \mathbb{R}^r$ . Let  $\hat{\psi}$  be the MLE of  $\psi$ . Augment the sample data with a new point  $(x, y)$ . Suppose that Assumption 1 holds. Let  $\hat{\psi}^{(x,y)}$  be the MLE of  $\psi$  with respect to the augmented data. Let  $\hat{F}^{(x,y)}(\cdot|x)$  be the estimated conditional distribution  $F(y|x)$  with  $\hat{\psi}^{(x,y)}$  plugged in. Given  $\lambda > 0$ , there is a numerical constant  $\chi'_\lambda$  such that*

$$\mathbb{P} \left\{ \sup_{x \in \mathcal{X}} \|\hat{F}^{(x,y)}(\cdot|x) - F(\cdot|x)\|_\infty \geq \chi'_\lambda r_n \right\} = O(n^{-\lambda}).$$

*Proof.* Let  $E$  be the event that  $|\hat{\psi}^{(x,y)} - \psi| < A'_\lambda r_n$  with  $\lambda$  and  $A_\lambda$  defined in Corollary 1 and note that  $\mathbb{P}(E^c) = O(n^{-\lambda})$  by Corollary 1. A Taylor expansion of  $\hat{F}^{(x,y)}(v|x)$  around  $F(v|x)$  yields

$$\begin{aligned} |\hat{F}^{(x,y)}(v|x) - F(v|x)| &= |\nabla_\psi F(v|x)'(\hat{\psi}^{(x,y)} - \psi) + o(|\hat{\psi}^{(x,y)} - \psi|)| \\ &= |\nabla_\psi F(v|x)'(\hat{\psi}^{(x,y)} - \psi) + o(r_n)|, \end{aligned}$$

on  $E$ . Boundedness of  $|\nabla_\psi F(v|x)|$  for all  $v$  and all  $\psi \in \mathfrak{N}_\mathcal{X}$  implies that  $|\nabla_\psi F(v|x)'(\hat{\psi}^{(x,y)} - \psi)| = O(r_n)$ . This then implies that there exists an  $N$  such that

$$\begin{aligned} |\nabla_\psi F(v|x)'(\hat{\psi}^{(x,y)} - \psi)| + o(r_n) &\leq |\nabla_\psi F(v|x)| |\hat{\psi}^{(x,y)} - \psi| + |o(r_n)| \\ &\leq |\nabla_\psi F(v|x)| A'_\lambda r_n, \end{aligned}$$

for all  $n > N$  on  $E$ . Our conclusion follows for some  $\chi'_\lambda > 0$ .  $\square$

We now build on Lemma 12.

**Lemma 13.** Define  $U_{lwr}(x) = F(a(x)|x)$  and  $U_{upr}(x) = F(b(x)|x)$  where  $(a(x), b(x))$  as defined in (17). Define  $\lambda > 0$  as in Lemma 11 and Lemma 12. Then there exists  $\eta_{lwr}, \eta_{upr} > 0$  such that

$$\mathbb{P}\left(\sup_{x \in \mathcal{X}} |\widehat{U}_{lwr}^{(x,y)} - U_{lwr}(x)| \geq \eta_{\lambda}^{lwr} r_n\right) = O(n^{-\lambda}), \quad \text{and} \quad \mathbb{P}\left(\sup_{x \in \mathcal{X}} |\widehat{U}_{upr}^{(x,y)} - U_{upr}(x)| \geq \eta_{\lambda}^{upr} r_n\right) = O(n^{-\lambda}).$$

*Proof.* Set  $\lambda > 0$  and let  $E$  be the event that  $\sup_{x \in \mathcal{X}} |(\hat{a}(x), \hat{b}(x)) - (a(x), b(x))| \leq \xi'_{\lambda} r_n$ , and  $\sup_{x \in \mathcal{X}} \|\widehat{F}^{(x,y)}(\cdot|x) - F(\cdot|x)\|_{\infty} \leq \chi'_{\lambda} r_n$ , where  $\xi'_{\lambda}$  is defined as in Lemma 11 and  $\chi'_{\lambda}$  is defined as in Lemma 12, and note that these two Lemmas give  $\mathbb{P}(E^c) = O(n^{-\lambda})$ . Then,

$$\begin{aligned} |\widehat{U}_{lwr}^{(x,y)} - U_{lwr}(x)| &= |\widehat{F}^{(x,y)}(\hat{a}(x)|x) \pm F(\hat{a}(x)|x) - F(a(x)|x)| \\ &\leq |\widehat{F}^{(x,y)}(\hat{a}(x)|x) - F(\hat{a}(x)|x)| + |F(\hat{a}(x)|x) - F(a(x)|x)| \\ &\leq r_n \chi'_{\lambda} + \left| \frac{F(\hat{a}(x)|x) - F(a(x)|x)}{\hat{a}(x) - a(x)} \right| |\hat{a}(x) - a(x)|. \end{aligned}$$

Arbitrarily choose  $\varepsilon > 0$ , then for  $n$  sufficiently large, we have that

$$\left| \frac{F(\hat{a}(x)|x) - F(a(x)|x)}{\hat{a}(x) - a(x)} \right| |\hat{a}(x) - a(x)| \leq (p_{\psi}(a(x)|x) + \varepsilon) \xi'_{\lambda} r_n.$$

We can pick  $L \in \mathbb{R}$  such that  $\sup_{x \in \mathcal{X}} p_{\psi}(a(x)|x) \leq L$ . Putting all of this together, we have

$$|\widehat{U}_{lwr}^{(x,y)} - U_{lwr}(x)| \leq (\chi'_{\lambda} + (L + \varepsilon) \xi'_{\lambda}) r_n,$$

for  $n$  sufficiently large. Set  $\eta_{\lambda}^{lwr} = (\chi'_{\lambda} + (L + \varepsilon) \xi'_{\lambda})$  and note that the right hand side of the above displayed equation does not depend on  $x$ . The same argument gives  $|\widehat{U}_{upr}^{(x,y)} - U_{upr}(x)| \leq \eta_{\lambda}^{upr} r_n$ , for  $n$  sufficiently large. Our conclusion follows.  $\square$

### Proof of Theorem 3

*proof of Theorem 3.* Let  $\lambda > 0$  be as defined in Lemma 13. Define  $\xi'_{\lambda}$  as in Lemma 11,  $\chi'_{\lambda}$  as in Lemma 12, and both  $\eta_{\lambda}^{lwr}$  and  $\eta_{\lambda}^{upr}$  as in Lemma 13. Let  $E$  be the event such that  $\sup_{x \in \mathcal{X}} |(\hat{a}(x), \hat{b}(x)) - (a(x), b(x))| \leq \xi'_{\lambda} r_n$ , and  $\sup_{x \in \mathcal{X}} \|\widehat{F}^{(x,y)}(\cdot|x) - F(\cdot|x)\|_{\infty} \leq \chi'_{\lambda} r_n$ , and  $\sup_{x \in \mathcal{X}} (|\widehat{U}_{lwr}^{(x,y)} - U_{lwr}(x)|) \leq \eta_{\lambda}^{lwr} r_n$ , and  $\sup_{x \in \mathcal{X}} (|\widehat{U}_{upr}^{(x,y)} - U_{upr}(x)|) \leq \eta_{\lambda}^{upr} r_n$ . Note that Lemmas 11-13 implies that  $\mathbb{P}(E^c) = O(n^{-\lambda})$ . Condition on  $E$  and note that

$$(n+1)U_{lwr}^{(x,y)} \geq (n+1)(U_{lwr}(x) - \eta_{\lambda}^{lwr} r_n),$$

and

$$(n+1)U_{upr}^{(x,y)} \leq (n+1)(U_{upr}(x) + \eta_{\lambda}^{upr} r_n).$$

With these specifications, we have that

$$\begin{aligned}
\widehat{U}_{\lfloor (n+1)\widehat{U}_{\text{lwr}}^{(x,y)} \rfloor}^{(x,y)} &\geq \widehat{U}_{\lfloor (n+1)(U_{\text{lwr}}(x) - \eta_{\lambda}^{\text{lwr}} r_n) \rfloor}^{(x,y)} \\
&= \widehat{F}^{(x,y)}(Y_{\lfloor (n+1)(U_{\text{lwr}}(x) - \eta_{\lambda}^{\text{lwr}} r_n) \rfloor} | X_{\lfloor (n+1)(U_{\text{lwr}}(x) - \eta_{\lambda}^{\text{lwr}} r_n) \rfloor}) \\
&\geq F(Y_{\lfloor (n+1)(U_{\text{lwr}}(x) - \eta_{\lambda}^{\text{lwr}} r_n) \rfloor} | X_{\lfloor (n+1)(U_{\text{lwr}}(x) - \eta_{\lambda}^{\text{lwr}} r_n) \rfloor}) - \chi'_{\lambda} r_n \\
&\geq U_{\lfloor (n+1)(U_{\text{lwr}}(x) - \eta_{\lambda}^{\text{lwr}} r_n) \rfloor} - \chi'_{\lambda} r_n - |O(n^{-1/2})|,
\end{aligned}$$

where  $U_{\lfloor (n+1)(U_{\text{lwr}}(x) - \eta_{\lambda}^{\text{lwr}} r_n) \rfloor}$  is the  $\lfloor (n+1)(U_{\text{lwr}}(x) - \eta_{\lambda}^{\text{lwr}} r_n) \rfloor$ th quantile of the sample of uniform random variables,  $F(Y_i | X_i)$ ,  $i = 1, \dots, n+1$  and the last inequality follows from Ferguson [1996, Theorem 13]. Now, let

$$z_n = \frac{\lfloor (n+1)(U_{\text{lwr}}(x) - \eta_{\lambda}^{\text{lwr}} r_n) \rfloor}{n+1},$$

and note that

$$U_{\lfloor (n+1)(U_{\text{lwr}}(x) - \eta_{\lambda}^{\text{lwr}} r_n) \rfloor} \geq z_n - n^{-1/2} |B_n(z_n)| - |O(n^{-1} \log(n))|,$$

where  $\{B_n(u) : 0 \leq u \leq 1\}$  is a sequence of Brownian bridges. This inequality follows from Csörgő and Révész [1978, Theorem 1] and Komlós et al. [1975] and a bit of algebra. We can pick  $\chi''_{\lambda}$  such that, for  $n$  sufficiently large,

$$z_n - n^{-1/2} |B_n(z_n)| - |O(n^{-1} \log(n))| - \chi'_{\lambda} r_n - |O(n^{-1/2})| \geq U_{\text{lwr}}(x) - \chi''_{\lambda} r_n.$$

A similar argument gives,

$$\widehat{U}_{\lfloor (n+1)\widehat{U}_{\text{upr}}^{(x,y)} \rfloor}^{(x,y)} \leq U_{\text{upr}}(x) + \chi''_{\lambda} r_n,$$

for sufficiently large  $n$ . We also have that  $|\widehat{U}_{n+1}^{(x,y)} - F(y|x)| \leq \chi'_{\lambda} r_n$ .

Putting all of this together, we have that

$$\widehat{C}_{\text{trans}}^{(\alpha)}(x) \subseteq \{y : U_{\text{lwr}}(x) - r_n(\chi'_{\lambda} + \chi''_{\lambda}) \leq F(y|x) \leq U_{\text{upr}}(x) + r_n(\chi'_{\lambda} + \chi''_{\lambda})\},$$

for  $n$  sufficiently large. Let  $F_x^{-1}(\cdot)$  be the inverse of  $F(\cdot|x)$ , then

$$\begin{aligned}
&\{y : U_{\text{lwr}}(x) - r_n(\chi'_{\lambda} + \chi''_{\lambda}) \leq F(y|x) \leq U_{\text{upr}}(x) + r_n(\chi'_{\lambda} + \chi''_{\lambda})\} \\
&= \{y : F_x^{-1}(F(a(x)|x) - r_n(\chi'_{\lambda} + \chi''_{\lambda})) \leq y \leq F_x^{-1}(F(b(x)|x) + r_n(\chi'_{\lambda} + \chi''_{\lambda}))\}.
\end{aligned}$$

For  $n$  sufficiently large, we can pick  $K > 0$  such that

$$\begin{aligned}
&\{y : F_x^{-1}(F(a(x)|x) - r_n(\chi'_{\lambda} + \chi''_{\lambda})) \leq y \leq F_x^{-1}(F(b(x)|x) + r_n(\chi'_{\lambda} + \chi''_{\lambda}))\} \\
&\subseteq \{y : a(x) - r_n(\chi'_{\lambda} + \chi''_{\lambda})K \leq y \leq b(x) + r_n(\chi'_{\lambda} + \chi''_{\lambda})K\}.
\end{aligned}$$

Note that

$$\nu(C_P(x) \triangle \{a(x) - r_n(\chi'_{\lambda} + \chi''_{\lambda})K \leq y \leq b(x) + r_n(\chi'_{\lambda} + \chi''_{\lambda})K\}) = 2r_n(\chi'_{\lambda} + \chi''_{\lambda})K.$$

A similar argument gives

$$\widehat{C}_{\text{trans}}^{(\alpha)}(x) \supseteq \{y : a(x) - r_n(\chi'_{\lambda} + \chi''_{\lambda})K' \leq y \leq b(x) + r_n(\chi'_{\lambda} + \chi''_{\lambda})K'\},$$



for some  $K' > 0$  and  $n$  sufficiently large, where

$$\nu(C_P(x) \Delta \{y : a(x) - r_n(\chi'_\lambda + \chi''_\lambda)K' \leq y \leq b(x) + r_n(\chi'_\lambda + \chi''_\lambda)K'\}) = 2r_n(\chi'_\lambda + \chi''_\lambda)K'.$$

Putting everything together yields

$$\nu\left(\widehat{C}_{\text{trans}}^{(\alpha)}(x) \Delta C_P(x)\right) \leq 4r_n(\chi'_\lambda + \chi''_\lambda) \max(K, K').$$

Set  $\chi_\lambda = 4(\chi'_\lambda + \chi''_\lambda) \max(K, K')$ . Therefore

$$\nu\left(\widehat{C}_{\text{trans}}^{(\alpha)}(x) \Delta C_P(x)\right) \leq \chi_\lambda r_n.$$

Our conclusion follows. □

## Supplementary Materials for “Efficient and minimal length parametric conformal prediction regions”

We provide additional technical and numeric results which demonstrate the advantages and disadvantages of our parametric conformal prediction region compared to the nonparametric conformal prediction region [Lei and Wasserman, 2014], the LS conformal prediction region [Lei et al., 2018] obtained from conformalized residual scores, the LSLW conformal prediction region [Lei et al., 2018, Section 5.2] obtained from conformalized locally weighted residual scores, and the highest density prediction region. In analyses with model misspecification, the parametric, LS, and LSLW conformal prediction regions and highest density prediction region are constructed under the misspecified model. The binning used to construct the parametric and nonparametric conformal prediction regions follows the bin width asymptotics of Lei and Wasserman [2014]. Comparative diagnostics are discussed in Section 5 of the main text.

We expand upon the three simulation settings in the sensitivity analysis in Section 5. These simulation settings are:

- A) Gamma regression with  $\beta = [1.25, -1]'$  and  $n \in \{150, 250, 500\}$ . In this setting the Gamma density is correctly specified for the parametric conformal and the highest density prediction regions. A cubic regression model is assumed for the LS and LSLW conformal prediction regions.
- B) Gamma regression with  $\beta = [0.5, 1]'$  and  $n \in \{150, 250, 500\}$ . In this setting the cubic regression model is assumed for the highest density prediction region and the misspecified parametric conformal, LS, and LSLW conformal prediction regions.
- C) Simple linear regression with normal errors and constant variance. We set  $\beta = [2, 5]'$ , and the normal errors to have variance  $\sigma^2 = 1$ . Results are considered for sample sizes  $n \in \{150, 250, 500\}$ . In this setting the regression model is correctly specified for the highest density prediction region and the parametric, LS, and LSLW conformal prediction regions.

In the next Section we show that all of the assumptions required for the asymptotic efficiency of  $\widehat{C}_{\text{loc}}^{(\alpha)}$  (see Section 2.3.1 in the manuscript) hold for GLMs.

### A Conformal prediction in the GLM setting

In this Section we establish that GLMs which can be parameterized as in (10) in the main text satisfy Assumptions 2-4 in the main text, and that the kernel density based conformal prediction region  $\widehat{C}_{\text{loc}}^{(\alpha)}(x)$  is appropriate for this class of GLMs. There is considerable overlap in the conditions required to achieve both goals, Assumptions 2-3 in the main text are established in the proof that our class of GLMs satisfies the conditions required for the asymptotic properties of  $\widehat{C}_{\text{loc}}^{(\alpha)}(x)$  to hold.

We verify that  $\widehat{C}_{\text{loc}}^{(\alpha)}(x)$  is asymptotically minimal at rate  $w_n = \{\log(n)/n\}^{1/(d+3)}$  when the underlying distribution is a GLM. This result is obtained by showing that our GLM parameterization satisfies the conditions of Theorem 1 in Lei and Wasserman [2014]. We now provide the conditions in Lei and Wasserman [2014] that are required for  $\widehat{C}_{\text{loc}}^{(\alpha)}(x)$  to be asymptotically of minimal length at rate  $w_n$ . The first of these

conditions are Assumptions 1-3 in the main text. We additionally require Assumption 5 below.

**Assumption 5** (Assumptions 1 (b) and (c) of Lei and Wasserman [2014]). (a) For all  $x$ ,  $p_\psi(\cdot|x) \in \Sigma(\eta, L)$ , where  $\Sigma(\eta, L)$  is a Hölder class of functions defined in Lei and Wasserman [2014, Appendix A.1]. Correspondingly, the kernel  $K$  used to construct the nonparametric conformal prediction band is a  $\beta$ -valid kernel; (b) For any  $0 \leq s < \lfloor \eta \rfloor$ ,  $p_\psi^{(s)}(y|x)$  is continuous and uniformly bounded by  $L'$  for all  $x$  and  $y$ .

See Lei and Wasserman [2014, Appendix A.1] for a definition of  $\beta$ -valid kernels, the Hölder class of functions for which  $p_\psi(\cdot|x)$  is assumed to belong to is defined below. Additional explanations of these conditions are given in Lei et al. [2013] and Lei and Wasserman [2014].

**Definition 7** (Hölder class). Given  $L > 0$  and  $\beta > 0$ , let  $l = \lfloor \beta \rfloor$  be the largest integer strictly less than  $\beta$ . The Hölder class  $\Sigma(\beta, L)$  is the family of functions  $f : \mathbb{R} \rightarrow \mathbb{R}$  whose derivative  $f^{(l)}$  satisfies

$$|f^{(l)}(y) - f^{(l)}(y')| \leq |y - y'|^{\beta-l}, \quad \text{for all } y, y'.$$

We now show that  $\widehat{C}_{loc}^{(\alpha)}(x)$  is asymptotically minimal at rate  $w_n$  when the underlying model is a GLM, where  $\beta$  in Assumption 5 is chosen so that  $0 < \beta < 2$ .

**Proposition 1.** Let  $(Y_1, X_1), \dots, (Y_n, X_n)$ ,  $Y_i \in \mathbb{R}^r$ ,  $X_i \in \mathbb{R}^m$ , be an independent and identically distributed sample of random variables with conditional density (12) and parameter space

$$\Theta_{\mathcal{X}} = \{\beta \in \mathbb{R}^m, \phi \in \mathbb{R}^{r-1} : c \{f(x'\beta, \phi)\} < \infty, \text{ for all } x \in \mathcal{X}\},$$

Assume that  $\mathbb{E}(Y_1|x) = g^{-1}(x'\beta)$  and that the canonical statistic vector is a one dimensional manifold. Suppose that Assumption 1 in the manuscript holds. Let  $0 < \alpha < 1$ . Then, for a given  $\lambda > 0$ , there exists a numerical constant  $\zeta_\lambda$  such that,

$$\mathbb{P} \left[ \sup_{x \in \mathcal{X}} \nu \left\{ \widehat{C}_{loc}^{(\alpha)}(x) \Delta C_P^{(\alpha)}(x) \right\} \geq \zeta_\lambda w_n \right] = O \left( n^{-\lambda} \right). \quad (18)$$

*Proof.* The one dimensional manifold assumption is to ensure that all changes in the density function with respect to the canonical statistic can be expressed through any one component of the canonical statistic vector. The result (18) follows from Theorem 1 in Lei and Wasserman [2014], provided that Assumptions 1-3 from the main text hold and that Assumption 5 holds. Assumption 1 is an assumed condition of this proposition. Exponential families are smooth functions over their parameter space. This implies that Assumption 2 from the main text holds for exponential families since  $\mathcal{X}$  is bounded.

We now show that Assumption 5 holds. WLOG, let the exponential family be regular full with density  $f_\theta(y) = e^{y\theta - c(\theta)}$ . Then, for every integer  $s \leq \lfloor \eta \rfloor$ , we have that  $f_\theta^{(s)}(y) = \theta^s f_\theta(y)$ . It follows that  $f_\theta^{(s)}(y)$  is continuous and uniformly bounded, and this establishes part (b) of Assumption 5. We now establish part (a) of Assumption 5 with  $0 < \beta < 2$ , with the only case left to prove is when  $1 < \beta < 2$  and  $s = 1$ . In this case, we can write

$$|f_\theta^{(1)}(y) - f_\theta^{(1)}(y')| = \theta f_\theta(y) |1 - \exp\{\theta(y' - y)\}|.$$

We can bound  $\theta f_\theta(y)$  by some  $M_1 > 0$  for all  $y$  and  $1 < \beta < 2$ , and we can bound  $|1 - \exp\{\theta(y' - y)\}|$  by  $M_2$  for all  $y, y'$ . Thus,

$$|f_\theta^{(1)}(y) - f_\theta^{(1)}(y')| \leq M_1 M_2 (y' - y)^{\beta-1}$$

for all  $y, y'$  such that  $|y - y'| \geq 1$ . We can choose  $\delta > 0$  such that  $\exp\{\theta(y' - y)\} \leq 1 + 2\theta|y' - y|$  for all  $y, y'$  such that  $|y' - y| \leq \delta$ . Thus, for all  $y, y'$  such that  $|y' - y| \leq \delta$ , we have that

$$|f_\theta^{(1)}(y) - f_\theta^{(1)}(y')| \leq 2M_1 (y' - y)^{\beta-1}.$$

Finally, for all  $y, y'$  such that  $\delta \leq |y - y'| < 1$ , we have that

$$|f_\theta^{(1)}(y) - f_\theta^{(1)}(y')| \leq 2M_1 M_2 \left( \frac{y' - y}{\delta} \right)^{\beta-1}.$$

Part (a) of Assumption 5 holds with  $L = 2M_1 M_2 \delta^{-2}$ .

We now verify that Assumption 3 from the main text holds when  $p_\psi(y|x)$  is an exponential family with density (12). We will assume WLOG that generating measure  $\mu$  is Lebesgue measure. Define  $t_x^{(\alpha)}$  such that  $\mathbb{P}\{y : p_\psi(y|x) \geq t_x^{(\alpha)}\} = \alpha$  and let  $A_{x,\varepsilon}^{(\alpha)} = \{y : |p_\psi(y|x) - t_x^{(\alpha)}| \leq \varepsilon\}$ . When  $p_\psi(y|x)$  is an exponential family with density (12) we can choose a  $\varepsilon_o > 0$  such that, for all  $\varepsilon < \varepsilon_o$ , we can pick  $a_1, a_2 \in \mathbb{R}$  for which

$$a_1 \varepsilon \leq \mu(A_{x,\varepsilon}^{(\alpha)}) \leq a_2 \varepsilon.$$

Let  $M(x) = \sup_{y \in A_{x,\varepsilon}^{(\alpha)}} \{p_\psi(y|x)\}$ . We can pick  $M_3 < \infty$  such that  $\sup_{x \in \mathcal{X}} M(x) \leq M_3$ . Then we have,

$$\begin{aligned} & \mathbb{P}\left[\left\{y : |p_\psi(y|x) - t_x^{(\alpha)}| < \varepsilon\right\} \mid X = x\right] \\ &= \int_{A_{x,\varepsilon}^{(\alpha)}} \exp[\langle y, f(x'\beta, \phi) \rangle - c\{f(x'\beta, \phi)\}] \mu(dy) \\ &\leq M(x) \mu(A_{x,\varepsilon}^{(\alpha)}) \leq a_2 M_3 \varepsilon. \end{aligned}$$

The upper bound in Assumption 3 follows from the choice of  $c_2 = a_2 M_3$ . Now pick  $\varepsilon_o$  such that  $\inf_x t_x^{(\alpha)} \geq \varepsilon_o$ . This choice of  $\varepsilon_o$  is possible since  $\alpha < 1$ . Let  $m(x) = \inf_{y \in A_{x,\varepsilon}^{(\alpha)}} \{p_\psi(y|x)\}$ . We can pick  $M_4 > 0$  such that  $\inf_{x \in \mathcal{X}} m(x) \geq M_4$ . Then we have,

$$\begin{aligned} & \mathbb{P}\left[\left\{y : |p_\psi(y|x) - t_x^{(\alpha)}| < \varepsilon\right\} \mid X = x\right] \\ &= \int_{A_{x,\varepsilon}^{(\alpha)}} \exp[\langle y, f(x'\beta, \phi) \rangle - c\{f(x'\beta, \phi)\}] \nu(dy) \\ &\geq m(x) \mu(A_{x,\varepsilon}^{(\alpha)}) \geq a_1 M_4 \varepsilon. \end{aligned}$$

The lower bound in Assumption 3 follows from the choice of  $c_1 = a_1 M_4$ . Therefore Assumption 3 holds when  $p_\psi(y|x)$  is an exponential family with density (12).  $\square$

We now verify that Assumption 5 in the main text holds, we show that If  $|\nabla_\psi F(v|x)|$  is bounded for all  $v$  and all  $\psi \in \Theta_{\mathcal{X}}$ .

The gradient of  $\log p_\psi(y|x)$  is then  $\nabla_\psi B(x) \{y - \nabla_\theta c(\theta)\}$  where

$$B(x) = \begin{pmatrix} x & 0 \\ 0 & I \end{pmatrix} \{\nabla_\psi f(x'\beta, \phi)\}',$$

and  $\theta = f(x'\beta, \phi)$ . From Trench [2013, Theorem 11], we have that

$$\begin{aligned}\nabla_{\psi}F(v|x) &= \nabla_{\psi} \int_{-\infty}^v p_{\psi}(u|x)du = \int_{-\infty}^v \nabla_{\psi}p_{\psi}(u|x)du \\ &= B(x) \int_{-\infty}^v \{u - \nabla_{\theta}c(\theta)\} p_{\psi}(u|x)du.\end{aligned}$$

The quantity  $B(x)$  is bounded in  $x$  since  $\mathcal{X}$  is bounded. Existence of moments of all orders for the random variables with conditional density  $p_{\psi}(u|x)$  with parameter space  $\Theta_{\mathcal{X}}$  implies that

$$\int_{-\infty}^v \{u - \nabla_{\theta}c(\theta)\} p_{\psi}(u|x)du$$

is bounded for all  $v$  and all  $x \in \mathcal{X}$ . Therefore  $|\nabla_{\psi}F(v|x)|$  is bounded for all  $v$  and all  $x \in \mathcal{X}$ . Therefore Assumption 5 holds for GLMs with densities (12).

## B Summary of simulation results

We provide additional numerical evidence that parametric conformal prediction regions perform well even when the model is misspecified. The guarantee of finite-sample marginal and local validity in the presence of model misspecification are noted benefits of both the parametric and nonparametric conformal prediction regions. However, the parametric and nonparametric conformal prediction regions are visually very different and give different prediction errors at small to moderate sample sizes as seen in Section C. We see that the both parametric conformal prediction regions adapt naturally to the data when the model is correctly specified or modest deviations from the specified model are present. Large deviations from model misspecification are not handled well as seen in the top 2 rows of Figures 9-11, although the parametric conformal prediction region does give nominal marginal and local coverage with respect to binning in finite-samples. When the model is correctly specified, the parametric conformal prediction region increasingly resembles the highest density oracle prediction region as the sample size increases. On the other hand, the nonparametric conformal prediction region does not adapt well to data obtained from a Gamma regression model or data obtained from a linear regression model with a steep mean function (steepness is relative to the variability about the mean function) in small to moderate sample sizes.

The LS conformal prediction region obtains marginal validity [Lei et al., 2018] but performs poorly when deviations about the estimated mean function are either not symmetric, not constant, or both. When heterogeneity is present, the LS conformal prediction region exhibits undercoverage in regions where variability about the mean function is large and overcoverage in regions where variability about the mean function is small. This conformal prediction region is very sensitive to model misspecification. The LSLS conformal prediction region also obtains marginal validity [Lei et al., 2018, Section 5.2] and it is far less sensitive to model misspecification than the LS conformal prediction region and it performs well under most model misspecification. However, the LSLW conformal prediction region is not appropriate when deviations about an estimated mean function are obviously not symmetric, as evidenced in Section C.1. Note that all conformal prediction regions are obtained using the software defaults. Therefore, observed deviations from guaranteed coverage properties can result from the precision (or lack thereof) of the default settings.

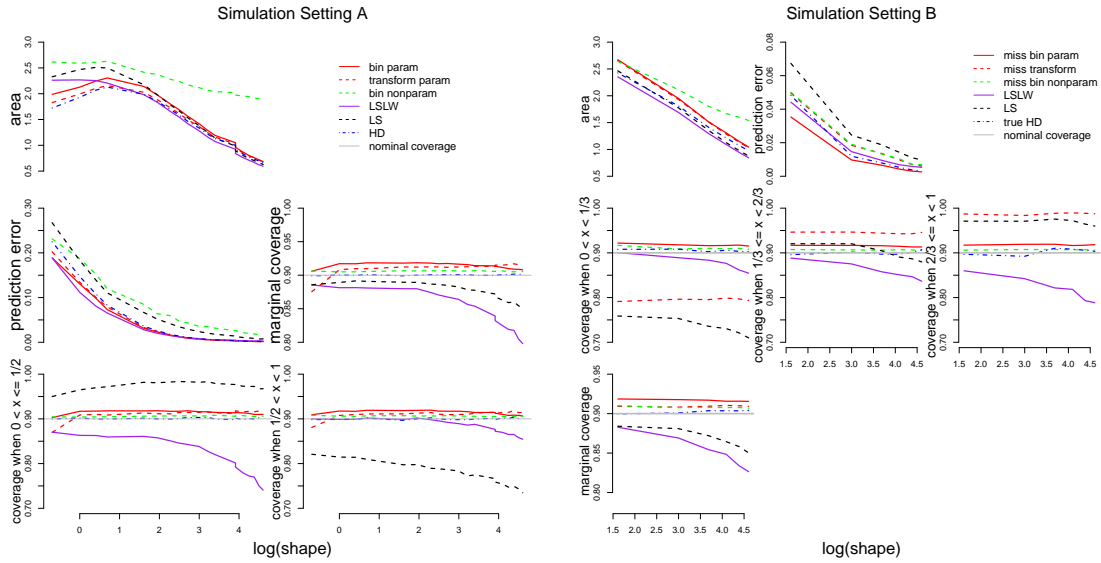


Figure 5: Area, prediction error, and bin-wise coverage for parametric, nonparametric, LS, LSLW conformal prediction region, and the highest density prediction region for gamma GLM regression with  $n = 250$ . Simulation setting A is shown at left, and setting B at right. The average of 50 Monte Carlo samples at each shape parameter value in these simulation settings form the lines that are depicted in this figure.

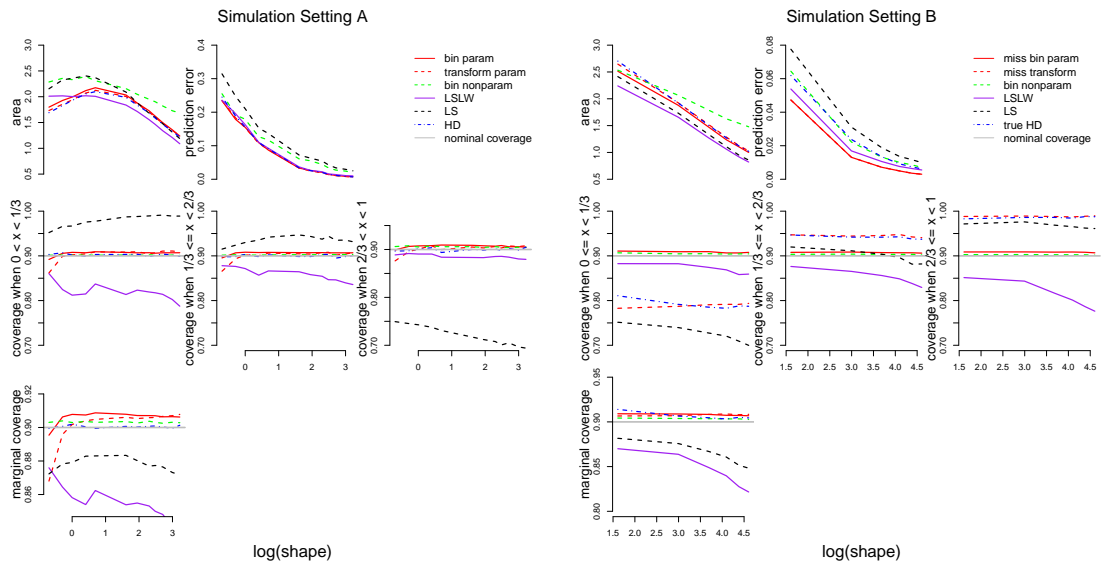


Figure 6: Area, prediction error, and bin-wise coverage for parametric, nonparametric, LS, LSLW conformal prediction region, and the highest density prediction region for gamma GLM regression with  $n = 500$ . Simulation setting A is shown at left, and setting B at right. The average of 50 Monte Carlo samples at each shape parameter value in these simulation settings form the lines that are depicted in this figure.

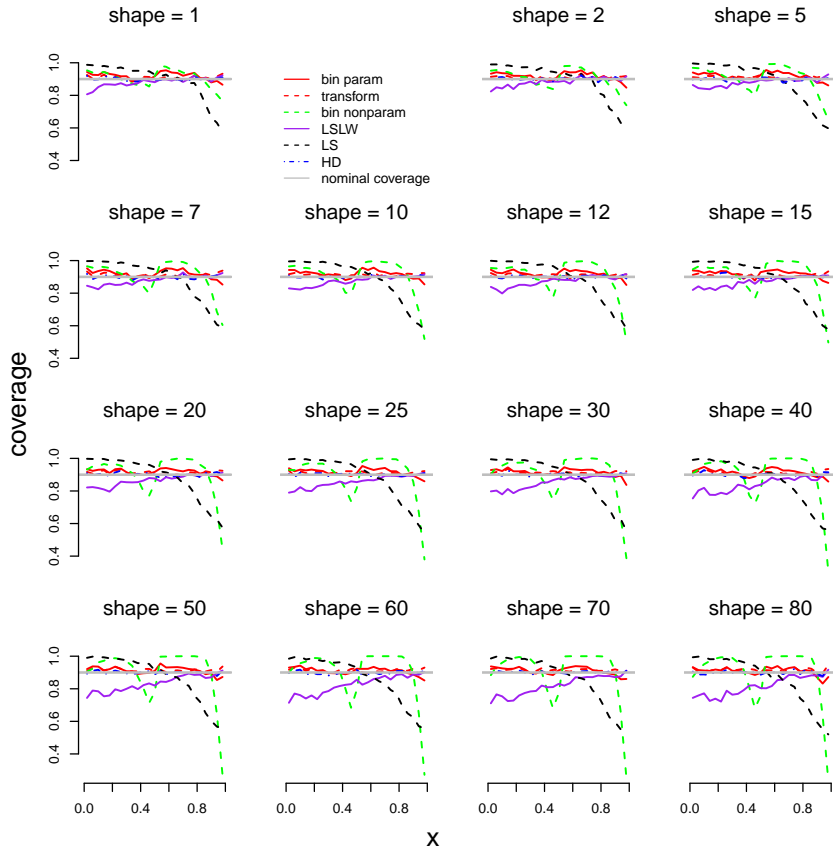


Figure 7: Plot of the estimated coverage probabilities of prediction regions across  $x$  and shape parameter values when the model is correctly specified,  $n = 150$ , and the number of bins is equal to 2. The average of 250 Monte Carlo samples at each shape parameter value in these simulation settings form the lines that are depicted in this figure.

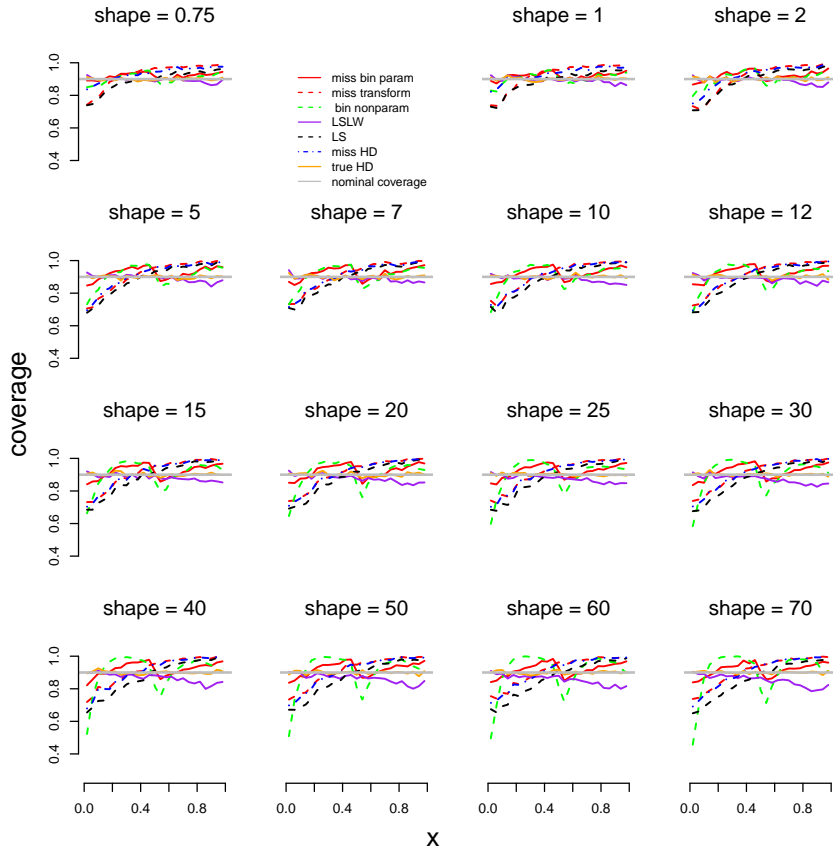


Figure 8: Plot of the estimated coverage probabilities of prediction regions across  $x$  and shape parameter values when the model is misspecified,  $n = 150$ , and the number of bins is equal to 2. The average of 250 Monte Carlo samples at each shape parameter value in these simulation settings form the lines that are depicted in this figure.



## C Plots of conformal prediction regions

### C.1 Plots when Gamma model is correctly specified

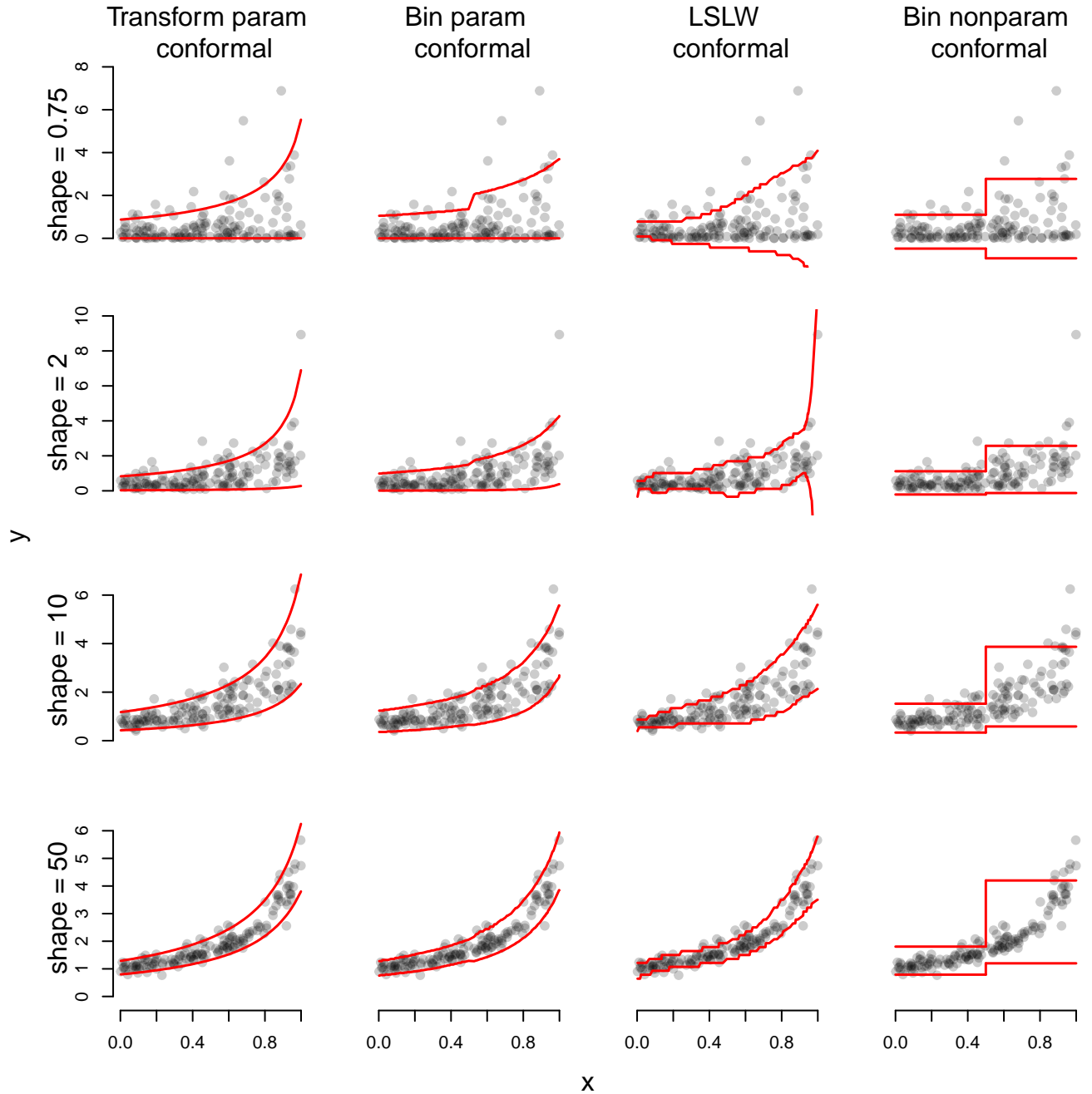


Figure 9: Illustration of conformal prediction regions for Gamma regression under simulation setting A with  $n = 150$ ,  $\alpha = 0.10$ , and the number of bins equals 2.

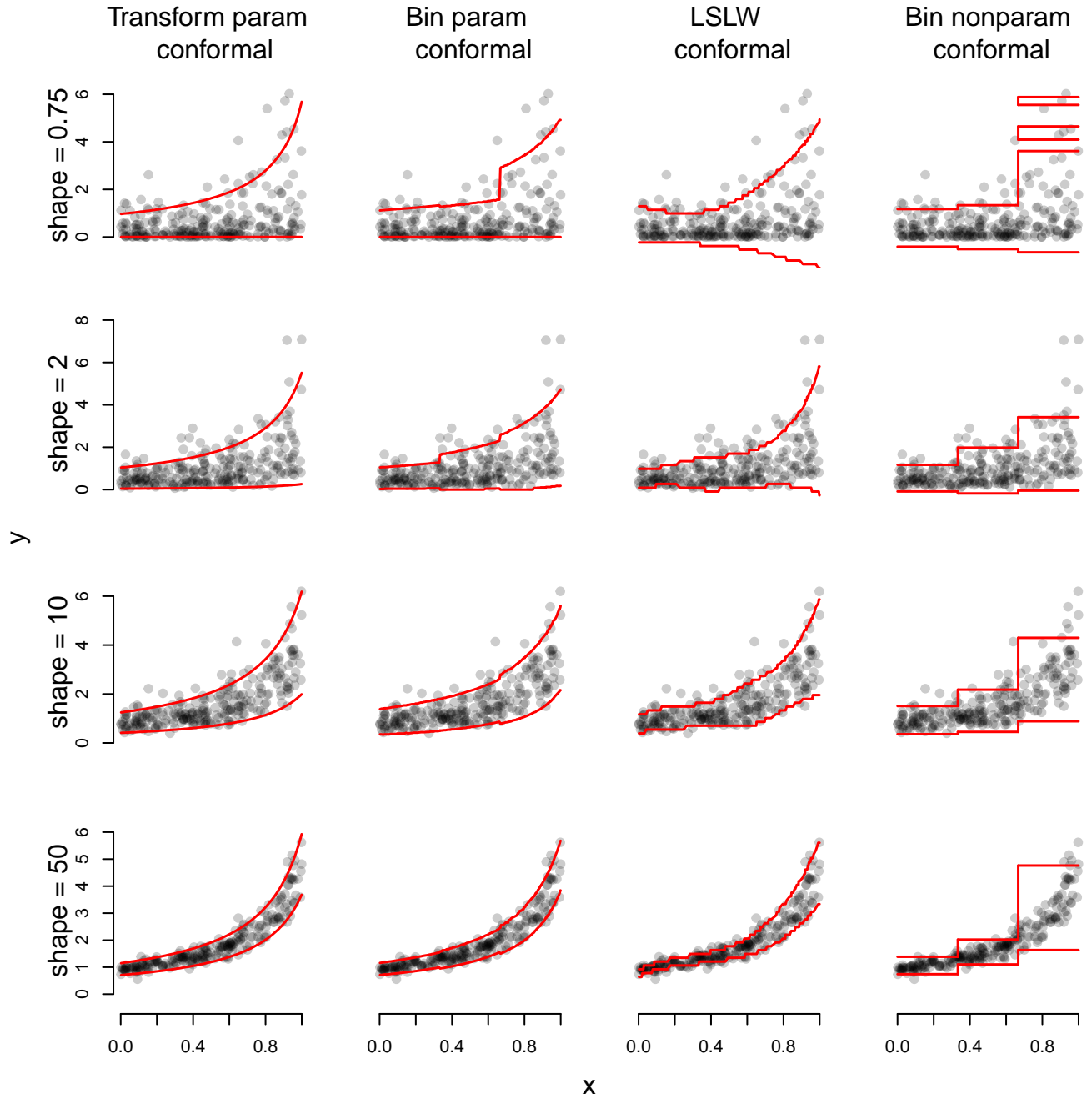


Figure 10: Illustration of conformal prediction regions for Gamma regression under simulation setting A with  $n = 250$ ,  $\alpha = 0.10$ , and the number of bins equals 3.

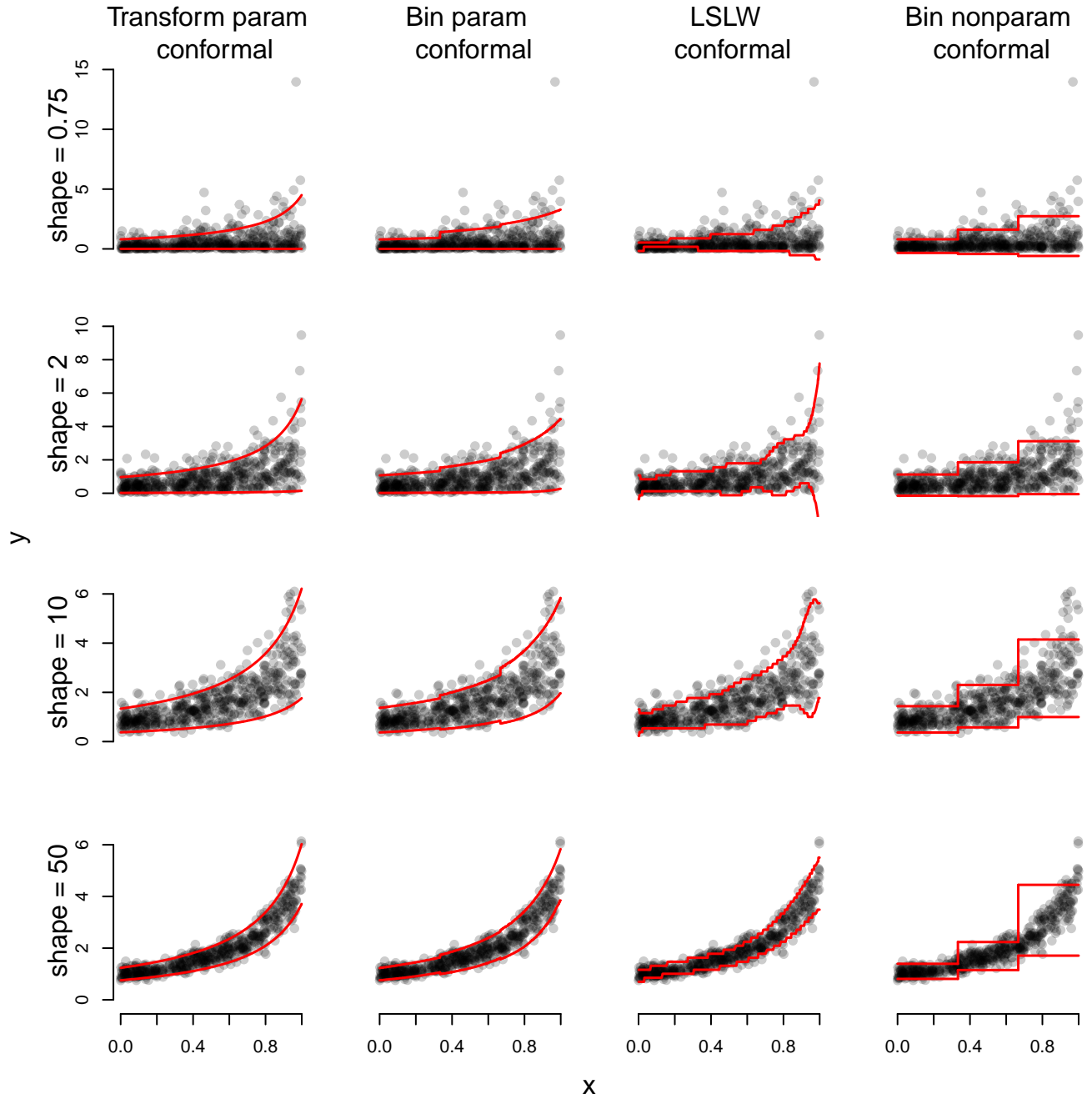


Figure 11: Illustration of conformal prediction regions for Gamma regression under simulation setting A with  $n = 500$ ,  $\alpha = 0.10$ , and the number of bins equals 3.

## C.2 Plots when model is misspecified

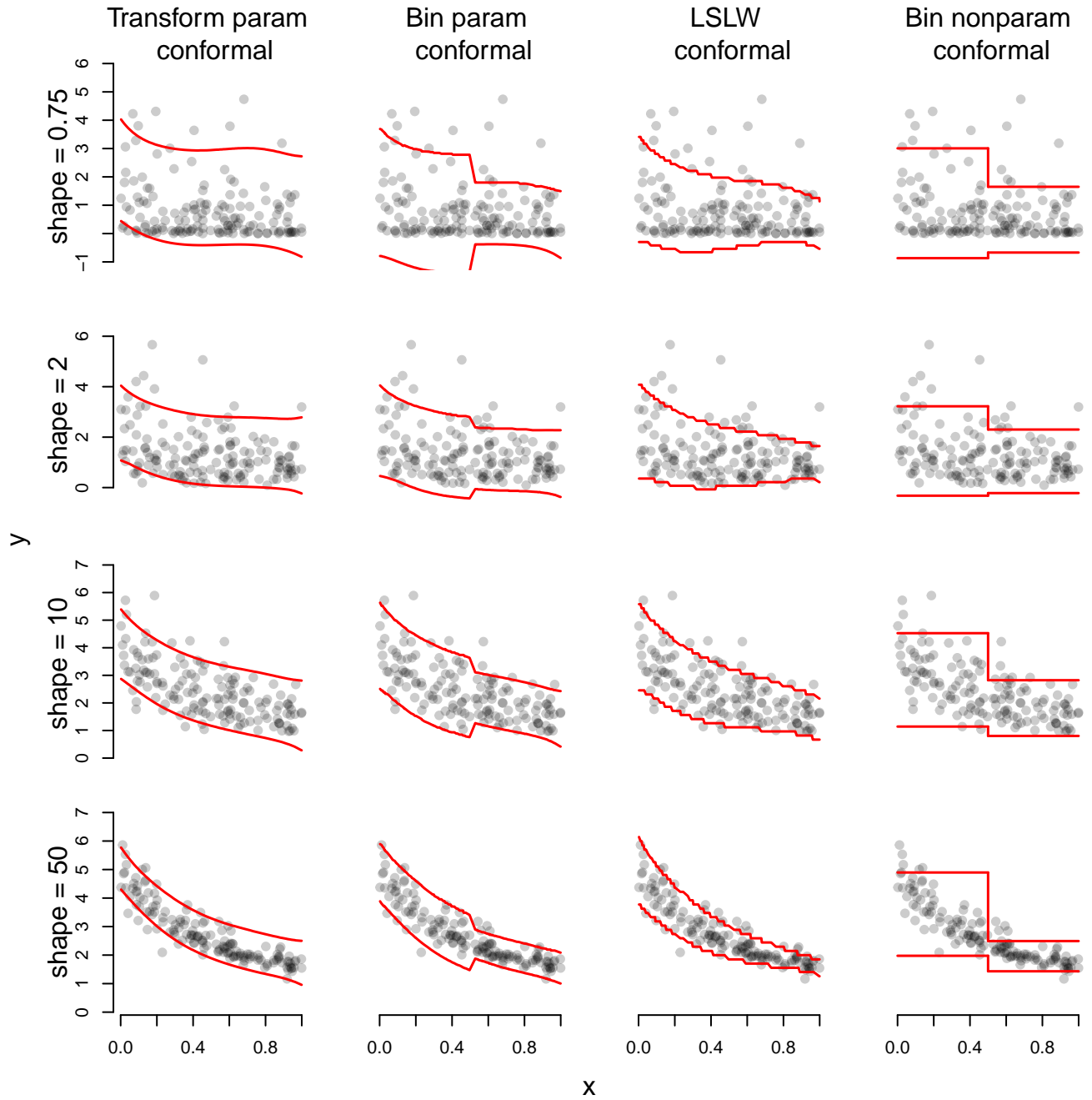


Figure 12: Illustration of conformal prediction regions for Gamma regression under simulation setting B with  $n = 150$ ,  $\alpha = 0.10$ , and the number of bins equals 2.

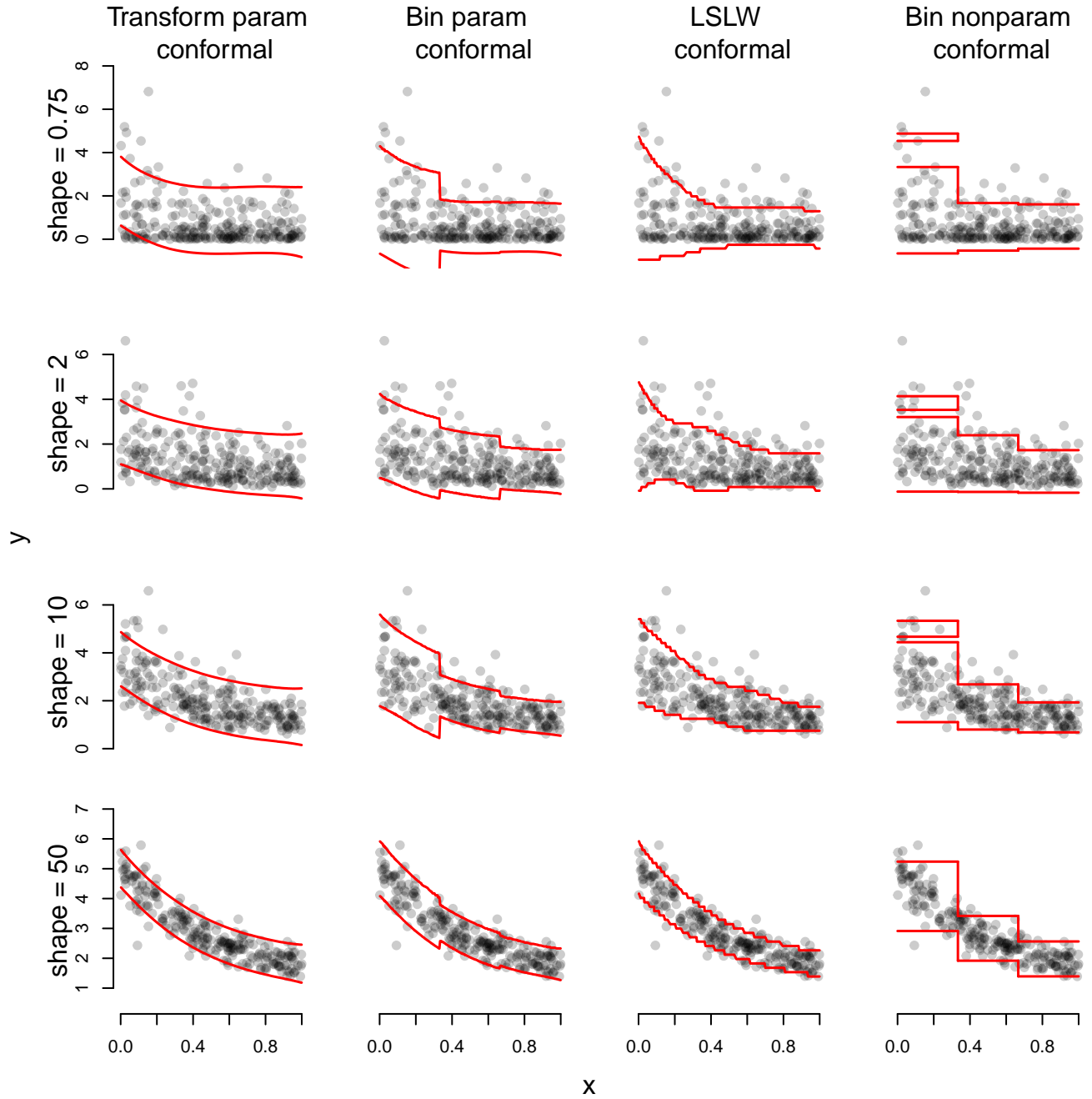


Figure 13: Illustration of conformal prediction regions for Gamma regression under simulation setting B with  $n = 250$ ,  $\alpha = 0.10$ , and the number of bins equals 3.

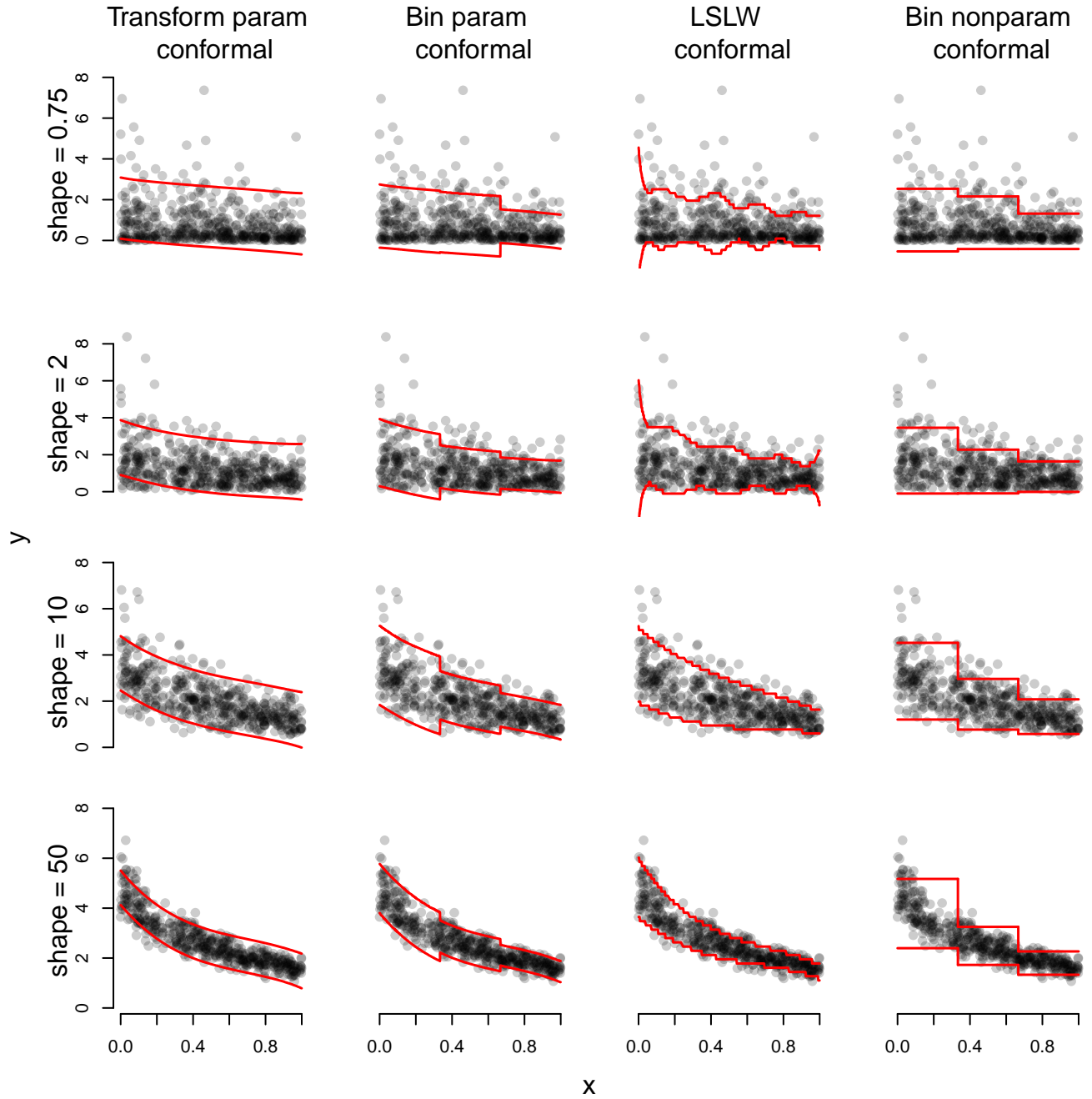


Figure 14: Illustration of conformal prediction regions for Gamma regression under simulation setting B with  $n = 500$ ,  $\alpha = 0.10$ , and the number of bins equals 3.

### C.3 Plots when linear regression model is correctly specified

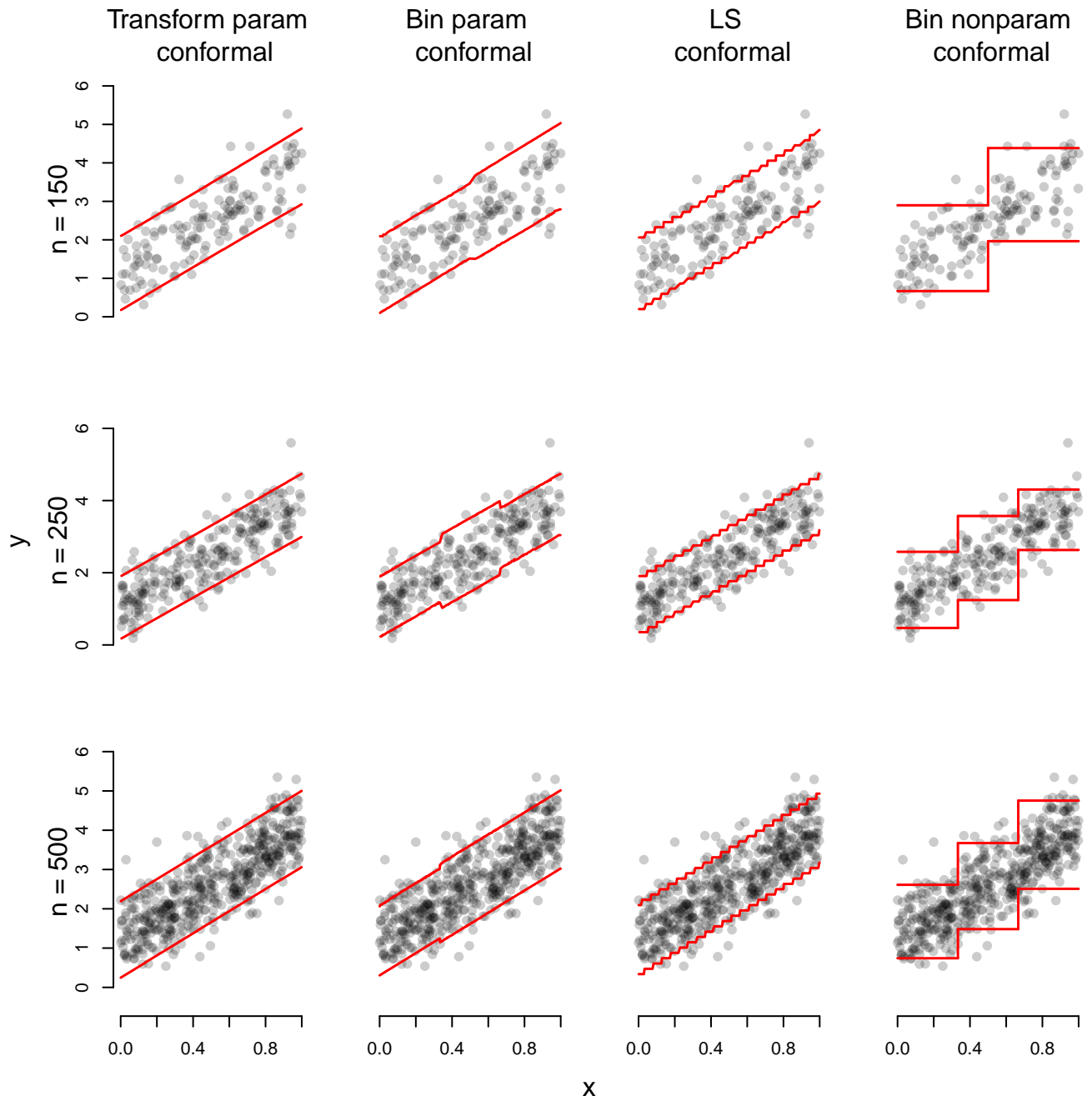


Figure 15: Illustration of conformal prediction regions for linear regression under simulation setting C with  $\alpha = 0.10$ .

## D Example from README file in Eck [2018]

In this section we illustrate conformal prediction regions through a gamma regression example with perfect model specification when the model is known, the model can be parameterized as in displayed equation 12 of the main text, and the model does not have additive symmetric errors. We also compare conformal prediction regions to the oracle highest density region under the correct model. This example is included in the README file of the corresponding R package Eck [2018].

In this example we set the sample size to  $n = 500$  and we consider the gamma regression model with a single predictor with inverse link function (default in `glm` package). The predictors were generated independently as  $X_i \sim U(0, 1), i = 1, \dots, n$ . We specified that  $\beta = [0.25, 2]'$ . The response variable was generated using `rgamma` with the shape parameter  $\phi = 2$  and the rate as  $2[1, X_i]'\beta$ . Therefore we have iid data  $(X_i, Y_i)$  from a continuous distribution where  $Y_i|X_i$  is a GLM that can be parameterized as in displayed equation 12 of the main text.

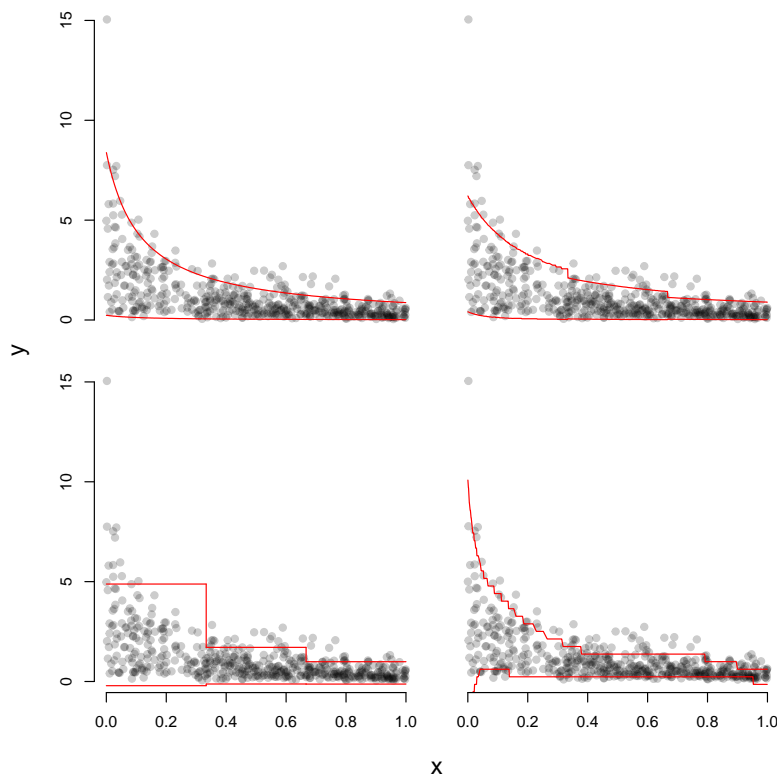


Figure 16: Depiction of four prediction regions when  $n = 500$ . The description of the gamma regression data generating process is outlined in the README file of the corresponding R package Eck [2018]. Sim setting: shape = 2, bins = 3. The regions are depicted as follows: transformation based parametric conformal prediction (top-left panel), binned parametric conformal prediction region (top-right panel), binned nonparametric conformal prediction region (bottom-left panel), and LSLW conformal prediction region (bottom-right panel).

Figure 16 shows prediction regions for four of the five prediction regions considered. The top row depicts the transformation parametric conformal prediction region (left panel) and the binned parametric conformal



prediction region (right panel). The bottom row depicts the binned nonparametric conformal prediction region (left panel) and the LSLW conformal prediction region (right panel). The bin width was specified as  $1/3$  for the binned conformal prediction regions. We see that the binned parametric conformal prediction region is a close discretization of the transformation conformal prediction region, the nonparametric conformal prediction region is quite jagged and unnatural, and the LSLW conformal prediction region includes negative response values and is jagged. In Figure 17 we see that the transformation based parametric conformal prediction region closely resembles the HD prediction region, and that the binned parametric conformal prediction region is a close discretization of the HD prediction region.

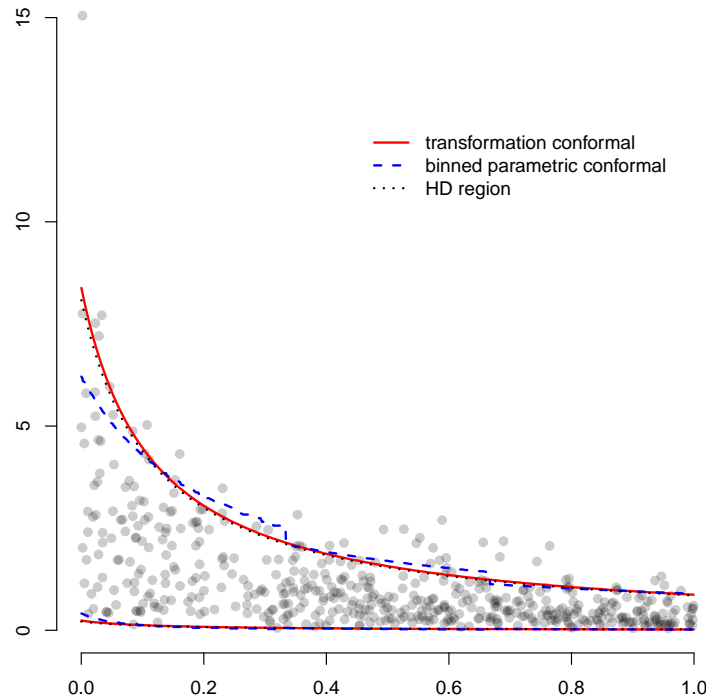


Figure 17: Depiction of both parametric conformal prediction regions in Figure 16 and the HD region.

All of the presented prediction regions exhibit close to finite-sample marginal validity and local validity with respect to binning. However, the transformation conformal prediction region, LSLW conformal prediction region, and the HD prediction region do not exhibit finite-sample local validity in the second bin and the HD prediction region does not quite possess finite-sample marginal validity. The binned parametric conformal prediction region is smallest in size with an estimated area of 2.19. The HD prediction region is a close second with an estimated area of 2.21. The transformation conformal prediction region is a respectable third with an estimated area of 2.26. LSLW conformal prediction region has an estimated area of 2.56 and The nonparametric conformal prediction region has an estimated area of 2.68. Under correct model specification, the parametric conformal prediction regions are similar in performance to that of the highest density prediction region.

Performance of these prediction regions under the same model specification in this example is investigated further in a Monte Carlo simulation study. The results of this Monte Carlo simulation study are consistent

with those presented here. Details are included in the reproducible technical report available at <https://github.com/DEck13/conformal.glm/tree/master/techreport>.

## References

- American Diabetes Association. Diagnosis and classification of diabetes mellitus. *Diabetes Care*, 33 (Supplement 1):S62–S69, 2010.
- Vineeth Balasubramanian, Shen-Shyang Ho, and Vladimir Vovk. *Conformal Prediction for Reliable Machine Learning: Theory, Adaptations and Applications*. Morgan Kaufmann, Boston, 2014.
- Sergej G Bobkov and Friedrich Götze. Exponential integrability and transportation cost related to logarithmic Sobolev inequalities. *Journal of Functional Analysis*, 163(1):1–28, 1999.
- Nicolas Bosc, Francis Atkinson, Eloy Felix, Anna Gaulton, Anne Hersey, and Andrew R Leach. Large scale comparison of QSAR and conformal prediction methods and their applications in drug discovery. *Journal of Cheminformatics*, 11(1):4, 2019.
- Evgeny Burnaev and Vladimir Vovk. Efficiency of conformalized ridge regression. In *Conference on Learning Theory*, pages 605–622, 2014.
- Victor Chernozhukov, Kasper Wüthrich, and Yinchu Zhu. An exact and robust conformal inference method for counterfactual and synthetic controls. *preprint*, 2018a. URL [arXiv:1712.09089](https://arxiv.org/abs/1712.09089).
- Victor Chernozhukov, Kasper Wüthrich, and Yinchu Zhu. Exact and robust conformal inference methods for predictive machine learning with dependent data. *preprint*, 2018b. URL [arXiv:1802.06300](https://arxiv.org/abs/1802.06300).
- Victor Chernozhukov, Kasper Wüthrich, and Yinchu Zhu. Distributional conformal prediction. *preprint*, 2019. URL [arXiv:1909.07889](https://arxiv.org/abs/1909.07889).
- NH Cho, JE Shaw, S Karuranga, Y Huang, JD da Rocha Fernandes, AW Ohlrogge, and B Malanda. IDF Diabetes Atlas: Global estimates of diabetes prevalence for 2017 and projections for 2045. *Diabetes Research and Clinical Practice*, 138:271–281, 2018.
- Mattia Ciollaro, Jessi Cisewski, Peter E. Freeman, Christopher R. Genovese, Jing Lei, Ross O’Connell, and Larry Wasserman. Functional regression for quasar spectra. *preprint*, 2018. URL [arXiv:1404.3168](https://arxiv.org/abs/1404.3168).
- Isidro Cortés-Ciriano and Andreas Bender. Deep confidence: A computationally efficient framework for calculating reliable prediction errors for deep neural networks. *Journal of Chemical Information and Modeling*, 2018.
- Isidro Cortés-Ciriano and Andreas Bender. Concepts and applications of conformal prediction in computational drug discovery. *arXiv:1908.03569*, 2019.
- Miklós Csörgő and Pál Révész. Strong approximations of the quantile process. *The Annals of Statistics*, pages 882–894, 1978.
- Dmitry Devetyarov, Iliia Nouretdinov, Brian Burford, Stephane Camuzeaux, Aleksandra Gentry-Maharaj, Ali Tiss, Celia Smith, Zhiyuan Luo, Alexey Chervonenkis, Rachel Hallett, Volodya Vovk, Mike Waterfield, Rainer Cramer, John F. Timms, John Sinclair, Usha Menon, Ian Jacobs, and Alex Gammerman. Conformal predictors in early diagnostics of ovarian and breast cancers. *Progress in Artificial Intelligence*, 1(3):245–257, 2012.

- Hacene Djellout, Arnaud Guillin, and Liming Wu. Transportation cost-information inequalities and applications to random dynamical systems and diffusions. *The Annals of Probability*, 32(3B):2702–2732, 2004.
- Robin Dunn and Larry Wasserman. Distribution-free prediction sets with random effects. *preprint*, 2018. URL [arXiv:1809.07441](https://arxiv.org/abs/1809.07441).
- Daniel J. Eck. *conformal.glm: Conformal Prediction for Generalized Linear Regression Models*, 2018. <https://github.com/DEck13/conformal.glm>.
- Martin Eklund, Ulf Norinder, Scott Boyer, and Lars Carlsson. The application of conformal prediction to the drug discovery process. *Annals of Mathematics and Artificial Intelligence*, 74(1-2):117–132, 2015.
- Julian Faraway. *faraway: Functions and Datasets for Books by Julian Faraway*, 2016. <https://cran.r-project.org/web/packages/faraway/index.html>.
- Thomas S. Ferguson. A course in large sample theory, 1996.
- Alexander Gammernan and Vladimir Vovk. Hedging Predictions in Machine Learning: The Second Computer Journal Lecture . *The Computer Journal*, 50(2):151–163, 02 2007.
- Kenneth E Heikes, David M Eddy, Bhakti Arondekar, and Leonard Schlessinger. Diabetes risk calculator: a simple tool for detecting undiagnosed diabetes and pre-diabetes. *Diabetes care*, 31(5):1040–1045, 2008.
- Rafael Izbicki, Gilson Y. Shimizu, and Rafael B. Stern. Distribution-free conditional predictive bands using density estimators. *preprint*, 2019. URL [arXiv:1910.05575](https://arxiv.org/abs/1910.05575).
- Changge Ji, Fredrik Svensson, Azedine Zoufir, Andreas Bender, and Alfonso Valencia. eMolTox: prediction of molecular toxicity with confidence. *Bioinformatics*, 1:2, 2018.
- Ulf Johansson, Henrik Linusson, Tuve Löfström, and Henrik Boström. Interpretable regression trees using conformal prediction. *Expert Systems With Applications*, 97:394–404, 2018.
- János Komlós, Péter Major, and Gábor Tusnády. An approximation of partial sums of independent  $r_v$ 's, and the sample df. i. *Zeitschrift für Wahrscheinlichkeitstheorie und verwandte Gebiete*, 32(1-2):111–131, 1975.
- Antonis Lambrou, Harris Papadopoulos, and Alex Gammernan. Evolutionary conformal prediction for breast cancer diagnosis. *Proceedings of 9th International Conference on Information Technology and Applications in Biomedicine*, pages 1–4, 2009.
- Michel Ledoux. Concentration of measure and logarithmic sobolev inequalities. *Lecture Notes in Math*, 1709:120–216, 1999.
- Michel Ledoux. *The Concentration of Measure Phenomenon*. American Mathematical Society, 2001.
- Jing Lei and Larry Wasserman. Distribution-free prediction bands for nonparametric regression. *Journal of the Royal Statistical Society series B*, 76, 1:71–96, 2014.
- Jing Lei, James Robins, and Larry Wasserman. Distribution-free prediction sets. *Journal of the American Statistical Association*, 108:278–287, 2013.
- Jing Lei, Alessandro Rinaldo, and Larry Wasserman. A conformal prediction approach to explore functional data. *Annals of Mathematics and Artificial Intelligence*, 74:29–43, 2015.

- Jing Lei, Max G Sell, Alessandro Rinaldo, Ryan J Tibshirani, and Larry Wasserman. Distribution-free predictive inference for regression. *Journal of the American Statistical Association*, 113(523):1094–1111, 2018.
- Peter McCullagh and John A Nelder. *Generalized Linear Models*. CRC press, 1989.
- Mike Meredith and John Kruschke. *HDInterval: Highest (Posterior) Density Intervals*, 2018. <https://cran.r-project.org/web/packages/HDInterval/>.
- Yu Miao. Concentration inequality of maximum likelihood estimator. *Applied Mathematics Letters*, 23(10):1305–1309, 2010.
- Ulf Norinder, Ernst Ahlberg, and Lars Carlsson. Predicting Ames mutagenicity using conformal prediction in the Ames/QSAR International Challenge Project. *Mutagenesis*, 2018a.
- Ulf Norinder, Glenn Myatt, and Ernst Ahlberg. Predicting aromatic amine mutagenicity with confidence: A case study using conformal prediction. *Biomolecules*, 8(3):85, 2018b.
- Harris Papadopoulos, Vladimir Vovk, and Alex Gammernan. Inductive conformal prediction: Theory and application to neural networks. *Journal of Artificial Intelligence Research*, 40:815–840, 2011.
- R Core Team. *R: A Language and Environment for Statistical Computing*. R Foundation for Statistical Computing, Vienna, Austria, 2019. <https://www.R-project.org/>.
- Yaniv Romano, Rina F. Barber, Chiara Sabatti, and Emmanuel J. Candés. With malice towards none: Assessing uncertainty via equalized coverage. *preprint*, 2019a. URL [arXiv:1908.05428](https://arxiv.org/abs/1908.05428).
- Yaniv Romano, Evan Patterson, and Emmanuel J. Candés. Conformalized quantile regression. *preprint*, 2019b. URL [arXiv:1905.03222](https://arxiv.org/abs/1905.03222).
- Matteo Sesia and Emmanuel J. Candés. A comparison of some conformal quantile regression methods. *preprint*, 2019. URL [arXiv:1909.05433](https://arxiv.org/abs/1909.05433).
- Glenn Shafer and Vladimir Vovk. A tutorial on conformal prediction. *Journal of Machine Learning Research*, 9:371–421, 2008.
- Fredrik Svensson, Avid M Afzal, Ulf Norinder, and Andreas Bender. Maximizing gain in high-throughput screening using conformal prediction. *Journal of Cheminformatics*, 10(1):7, 2018a.
- Fredrik Svensson, Natalia Aniceto, Ulf Norinder, Isidro Cortes-Ciriano, Ola Spjuth, Lars Carlsson, and Andreas Bender. Conformal regression for quantitative structure–activity relationship modeling–quantifying prediction uncertainty. *Journal of Chemical Information and Modeling*, 58(5):1132–1140, 2018b.
- Ryan Tibshirani. *conformalInference: Tools for conformal inference in regression*, 2016. <https://github.com/ryantibs/conformal>.
- Paolo Toccaceli, Ilia Nouretdinov, and Alexander Gammernan. Conformal prediction of biological activity of chemical compounds. *Annals of Mathematics and Artificial Intelligence*, 81(1-2):105–123, 2017.
- William F. Trench. *Introduction to Real Analysis*. 2013. Relevant material from Supplement 1.
- Cédric Villani. *Optimal Transport: Old and New*, volume 338. Springer Science & Business Media, 2008.
- Vladimir Vovk. Conditional validity of inductive conformal predictors. *Proceedings of Machine Learning Research*, 25:475–490, 2012.

- Vladimir Vovk, Alex Gammerman, and Glenn Shafer. *Algorithmic Learning in a Random World*. Springer, 2005.
- Martin J. Wainwright. *High-Dimensional Statistics: A Non-Asymptotic Viewpoint*. Cambridge Series in Statistical and Probabilistic Mathematics, 2019. URL [https://www.stat.berkeley.edu/~mjlwain/stat210b/Chap2\\_TailBounds\\_Jan22\\_2015.pdf](https://www.stat.berkeley.edu/~mjlwain/stat210b/Chap2_TailBounds_Jan22_2015.pdf).
- Di Wang, Ping Wang, and Junzhi Shi. A fast and efficient conformal regressor with regularized extreme learning machine. *Neurocomputing*, 304:1–11, 2018.
- James P Willems, J Terry Saunders, Dawn E Hunt, and John B Schorling. Prevalence of coronary heart disease risk factors among rural blacks: a community-based study. *Southern Medical Journal*, 90(8): 814–820, 1997.
- World Health Organization. Use of glycated haemoglobin (HbA1c) in diagnosis of diabetes mellitus: abbreviated report of a WHO consultation. Technical report, Geneva: World Health Organization, 2011.